

Stephen F. Austin State University

SFA ScholarWorks

Electronic Theses and Dissertations

Spring 5-16-2018

The Effect of Compound L19 on Human Colorectal Cells (DLD-1)

Sepideh Mohammadhosseinpour
mohammads@jacks.sfasu.edu

Follow this and additional works at: <https://scholarworks.sfasu.edu/etds>



Part of the [Biotechnology Commons](#)

[Tell us](#) how this article helped you.

Repository Citation

Mohammadhosseinpour, Sepideh, "The Effect of Compound L19 on Human Colorectal Cells (DLD-1)" (2018). *Electronic Theses and Dissertations*. 188.
<https://scholarworks.sfasu.edu/etds/188>

This Thesis is brought to you for free and open access by SFA ScholarWorks. It has been accepted for inclusion in Electronic Theses and Dissertations by an authorized administrator of SFA ScholarWorks. For more information, please contact cdsscholarworks@sfasu.edu.

The Effect of Compound L19 on Human Colorectal Cells (DLD-1)

Creative Commons License



This work is licensed under a [Creative Commons Attribution-Noncommercial-No Derivative Works 4.0 License](https://creativecommons.org/licenses/by-nc-nd/4.0/).

The Effect of Compound L19 on Human Colorectal Cells (DLD-1)

By

Sepideh Mohammadhosseinpour, Master of Science

Presented to the Faculty of the Graduate School of

Stephen F. Austin State University

In Partial Fulfillment

Of the Requirements

For the Degree of

Master of Science in Biotechnology

STEPHEN F. AUSTIN STATE UNIVERSITY

May, 2018

The Effect of Compound L19 on Human Colorectal Cells (DLD-1)

By

Sepideh Mohammadhosseinpour, Master of Science

APPROVED:

Dr. Beatrice A. Clack, Thesis Director

Dr. Josephine Taylor, Committee Member

Dr. Rebecca Parr, Committee Member

Dr. Stephen Mullin, Committee Member

Pauline Sampson, Ph.D.
Dean of Research and Graduate Studies

ABSTRACT

Colorectal cancer is the third most common type of cancer in the world and the second leading cause of death among humans. Extracts of water soluble compounds from the roots and leaves of *Rumex crispus* were screened for compounds that induced apoptosis in DLD-1 cells. A compound referred to as L19 was isolated using Accelerated Solvent Extraction (ASE) followed by High Performance Liquid Chromatography (HPLC). Gas chromatography coupled with mass spectrometry was used to identify the L19 as a tetrahydrofuran with a molecular weight of 72.11 g/mole. Each HPLC fraction resulted in 94.4% purity. In the present research, specific genes involved in apoptosis induction with the treatment of the DLD-1 cells with L19 were identified. Apoptosis was measured by detecting levels of caspase 3 and 7 using the APO-one assay after treating synchronized DLD-1 cells with varying concentrations of L19 for 24 hrs. Furthermore, the mechanism of apoptosis was determined using quantitative real-time polymerase chain reaction (qRT-PCR) and gene specific primers for caspases 6, 8, 10 (extrinsic pathways), 9 (intrinsic), 1, 4, 5 and 12 (ER stress). RT² Profiler PCR array for human apoptosis genes was used to explore additional changes in apoptotic gene expression. Microarray analysis was performed using the Human OneArray® Microarray from Phalanx Biotech Group to determine which genes of other key cellular pathways were affected by L19. Exposure of the DLD-1 cells to L19 for 6, 8, 12, and 24 hours and subsequent gene expression

analysis indicated primarily that ER stress was the mechanism of apoptosis along with inflammation. The qRT-PCR results showed *CASP 1* and *12* exhibited up-regulation by 12 hours, after which, results from the RT² Profiler™ PCR array showed BCL2 an inhibitor for apoptosis down-regulated. Apoptosis genes, *CASP 3*, APAF-1 and BAX and those involved in ER Stress, BH3, FAS, and FASLG were up-regulated as were the genes involved in inflammation, *CASP 1, 12*. Based on these results, L19 induces ER stress, *AIF* pathway (apoptosis pathways) and inflammatory pathways were shown. The microarray results show many more neurological, metabolic, and cell cycle processes affected by L19 that need to be investigated.

ACKNOWLEDGMENTS

It was thanks to the incredible hard work of my professors and the support of the university staff that I was able to achieve such honors as the “Travel award” and admission to a Ph.D. program. Now, at the junction of ending of one era and beginning of a new one, I would like to show my deepest gratitude for my honorable professors, especially Dr. Clack, Dr. Taylor, and Dr. Parr, for their compassion and superb support. As my primary advisor, Dr. Clack has been somewhat of a mother-figure to me, and she has been my pillar of strength. Furthermore, I would like to extend my special thanks to Dr. Mullin for his guidance. It was because of his confidence in me that I was able to work as a Laboratory Instructor and gain some of my best experiences. Additionally, I would like to thank my family, especially my parents and sisters, for their never-ending support and love, and all my friends, whose strength and mutual interest in science allowed me to overcome multiple obstacles in my professional or personal life.

Research and exploration in the field of biotechnology has opened a new path in my life. It is my pleasure to share the heartwarming feeling of satisfaction from Stephen F Austin State University and its incredible professors. This great feeling encourages me to continue in this course; happier, determined and stronger than ever.

TABLE OF CONTENTS

| | |
|---|-----|
| ABSTRACT | i |
| ACKNOWLEDGMENTS | iii |
| LIST OF FIGURES | ix |
| LIST OF TABLES | xii |
| INTRODUCTION | 1 |
| Colorectal Cancer | 1 |
| Apoptosis..... | 2 |
| Extrinsic pathway | 4 |
| Intrinsic pathway..... | 5 |
| ER stress pathways | 8 |
| DLD-1 Cell Line | 10 |
| Rumex crispus | 10 |
| Doxorubicin | 13 |
| Determination of Levels of Gene Expression by Quantitative Real Time PCR..... | 14 |

| | |
|---|-----------|
| Use of Microarrays to Analyze Gene Expression in DLD-1 Cells..... | 15 |
| OBJECTIVES | 18 |
| MATERIALS AND METHODS..... | 19 |
| Media Preparation | 20 |
| Cell culture..... | 20 |
| Synchronization of Cells Prior to Dox or L19 Exposure | 21 |
| Acquiring Leaf Extract by Accelerated Solvent Extraction | 21 |
| Separation of Compound L19 by High Performance Liquid Chromatography..... | 22 |
| Gas Chromatography-Mass Spectrometry | 23 |
| Optimization of the Number of Cells per well for Cell Viability Assays | 23 |
| Measuring Dose-Response for L19 and Dox using Cell Viability | 24 |
| Determination of Apoptosis Induction by Apoptotic Assay | 25 |
| Extraction of Total RNA of Treated and Untreated Cells for qRT-PCR..... | 26 |
| cDNA Synthesis for Quantitative Real Time PCR..... | 28 |
| cDNA Purification | 28 |

| | |
|---|-----------|
| Quantitative Real Time PCR of cDNA Isolated from Untreated and Treated Cells at | |
| Different Time Points | 29 |
| RT2 Profiler Human Apoptosis Array | 32 |
| Microarray Analysis- | 35 |
| Fluorescent Labelling of cDNA- | 37 |
| Microarray Assay- | 38 |
| Hybridization- | 39 |
| Post Hybridization- | 40 |
| Image Acquisition and Data Analysis- | 40 |
| BRB-ARRAY Tools | 43 |
| RESULTS | 44 |
| Accelerated Solvent Extraction (ASE) | 44 |
| High Performance Liquid Chromatography (HPLC) | 44 |
| Gas Chromatography-Mass Spectrometry | 46 |
| Optimization of Cell Viability Assay and Confirmation of Cytotoxicity of L19 | 46 |
| Dose-Response Assay | 49 |

| | |
|--|------------|
| Induction of Caspase 3 and 7 and Cell viability of DLD-1 Cells Treated with Different | |
| HPLC Fractions | 54 |
| Induction of Caspase 3 and 7 and Cell Viability on DLD-1 by L19 | 57 |
| Isolation of RNA | 57 |
| cDNA Synthesis for qRT PCR | 60 |
| Determination of Changes in Caspase Gene Expression Using Quantitative Real Time | |
| PCR..... | 60 |
| RT² Profiler™ PCR Human Apoptosis Array | 65 |
| Comparison of The Two qRT-PCR Results | 71 |
| Microarray cDNA Quantification..... | 76 |
| Microarray Data Normalization Analysis | 79 |
| Genes Affected by L19 | 87 |
| DISCUSSION | 123 |
| Pathway 2: Inflammatory..... | 126 |
| Non-Apoptotic Genes Affected by L19..... | 127 |
| REFERENCES | 129 |

| | |
|--------------------------|------------|
| APPENDIX I | 136 |
| APPENDIX II | 143 |
| VITA | 156 |

LIST OF FIGURES

| | |
|--|----|
| Figure 1. Intrinsic and extrinsic apoptosis pathways..... | 7 |
| Figure 2. ER stress apoptosis pathway.. | 9 |
| Figure 3. <i>Rumex crispus</i> plant sample used in this study harvested at 31.6024865° N, 94.5677874° W in April, 2014. | 12 |
| Figure 4. Human OneArray® v7 0412310923.. | 17 |
| Figure 5. Overview of materials and methods.. | 19 |
| Figure 6. RT2 Profiler Human Apoptosis PCR array (Cat no: PAHS-01Z) from SA Biosciences for analyzing 84 apoptosis and non-apoptosis (Qiagen, CA)... .. | 34 |
| Figure 7. HPLC chromatograph of leaf ASE extract.. | 45 |
| Figure 8. GC-MS chromatograph of L19 compound (A) and Tetrahydrofuran molecular mass and structure (B)..... | 47 |
| Figure 9. Cell viability of untreated DLD-1 Cells for optimizing the Aqueous One Assay..... | 48 |
| Figure 10. Cell viability for treated DLD-1 Cells treated with different HPLC fractions..... | 51 |
| Figure 11. Dose Response curve for L19. | 52 |
| Figure 12. Dose Response curve for Doxorubicin. | 53 |

| | |
|--|----|
| Figure 13. Histogram of Caspase 3/7-fold change and percentage of cell viability by induction of HPLC Fractions DLD-1 cell Line..... | 55 |
| Figure 14. Histogram of Caspase 3/7-fold change and percent cell viability in DLD-1 cells in response to different Dox concentrations.. | 56 |
| Figure 15. Caspase 3/7-fold change and percentage of cell viability by induction of L19 on DLD-1 cell Line..... | 58 |
| Figure 16. Quality Assessment of total RNA by 1% native agarose gel. | 59 |
| Figure 17. qRTPCR of CASP Gene Expression in Response to L19 Exposure. y. | 64 |
| Figure 18. qRTPCR of DLD1 Cells Exposed to L19 at 6, 8, and 12 hours Using the RT2 Profiler Human Apoptosis PCR Array (Cat no: PAHS-01Z). | 70 |
| Figure 19. Absorption spectra of Alexa Fluor® 555 labeled cDNA and Alexa Fluor® 647..... | 77 |
| Figure 20. Flip dye Histogram of distribution Alexa 555 vs Alexa 647 at different time points..... | 80 |
| Figure 21. Scatter plots of the average distribution Alexa 555 vs Alexa 647 for raw intensity and log intensity at different time points in dye-swap experiment..... | 81 |
| Figure 22. Specific intensity-dependent log (IB/A) plot (R-I plot). | 83 |

Figure 23. Diagnostic plots for two different arrays in the dye-swap experiments.

Blue scatter plots denoted Alexa 555 treated and Alexa 647 untreated and

red plots represented Alexa 647 treated and Alexa 555 untreated DLD-1

cells. 85

Figure 24. Hypothetical apoptosis pathway in treated colorectal cancer cells

(DLD-1) by L19 through the qRT-PCR, and RT2 Profiler™ PCR Array

results for 6, 8, and 12 hours. 128

LIST OF TABLES

| | |
|--|----|
| Table 1. Caspase primer sequences obtained from the National Cancer Institute (NCI) primer database. | 31 |
| Table 2. Quality and total concentration of total RNA for representative L19 treated and untreated DLD-1 cells at 6,8,12, and 24 hour exposure times.. | 62 |
| Table 3. cDNA isolated from L19 treated and untreated DLD-1 Cells at different time points of exposure for qRT-PCR..... | 63 |
| Table 4. RT ² Profiler™ PCR Human Apoptosis Array (SA Biosciences, Cat no: PAHS-012Z) fold change ($2^{-\Delta\Delta Ct}$) for 6, 8, and 12 hours. | 67 |
| Table 5. Comparison of fold changes for CASP genes over different time intervals using RT ² Profiler™ PCR Human Apoptosis Array (SA) and qRT-PCR results (reported as means \pm 1 SD). | 73 |
| Table 6. Summary of gene expression for three independent time points (Group) across genes for RT2 Profiler Human Apoptosis PCR array results. | 75 |
| Table 7. A two-factor analysis of variance for three independent time point groups (across genes) for RT2 Profiler Human Apoptosis PCR array results, that indicates F and P-value for total intensities of different time points and genes of RT2 Profiler Human Apoptosis PCR array results.. | 75 |

| | |
|---|----|
| Table 8. Yield of labeled cDNA for both Alexa Fluor 555 and Alexa Fluor 647, amount of dye incorporation and frequency of incorporation (FOI) for two samples of treated and untreated cells..... | 78 |
| Table 9. Results of an analysis of variance for three independent time points groups for microarray gene expression results..... | 86 |
| Table 10. Results of a one-way analysis of variance of three independent time points groups for Microarray gene expression results, F and P-value for total intensities of different time points for Microarray fold change results. | 86 |
| Table 11. Microarray genes affected by L19 at 6, 8, and 12 hours..... | 88 |

INTRODUCTION

Colorectal Cancer

As reported by the American Cancer Society (ACS, 2017), colorectal cancer (CRC) is the third most common type of cancer in the world. Approximately 95,520 Americans were diagnosed with colon cancer in 2017. CRC begins in either the colon or the rectum, sharing common symptoms and features. All data reported for the disease represent a combination of both cancers, collectively termed “colorectal cancer” (ACS, 2017) which are located in the ascending and transverse colon. This region of colon is referred to as the proximal or descending and sigmoid colon, or the distal colon. According to the ACS (2017), the mortality rate attributable to CRC has decreased in the last two decades because of a decrease of red meat consumption and smoking, as well as an increase in the usage of aspirin. In 2011, Zhang et al. showed that surgery followed by chemotherapy has been the most successful treatment to reduce the cancer. A recent study has shown various metabolites from plant tissue culture known as stilbenoids play a role in treating cancer (Redondo-Blanco et al., 2017). Stilbenoids are inducible phenolic compounds produced as a self-defense mechanism against biotic and abiotic stresses in peanuts, grapes, and berries. In addition to their role in plant defense, they have potential applications in human

health because of their anticancer properties (Redondo-Blanco et al., 2017). Redondo-Blanco's study illustrated the importance of stilbenoids in fruits and vegetables, using parsley as a model, to exhibit growth inhibition and cell cycle arrest in CRC (Redondo-Blanco et al., 2017). Redondo-Blanco et al. (2017) showed that the addition of resveratrol enhanced the effects of 5-fluorouracil in chemotherapy to induce apoptosis in CRC and inhibit its growth. Identifying additional anti-cancer compounds from plants is necessary for enhancing chemotherapy effects and reducing harmful side-effects. Induction of apoptosis and not inflammation or toxicity is the focus of identifying new anticancer compounds from *Rumex crispus*, and is the focus of the study herein. Previously, numerous extracts from *Rumex crispus* have been shown to contain compounds that induce apoptosis in CRC (Inkollu, 2007; Bhandari, 2015). Apoptosis is a hallmark of cancer; cells failing to commit to apoptosis is one of the key reasons for the uncontrollable cell growth that leads to cancer (Gerl & Vaux, 2004).

Apoptosis

Apoptosis, cell death pathway, exhibits morphological characteristics including cell shrinking, membrane blebbing, chromatin condensation, and nuclear DNA fragmentation (Lowe & Lin, 2000). Abnormalities in apoptotic function drive both the pathogenesis of CRC and resistance to chemotherapy drugs and radiotherapy which are both vital in killing cancer cells (Riganti et al., 2005). The

presence of several proteins in three major pathways, extrinsic, intrinsic and ER stress pathways, are key to cells undergoing apoptosis. As a result, the proteins involved in apoptosis that have been mutated or whose expression has been down-regulated resulting in cancer formation are targets for the identification of new chemotherapy agents. There are several genes that are downregulated in CRC which should promote apoptosis, such as *Bax*, *p53*, *CytC*, and *CASP9* (AVIVA System Biology, San Diego, CA). Zhang et al. (2017) found that Apaf-1-caspase 9 complex formation was associated with mitochondrial mediated TRAIL-induced apoptosis (TNF-related apoptosis-inducing ligand) in cancer stem cells. In addition, cytochrome C inhibition in CRC led to a delay in apoptosis (Jing et al., 2016). Bhardwaj et al. (2016) found DNA damage in CRC treated with 5-Hydroxy-7-methoxyflavone (HMF). Cytochrome C was released from the mitochondria and Bcl2 proteins were inhibited. Bhardwaj et al. (2016) reported a down regulation of Bcl2 protein which caused activation of *BID*, *Bax* and *CASP3*.

There are three pathways that result in apoptosis: extrinsic, intrinsic, and ER stress. Each of these pathways are activated by cell death-receptors. Common to each pathway are the executioner caspases, 3 and 7; however, upstream, the pathways utilize different initiator caspases. Caspases 8 and 10 release DISC (death inducing signal complex) in the cytosol which can activate caspase 3 and 7 (Malike et al., 2016). Caspase 3 must be cleaved by an initiator caspase 9 for activation (McIlwain et al., 2013). Zhao et al. (2017) demonstrated that caspase 3

activation was dependent on the presence of caspase 5 (inflammatory caspase) in stretch induced apoptosis. Also, caspase 1 is activated by inflammasome factors such as HIN protein (hematopoietic expression, interferon-inducible nature) and NLR (nucleoid-binding domain, Leucine-rich repeat) which participate in autoinflammatory disease, tumor suppression and tissue repair (Man & Kanneganti, 2016). In addition, Caspase 1, 4, and 5 are inflammatory caspases which can cause pyroptosis, a form of inflammation in humans to defend against bacterial, viral, or fungal infections (Man & Kanneganti, 2016). Caspase 12 (inflammatory response) could also induce apoptosis by cleaving pro-caspase 3 for activation (Zhang et al., 2016; McIlwain et al., 2013).

Extrinsic pathway

The extrinsic pathway is activated by death-receptors upon extracellular surface binding by ligands such as hormones, toxins, or growth factors (Figure 1). The death-receptors have 2 domains, one of which is an extracellular cysteine rich domain for ligand binding while the other is intracellular for transmitting apoptosis signals for the recruitment of effector caspases 8 and 10. DISC is formed upon binding a pre-apoptosis ligand, tumor necrosis factor (TNF). TNF plays an essential role in the extrinsic pathway and can be either on the cell surface bound to its receptor or released into the extracellular space. Pro-caspase 8 or 10 binds to DISC which then in turn activates caspase 8/10 resulting in cleaving procaspase

3, 6 and/or 7 with subsequent activation of caspase 3, 6 and/or 7. The extrinsic pathway has two different sub-pathways. The first pathway does not involve the mitochondria and occurs when pro-caspase 8 or 10 is produced and binds to DISC in the cells as described above. Conversely, the second pathway occurs when caspase 8 is not present (Figure 1) and instead, crosses over to play a role in the intrinsic pathway activating Bid through proteolysis (Favaloro et al., 2012).

Intrinsic pathway

The intrinsic pathway occurs intracellularly and causes the activation of caspase 3 and 7 via caspase 9. The intrinsic pathway is managed by Bcl-2 proteins and the mitochondria and is initiated by a response to stress signals such as heat and/or viral infection. Some factors, like growth factors, can cause activation of this pathway. For example, Patra et al. (2016) confirmed, that the high expression of *Bax* and cytosolic cytochrome C plus suppression of apoptosis by inhibiting caspase 9, prevented apoptosis indicating that the intrinsic pathway was the mechanism of apoptosis in liver cells treated with *Parkia javanica* HPLC extract. Patra et al. (2016) reported an up-regulation of *p53*, *p21*, *Bax/Bcl2*, *CytC* and *CASP9*, all part of the intrinsic pathway of apoptosis. Mitochondrial apogenic proteins are then expressed such as cytochrome C, apoptosis inducing factor and RNA/DNA endonuclease. Cytochrome C is released from the mitochondria along with *Apaf-1* and procaspase-9 to create the apoptosome complex. The

apoptosome complex cleaves procaspase-9 to the activated caspase 9 which in turn activates caspase 3, 6 and 7 after cleaving procaspases 3, 6 and 7 (Figure 1).

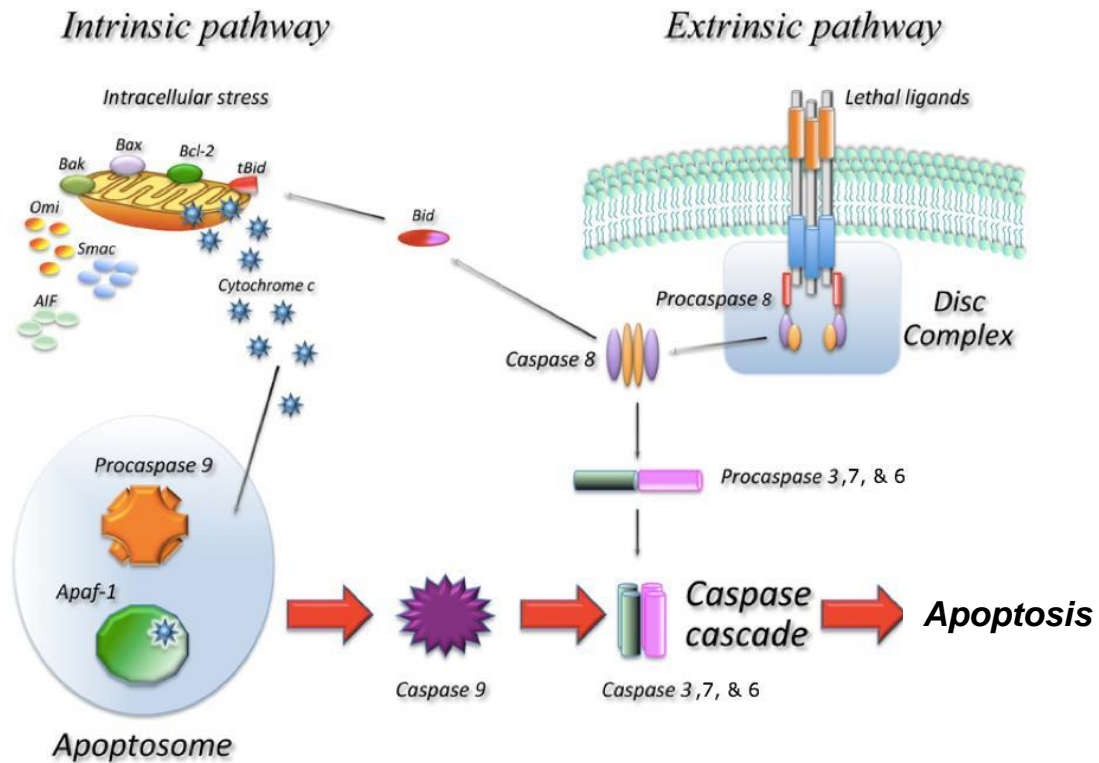


Figure 1. Intrinsic and Extrinsic Apoptosis Pathways. The intrinsic pathway is activated by many different forms of cellular stresses. Activation is controlled by BH3 (a member of the Bcl-2 family) causing the release of CytC from the mitochondria which in turn activates caspase 9. The extrinsic pathway, which is the essential effector mechanism in the immune system, is activated by death receptors at the cell surface. When ligand binds to the cell membrane it forms a DISC complex that results in the activation of caspase 8. Caspase 8 and 9 activate caspases 3, 6, and 7 to initiate apoptosis (Favaloro et al., 2012).

ER stress pathways

Bhardwaj et al. (2016) and Czabotar et al. (2014) demonstrated that endoplasmic reticulum (ER) stress plays an important role in apoptosis. Accumulation of unfolded proteins in the ER can cause stress to the ER resulting in the cellular machinery for transcription and translation to express the necessary factors for cell death, such as the Bcl-2-interacting domain (BID) and Bax proteins (Bhardwaj et al., 2016). The cell normally attempts to maintain homeostasis by removing unfolded proteins. However, cells can fail to properly remove unfolded proteins resulting in large amounts accumulating in the ER. ER stress will also result in the up-regulation of the Bcl-2-interacting killer (BIK) and BID which determines the commitment of cells to apoptosis. Terminal activation of caspase 3 and apoptosis is managed by the ER membrane-resident caspase 4 and 8 for ER stress induced apoptosis (Figure 2). Caspase 4 may directly activate caspase 3 during ER stress induced apoptosis (Czabotar et al., 2014).

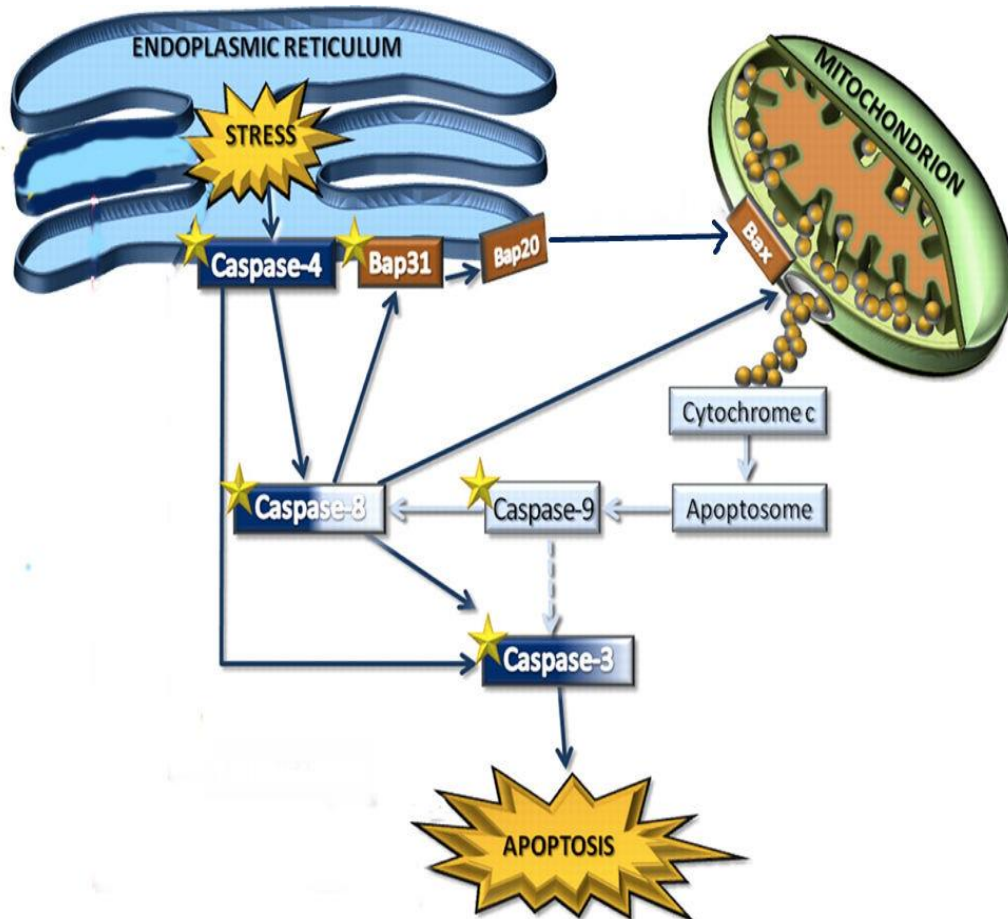


Figure 2. ER stress Apoptosis Pathway. ER stress is activated by ER membrane-resident caspase 4, then caspase 4 activates caspase 8 by breaking pro-caspase 8 and then caspase 8 cleaves pro-caspase 3 and induce caspase 3. Caspase 8 also binds to the ER and mitochondrial membranes to cleave ER proteins Bap31 producing Bap20. Cytochrome C is then released from the mitochondria. Cytochrome C activates caspase 9 then 8, followed by activation of caspase 3 (Rosati et al., 2010).

DLD-1 Cell Line

The cell line used in this study, DLD-1 which was originally isolated and established by Dexter et al. (1979), was purchased from the American Type Culture Collection (ATCC CCL-221TM). DLD-1 cells are commonly used in colorectal cancer research, originally removed during surgery from a patient who did not use tumor suppression medication (Tibbettes et al., 1977). DLD-1 cells contain a mutation in the p53 gene and overexpression of Cluster of Differentiation 47 (CD47), which is also known as integrin associated protein (IAP; Rodrigues et al., 1990). DLD-1 cells are characterized by mutations in *C-MYC*, *K-RAS*, *H-RAS*, *N-RAS*, *MYB*, *SIS*, and *FOS* which are pro-oncogenes and are part of the family of retroviral-associated DNA sequences (Ahmed et al., 2013). *C-MYC* and *FOS* code for a gene involved in cellular response to growth factors and nucleic acid metabolism. Overexpression of *MYB* and *SIS* which are coded transcriptional regulators cause tumors in humans. *RAS* (retroviral-associated DNA sequence) sequences correlated with *Kristen-RAS*, *Harvey-RAS* and *Neuroblastoma-RAS* have the same intron and exon and code for *p21* protein.

Rumex crispus

Rumex crispus, in Family Polygonaceae, is a wild herbaceous plant commonly called yellow dock or French Sorrel (Figure 3). *Rumex crispus* is found

in temperate climates and vegetates in acidic soil (Shiwani et al., 2012). This plant is native to Europe and Africa and has spread globally. Its root has been shown to consist of anthraquinones and glycosides with a variety of tannins and oxalates that are poisonous (Wynn, 2007). In a review by Wynn (2007), the leaves were utilized as a component of an herbal cancer remedy, Essiac tea in 1930, but its medical use was not supported by most medical professionals. Studies elucidated that mixtures of this herb killed prostate cancer cells *in vitro* (Wynn, 2007). Other researchers found *R. crispus* to have anti-cancer and anti-inflammatory effects in animal models (Tokarnia et al., 2002). Specific water-soluble extracts of *R. crispus* leaf extract have demonstrated increased apoptosis in DLD-1 cells in particular L19, a HPLC fraction of the water-soluble extract and the focus of this study (Bhandari, 2015).



Figure 3. *Rumex crispus* plant sample used in this study harvested at 31.6024865° N, 94.5677874° W in April, 2014.

Doxorubicin

Doxorubicin (Dox) was used as a positive control in this study. Therefore, the effect of Dox on cell viability for inducing apoptosis was compared with the effect of L19 on the cells. Dox is a chemotherapy drug that is an anthracycline, shown to slow or stop the proliferation of cancer cells by blocking topoisomerase II (Stewart & Wild, 2017). Dox has been shown to inhibit DNA polymerase activities and to suppress the Signal Transducer and Activator of Transcription 3 (STAT 3) signaling pathway (Jang et al., 2013). Dox also has been shown to elicit the expression of *p53* and *Bax* as well as expression of *CASP9* and 3 in carcinoma cancer cells (A549; Sørensen et al., 2016). Dox has shown activation of caspases and disruption of the mitochondrial membrane (Eom et al., 2005) suggesting the intrinsic pathway is induced. Jang et al. (2013) demonstrated swelling and apoptotic shrinkage in human myeloma cells treated with Dox. In addition, Dox has been shown to induce apoptosis in DLD-1 cells (Sonavane, 2012; Kandaveeti, 2015).

Different concentrations of Dox show different effects depending on the cell type. A low dose (50 ng/mL) of Dox in human hepatocarcinoma cells (Huh-7) in culture showed down-regulation of mitotic proteins such as *CENP-A/Mad 2* (Centromere protein-A/Mitotic arrest deficient 2 gene), *BudR1* (mitotic checkpoint kinase gene) and *ChK1* (Checkpoint kinase 1 gene). A high dose of Dox at

10µg/mL, however, shows activation of *NF-κβ*, *p53*, *c-Jun*, and *CASPs*. Thus, both low and high doses of Dox demonstrate apoptosis in the Huh-7 cell line by releasing *cytochrome C* from the mitochondria to the cytosol (Eom et al., 2005).

Determination of Levels of Gene Expression by Quantitative Real Time PCR.

Quantitative Real Time PCR (qRT-PCR) allows for the quantification of gene expression by measuring the amount of double strand DNA products after each amplification cycle of the cDNA template. The detection is based on the increase in fluorescence attributable to either SYBR green present in the reaction mix or fluorescently labeled primer pairs. The SYBR green detection was utilized in this study. SYBR green binds nonspecifically to double stranded DNA producing a fluorescent signal. The more amplicon produced, the higher the relative fluorescence signal (RFU). qRT-PCR can be used to calculate the level of gene expression with high detection sensitivity, specificity, reproducibility and precision (Kralik & Ricchi, 2017). The housekeeping genes such as glyceraldehyde-3-phosphate dehydrogenase (GAPDH) and/or β-actin were used to normalize the gene expression of the genes being analyzed. The work presented here in, utilizes qRT-PCR with the following 1) primer pairs complimentary to *CASP1*, 3, 4, 5, 6, 7, 8, 9, 10 and 12; and 2) gene specific primers for 84 apoptotic related genes in the commercially available RT² Profiler Human Apoptosis array (SA Biosciences, Qiagen Corp., CA). Already knowing that L19 induces apoptosis (Bhandari, 2015),

qRT-PCR was used to determine which apoptosis pathways were induced within the DLD-1 cells after 0, 6, 8, 12, 16 and 24 hrs exposure to L19 and compared to gene expression in untreated cells. The $2^{-\Delta\Delta Ct}$ was determined for apoptosis specific gene expression over time of exposure of DLD-1 cells to L19.

Use of Microarrays to Analyze Gene Expression in DLD-1 Cells.

Microarrays were utilized for monitoring gene expression and gene pattern profiling. Microarrays are plastic or glass slides which contain a grid on the surface. Each grid depends on the research purpose and can have thousands of synthetic short single strand DNA sequences spotted within. The spots of oligonucleotides of known sequence complimentary to the target cDNA along with spot controls are located in discreet rows and columns for identification.

Microarray assays are used for examining gene expression and determining which genes are being expressed or suppressed in different cells or tissues such as cancer cells. The information obtained from microarray analysis has been used to prescribe the best chemotherapy drugs for different cancers (Potaman & Sinden, 2000). Huang et al. (2016) examined levels of gene expression in different CASP genes such as, *CASP 8, 3, 4, 6, 7* and confirmed *Fas* and mitochondria-mediated pathways were active through the analysis of microarray results for HL-60 cells treated by 18 α -glycyrrhetic acid (18 α -GA)

In this study, whole human genome microarrays were used to detect the

effects of L19 on the mRNA expression of genes representing major cellular pathways in the DLD-1 cells. The Human OneArray® v7 (OneArray Corp. CA) was utilized to compare the gene expression of 29,000 human genes in the treated cells as compared to the untreated DLD-1 cells. This data suggests a mechanism of action of L19 in the DLD-1 cells as well as to confirm specific apoptosis pathways in DLD-1 cells. A reciprocal labelling method called dye-swap method was used with two dyes and two arrays for each sampling to account for dye bias and to serve as replicates within the microarray experiment. Oligonucleotides representing 29,000 human transcriptomes were spotted in a 50 ×16 mm area on a 25.1 x 72 mm flat glass slide (Figure 4). Spot layout per block was 112 columns x 350 rows with X, 142.8 µm Horizontal and Y, 142.8 µm Vertical spot pitch and 80 ± 10 µm diameters. Each Human OneArray® v7 was barcoded by the manufacturer for tracking and identification.

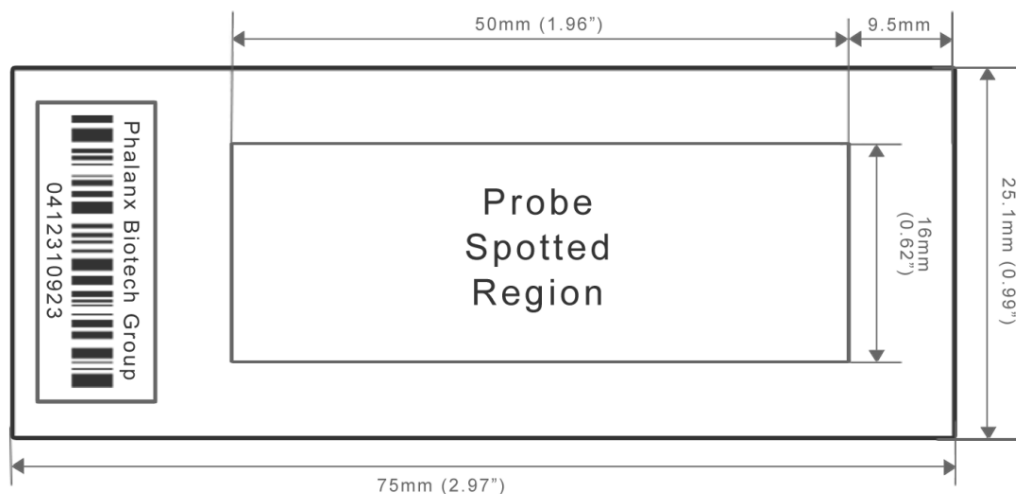


Figure 4. Human OneArray® v7 0412310923. Oligonucleotides of human transcriptomes spotted on a 50 ×16 mm area on a 25.1 x 72 mm flat glass slide. The grid was composed of one block of 112 columns by 350 rows.

OBJECTIVES

Objective 1. Extract a large amount of L19 using ASE and HPLC. L19 was isolated utilizing the methods established by Bhandari (2015).

Objective 2. Obtain four independent fractions from the L19 isolates.

Objective 3. Identification of the apoptosis pathways in DLD-1 cells induced by L19. qRT-PCR was used with the caspase gene specific primers for *CASP8*, 6 and 10 to recognize the extrinsic pathway; Caspase 9 for the intrinsic pathway; and caspase 4, 5 and 12 for ER stress pathway (Nakagawa et al., 2000). Additionally, gene expression of caspase 1, 3, and 7 were determined. The cDNAs of treated and untreated cells after 0, 6, 8, 12 and 24 hr. exposure to L19 were used as template.

Objective 4. The fourth goal of this research was to use Microarray analysis of the entire human transcriptome to determine if the genes of other key cellular pathways were affected by L19. As in Objective 3, cDNA of treated and untreated cells was used as a template, however, the cDNA in the microarray experiments were fluorescently labeled for dye swap experiments.

MATERIALS AND METHODS

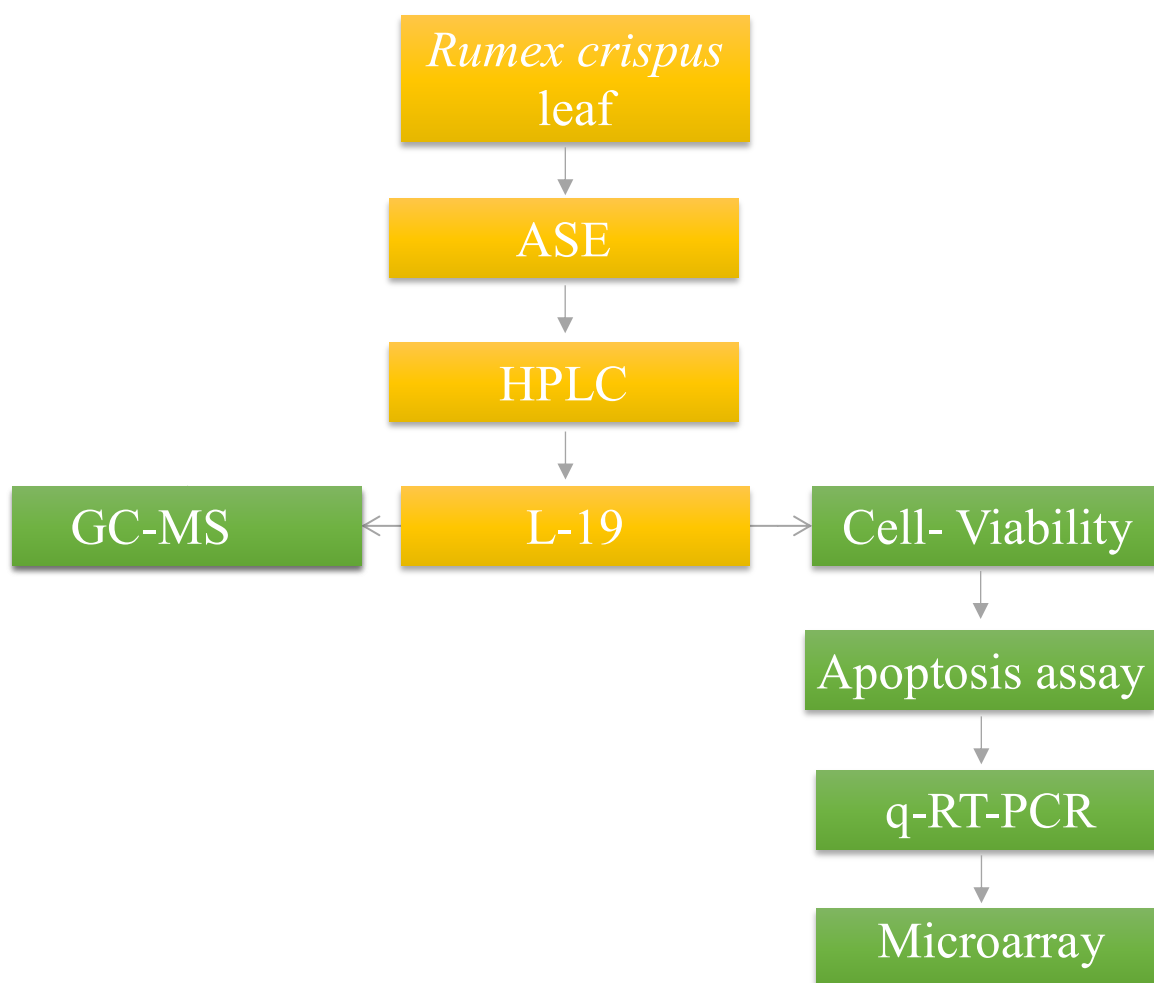


Figure 5. Overview of materials and methods. *Rumex crispus* leaves were extracted by Accelerated Solvent Extraction and analyzed by High Performance Liquid Chromatography. The compound L19 was identified by Gas Chromatography-Mass Spectrometry. The percentage of cell viability of DLD-1 cells remaining after treatment with L19 was calculated. Apoptosis assays were used to detect the level of caspase 3/7 present. Then qRT-PCR and Microarray technique were used to identify the apoptosis pathways in colorectal cancer cells.

Media Preparation

Roswell Park Memorial Institute (RPMI) Media 1640 (Gibco Thermo Fisher Scientific, Waltham, MA, USA) consisting of 300 mg/L of L-Glutamine supplemented with 10% (v/v) Fetal Bovine Serum (FBS) (Atlanta Biologicals, Norcross, GA, USA) was used as cell culture medium. Penicillin and streptomycin antibiotics were added to a final 100 U/ML and 0.1 mg/mL, respectively. This media was referred to as RPMI-plus.

Cell culture

DLD-1 human colorectal cells (ATCC CCL-221TM) were originally purchased from the American Type Culture Collection (ATCC, Manassas, VA) and stored in liquid nitrogen. Cells were thawed at 37°C using a water bath and plated into 10 cm² polystyrene tissue culture dishes consisting of 20 mL of RPMI-plus. Cells were incubated at 37°C in a humidified 6% CO₂ incubator. The media was changed every 2 to 3 days until cell growth reached approximately 85% confluent at which time the cells were subcultured and split 1 into 3 plates to proliferate cells

for storage and for the assays described below. Sub-culturing consisted of trypsinizing the cells with 0.25% (1x) Trypsin solution (JR Scientific Inc., Woodland, CA) using standard cell culture techniques (Bhandari, 2015).

Synchronization of Cells Prior to Dox or L19 Exposure

Cells were cultured with RPMI-plus medium and incubated at 37°C in a humidified 6% CO₂ incubator for approximately 6 hours until they attached to the polystyrene tissue culture dishes. Then, media was discarded and replaced with RPMI-plus without FBS and placed in the incubator for 24 hours. After this period, cell recovery was achieved by replacing old medium with RPMI-plus containing the FBS and incubated for 12 hours. Cells were then ready for being treated by either L19 or Dox.

Acquiring Leaf Extract by Accelerated Solvent Extraction

Rumex crispus, harvested by Bhandari in 2014 and stored in a -80°C freezer, was used as the sample source for these studies. Three grams of leaf powder obtained from liquid nitrogen pulverizing were weighed, mixed with sand at a 1:2 ratio and loaded into an 11-mL stainless steel extraction vessel according to the instruction manual for the Dionex Model ASE200 (Dionex Corp., Sunnyvale, CA, USA) Accelerated Solvent Extraction system (ASE). The extractions were performed at 85°C oven heat at 1500psi for 5min for three 11 mL cycles with a

final pooled elution volume of 35 mL. Deionized water and compressed nitrogen were used as solvent and to pressurize the system respectively. The extract was transferred to 50 mL polypropylene conical tubes and lyophilized using a Labconco Lymph-Lock 6 Lyophilizer Freeze Dryer (Labconco Corp., Woburn, MA).

Separation of Compound L19 by High Performance Liquid Chromatography

Twenty-five milligrams of lyophilized ASE extract were measured and suspended in 1 mL of 95% acidified water (pH 2.2) plus 5% acetonitrile (ACN). This extract was filtered through a 0.2-micron filter and transferred to a 1 mL HPLC sample vial. Acidified deionized H₂O at pH 2.2 with HPLC grade phosphoric acid and HPLC grade acetonitrile (ACN) were utilized as solvent A and B, respectively. A sample volume of 100 µL was injected onto a Zorbax® Eclipse Plus 18, 3.5 µm, 4.6 ×100 mm column (reverse phase C18) with an AlphaBond C18 10-micron Supelco® guard column attached (Sigma-Aldrich, St. Louis, MO, USA). Peak fractions were separated using a Waters 2695 HPLC Separation Module and detected at 210 nm using a Waters 2487 Lambda Dual Absorption detector (Agilent Corp., Santa Clara, CA). The eluate was collected at 1 mL/min in 1 mL aliquots at room temperature, labeled and stored in the dark at -20°C. All fractions were collected with fraction 19 being utilized for downstream experiments. Other fractions were lyophilized and stored at -80°C for future experiments. HPLC was continually repeated to accumulate enough L19 for downstream experiments.

Gas Chromatography-Mass Spectrometry

Gas chromatography-mass spectrometry (GC-MS) was used to identify the chemical composition of L19 and its purity. Four independent isolations of L19 samples were individually collected in 1.5 mL microfuge tubes, frozen in -80°C overnight then lyophilized and were sent to the Moore Analytical Lab (Houston, Texas). GC-MS was performed for each sample resulting in four replicate determinations. Acetonitrile was used as the solvent. The sample volume analyzed was 10 μ L.

Optimization of the Number of Cells per well for Cell Viability Assays

The CellTiter 96® AQueous One Solution Cell Proliferation Assay (Promega Corp., Madison, WI, USA) was used to determine the number of viable cells during maintenance of the cells and in parallel to dose response assays. This method uses 3-(4,5-dimethylthiazol-2-yl)-5-(3-carboxymethoxyphenyl)-2-(4-sulfophenyl)-2H-tetrazolium and Phenazine Methosulfate (PMS) as substrate in cells with intact mitochondria and electron transport chains (Promega Corp., Madison, WI, USA). The MTS is oxidized to a Formazan product detected at 490 nm. As per the instructions, 20 μ L of AQueous One Solution was added to cells containing 100 μ L of RPMI-plus in each well of a 96 well assay plate. The cells were incubated at 37°C, 6% CO₂ for 1-4 hours. Each hour, the absorbance in the

wells was measured at 490 nm. Assays were optimized by varying the number of cells per well (10^3 , 10^4 , 2×10^4 , 10^5 cells/well) and the time of incubation of cells in the substrate. The number of cells and time of incubation that resulted in the absorbance being less than 1 were chosen for optimal results. Because the Aqueous One assay detected only the live cells, standard trypan blue staining (GMP-Compliant Corp, Grand Island, NY) was also used to detect the number of living and dead cells during routine subculturing of cells. Viable cells are impermeable to the dye whereas dead cells are permeable and take up the dye (Promega Corp., Madison, WI, USA). Trypan blue staining provided the ratio of live to dead cells which was needed for normalization of the viability assays and the apoptosis assays.

Measuring Dose-Response for L19 and Dox using Cell Viability

For every experiment where cells were treated with varying concentrations of L19 or Dox, cell viability of treated as compared to untreated cells were determined in order to generate a dose response curve. Cells were seeded into 96-well tissue culture plates at the density of 1×10^4 cells/well in triplicate with 200 μ L of RPMI-plus media and incubated for 20 hrs at 37°C, 6% CO₂ to attach to the well surface. The medium was removed followed by addition of 200 μ L of RPMI-plus containing 10-fold dilutions ranging from 10^0 to 10^7 of either Dox at an initial concentration of 26.8 mM or L19 at 27.73 μ M followed by incubation at 37°C,

6% CO₂ for 24 hours. The negative control for the dose response assays was RPMI-plus only and the positive control was Dox. After 24 hours, the medium was removed and 10 µL of Aqueous One solution reagent and 100 µL of RPMI plus media was added to each well and incubated at 37°C, 6% CO₂ for 4 hrs. The absorbance was measured at 490 nm in order to calculate the percent viability of the treated cells relative to the untreated cells using the following formula:

$$\text{Percent of cell viability (\%)} = \frac{\text{Absorbance of treated cells (A}_t\text{)}}{\text{Absorbance of untreated cells (A}_{ut}\text{)}} \times 100 \quad (1)$$

A_t was the absorbance at 490 nm obtained from the treated cells. A_{ut} was the absorbance at 490 nm for the untreated cells.

Determination of Apoptosis Induction by Apoptotic Assay

The Apo-ONE™ Homogeneous Caspase-3/7 Assay (Promega Corp., Madison, WI, USA) was used to detect the level of caspase 3/7 induction in response to L19 and DOX (positive control). Based on the cell viability assay results, the cell culture plate was seeded with 1x10⁴ DLD-1 cells/100 µL/well and was incubated in 6% CO₂ at 37°C overnight. The media was then removed. The positive control contained 100 µL of 50 µM DOX (Sigma-Aldrich, St. Louis, MO, USA) in RPMI-plus while the negative control was the untreated cells. The unknown was the L19 at varying concentrations starting at 27.73 and 30.5 µM. The plate was incubated in 6% CO₂ at 37°C for 24 hours. The media from all wells was

removed and replaced with 25 μ L of fresh RPMI-plus media. A working solution of Apo-ONE homogenous caspase-3/7 reagent (Promega Corp., Madison, WI, USA) was prepared by mixing the caspase-3/7 substrate, Z-DEVD-rhodamine 110 conjugate and a lysis buffer provided according to the manufacturer's technical bulletin #TB323 (Promega Corp., Madison, WI, USA). In each well, 25 μ L of the working solution was added, mixed and incubated in the dark for one hour at room temperature as described previously by Bhandari (2015). The fluorescence was measured using the Typhoon™ FLA9500 (GE Healthscience, Pittsburgh, PA) with excitation at 499 nm and emission at 521 nm. The trypan blue staining was used to provide the number of live to dead cells remaining after exposure with either L19 or DOX and for normalization of Apo-ONE assays and large scale L19 or Dox treatment.

Extraction of Total RNA of Treated and Untreated Cells for qRT-PCR

The total RNA was extracted from three 10 cm² plates of 10⁶ DLD-1 cells for each time point using the TRizol® Plus RNA purification kit (Ambion™ Corp., Austin, TX). After treating the cells with L19, the total 10mL of media on the cells in the 10 cm² plates was collected into 15 mL conical tubes to collect any dead cells and/or floaters. The cells were removed from the plate surface with 0.25% (1x) trypsin solution (JR Scientific Inc., Woodland, CA, USA) and then collected in the same tube as any dead cells and centrifuged at room temperature for 5 minutes

at 256xg. The media was then removed followed by the addition of 1 mL of TRIzol™ Reagent (ThermoFisher Scientific Corp., Grand Island, NY) pre-chilled to 4°C. The lysate was either stored at -80°C or incubated at room temperature for 5 minutes after mixing well. For every 1 mL of TRIzol, 200 µL of chloroform was added and incubated at room temperature for 2-3 minutes. Samples were then centrifuged for 15 minutes at 12,000xg at 4°C. The RNA contained in the upper layer solution was transferred to a new 1.7 mL microcentrifuge tube to which an equal volume of 70% ethanol was added and mixed well. The solution was added in 700 µl increments to a spin cartridge provided in the Invitrogen PureLink RNA Mini Kit and processed according to the manufacturer's instructions (Ambion™, Corp, Austin, TX). After incubating with 50µL of RNAase free water for 1-2 minutes, the RNA was eluted by centrifuging at 12000xg for 2 minutes. The RNA was stored at -80°C. A native 1% w/v agarose gel in TAE buffer (40 mM Tris-acetate, 1 mM EDTA) was used to check the quality of the RNA followed by quantification of the RNA using a Varian Carry 50 spectrophotometer (Agilent Corp., Santa Clara, CA). RNA concentrations were determined using the following formula:

$$\text{RNA concentration (}\mu\text{g/mL)} = \text{Abs}_{260} \times \text{pathlength} \times \text{Dilution Factor} \times 40 \mu\text{g/mL} \quad (2)$$

(Promega Corp., Madison, WI, USA)

cDNA Synthesis for Quantitative Real Time PCR

GoScript™ reverse transcriptase (Promega Corp., Madison, WI) was used to synthesize complementary DNA (cDNA) for quantitative Real time PCR (qRT-PCR). According to the manufacturer's instructions, GoScript reverse transcriptase can convert up to 5 µg of total of RNA to first strand cDNA. Approximately 5 µg of total RNA was converted to cDNA in each process. A BioRad Mycycler thermocycler was used for all incubations. To synthesize the cDNA, the reverse transcriptase reaction was incubated at 42°C for 3 hours instead of one hour as suggested by the manufacturer. The RNA was then hydrolyzed by adding 15 µL of 1N NaOH and incubated at 70°C for 10 minutes. The reaction was neutralized by adding 15 µL of 1N HCL with subsequent purification.

cDNA Purification

The cDNA was purified using the Wizard® SV Gel and PCR Clean Up System (Promega Corp., Madison, WI). Equal volumes of membrane binding solution were added to the cDNA mixture and mixed. The mixture was transferred to a spin cartridge, incubated for 1 minute at room temperature, and then centrifuged at 16000 rpm for 1 minute. The spin cartridge was transferred to the recovery tube, then 50 µL of nuclease free water was added and incubated for 5

minutes at room temperature. The recovery tubes were centrifuged at 16000xg for 2 minutes. The eluate was stored at -80°C. The cDNA was quantified using the Varian Carry 50 spectrophotometer (Agilent Corp., Santa Clara, CA). The cDNA concentration was calculated using the following formula:

$$\text{cDNA concentration } (\mu\text{g/mL}) = A_{260} \times \text{pathlength} \times \text{dilution factor} \times 37 \mu\text{g/mL} \quad (3)$$

(Promega Corp., Madison, WI, USA)

Quantitative Real Time PCR of cDNA Isolated from Untreated and Treated Cells at Different Time Points

The cDNA was used as a template in qRT PCR to determine the fold change in gene expression of *CASP1*, 3, 4, 5, 6, 7, 8, 9, 10 and 12. Glyceraldehyde-3-Phosphate Dehydrogenase (*GAPDH*), a housekeeping gene which shows no changes in gene expression after DOX treatment, was used for normalization of the qReal-Time PCR data. The respective caspase gene specific forward and reverse primers, listed in Table 1, were added to a final concentration of 0.5 μM and 10 μL of 2X SYBR® Green Master Mix which contained the Taq and the dNTPs (Promega Corp., Madison, WI). cDNA (20 ng) and nuclease free water were added to obtain 20 μL final volume per well. The RT PCR conditions, determined previously by Kondaveeti (2015), were: An initial denaturation at 95°C for 10 min followed by 40 cycles of denaturation temperature at 95°C for 30 sec, annealing temperature at 60°C for 60 sec and an extension temperature at 72°C for 30 sec. Detection of amplicons was programmed after each annealing step. A melting

curve from 65°C to 95°C was programmed to occur for each well after the completion of the PCR to ensure that only one size amplicon was produced by each primer pair and therefore, specific binding of primers to the template.

The qRT-PCR resulted in Ct (Cycle threshold) values for each gene expressed in proportion to the copy number for the respective cDNA. Both untreated and treated cDNAs were used as templates. The $\Delta\Delta\text{Ct}$ values for each cDNA were determined using the following formulas for cDNA_X (X is the respective gene):

$$\text{Ct Untreated} - \text{Ct GAPDH Untreated} = \Delta\text{Ct Untreated} \quad (4)$$

$$\text{Ct Treated} - \text{Ct GAPDH Treated} = \Delta\text{Ct Treated} \quad (5)$$

$$\Delta\text{Ct Treated} - \Delta\text{Ct Untreated} = \Delta\Delta\text{Ct of cDNA}_X \quad (6)$$

The $2^{-\Delta\Delta\text{Ct}}$ of each caspase cDNA represented the fold change in gene expression (Schmittgen & Livak, 2008) and in this case, which caspases were up-regulated or down-regulated in response to L19.

Table 1. Caspase primer sequences obtained from the National Cancer Institute (NCI) primer database. The respective forward and reverse primer pairs were used in the qRT-PCR. Primers were designed to give a PCR product of 200 bp +/- 10. Primers for caspase 12 were not found at the NCI primer database and therefore were designed using NCBI Primer-BLAST (Ye et al., 2012).

| Primers | Primer Sequences | Accession Numbers |
|------------------|--------------------------|--------------------------|
| CASP3(Forward) | 5'AGAACTGGACTGTGGCATTGAG | NM_032991 |
| CASP3(Reverse) | 5'GCTTGTCGGCATACTGTTTCAG | NM_032991 |
| CASP4(Forward) | 5'ATGGCAGGACAAATGCTTCT | NM_033306.2 |
| CASP4(Reverse) | 5'TGCGGTTGTTTCTCTCCTTT | NM_033306.2 |
| CASP5 (Forward) | 5'CTGGGCTACACTGTGGTTGA | NM_001136112.1 |
| CASP5 (Reverse) | 5'GCAGTTGCGGTTGTTGAATA | NM_001136112.1 |
| CASP6 (Forward) | 5'AAGAGGAGGGCAAGGTGTCT | NM_000305.2 |
| CASP6 (Reverse) | 5'GCAATTCCTCTCCTCCTGTG | NM_000305.2 |
| CASP7 (Forward) | 5'TCAGTGGATGCTAAGCCAGA | NM_001267056.1 |
| CASP7 (Reverse) | 5'GAACGCCCATACCTGTCACT | NM_001267056.1 |
| CASP8 (Forward) | 5'CGGAATGTAGTCCAGGCTCA | NM_001080125.1 |
| CASP8 (Reverse) | 5'GGTCACTTGAACCTTGGGAA | NM_001080125.1 |
| CASP9 (Forward) | 5'CACGGCAGAAGTTCACATTG | AB026979.1 |
| CASP9 (Reverse) | 5'ACACCCAGACCAGTGGACAT | AB026979.1 |
| CASP10 (Forward) | 5'GGGAGGTAAAGCTGTGGTTG | NM_032974.4 |
| CASP10 (Reverse) | 5'GCCGAGTCGTATCAAGGAGA | NM_032974.4 |
| CASP12 (Forward) | 5'CCATCCAACGGTGTTCTGGT | NM_001191016.2 |
| CASP12 (Reverse) | 5'GCCTGCAATTTGAGCTGTCT | NM_001191016.2 |
| GAPDH (Forward) | 5'GAGTCCACTGGCGTCTTCA | NM_001289746.1 |
| GAPDH (Reverse) | 5'GGGGTGCTAAGCAGTTGGT | NM_001289746.1 |

RT² Profiler Human Apoptosis Array

RT² Profiler Human Apoptosis PCR array (Cat no: PAHS-01Z) from SA Biosciences (Qiagen, CA) was used to analyze 84 apoptosis and non-apoptosis genes in untreated and L19 treated DLD-1 cells. Gene specific primer pairs were provided in the 96-tube plate to which 10 µL of 2X SYBR green master mix (Promega Corp., Madison, WI) and 20 ng cDNA template, provided buffer and nuclease free water were added to have a 20 µL final reaction volume. The cDNA for either untreated or treated samples was prepared as a master mix and distributed into the 96 tubes within the plate. The plates were sealed with a thin plastic film and centrifuged at 300xg for 5 minutes to remove any bubbles then placed into a BioRad CFX96 Real-Time PCR thermocycler with the same setup as the qRT-PCR described above.

One 96-tube plate was used for the cDNA isolated from the treated cells and another 96-well plate was used for the cDNA isolated from the untreated cells for each respective time point. This was done for normalizing the data at each of the different time points. Based on Figure 6, the plate contained 84 apo- and non-apoptosis genes and controls which are listed in Appendix I. The controls included housekeeping genes (HK), Genomic DNA Contamination (GDC), Reverse Transcription Control (RTC) and Positive PCR Controls (PPC). There were 5 different HK for normalization of the data. Of these, only those that did not change

because of the treatment over time were used in the normalization; HK should not change between treated and untreated cells. The HK genes were located in wells H1-H5 (Figure 6). GDC, located in well H6, had the purpose of detecting non-transcript genomic DNA. RTC (wells H7-H9) and PPC (wells H10-H12) measured the efficiency of the RT² Profiler array reaction and PCR, respectively (Figure 6).

For data analysis, the www.sabiosciences.com website was used. At this website, under the resource tab, the data analysis option was chosen. Then, Web-based software for Cataloged and Custom Arrays was chosen under the RT² Profiler PCR array option. Standard RT² PCR Array was selected under the Experiment Performed section and the code Cat no: PAHS-012Z was used for the Cataloged PCR Array. Ct values from RT-PCR of treated and untreated cells were both saved in one single Excel sheet in XLS format as per the template provided then uploaded into the software available at the SA Biosciences website (Qiagen Corp., CA).

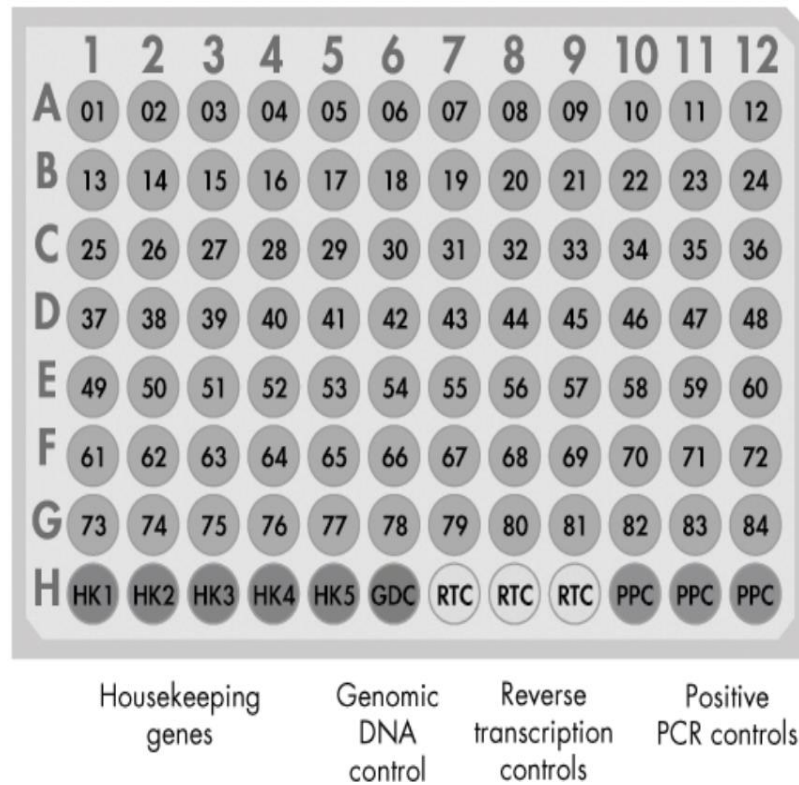


Figure 6. RT² Profiler Human Apoptosis PCR array (Cat no: PAHS-01Z) from SA Biosciences for analyzing 84 apoptosis and non-apoptosis (Qiagen, CA). Controls included Housekeeping genes (HK), Genomic DNA Contamination (GDC), Reverse Transcription Control (RTC) and Positive PCR Control (PPC). There were 5 different HK to normalize data because HK should not change between treated and untreated cells, they were located in wells H1-H5. GDC had the role of detecting non-transcript genomic DNA in well H6. RTC (wells H7-H9) and PPC (wells H10-H12) controlled the efficiency of RT² Profiler array reaction and PCR, respectively. The specific genes targeted in each well are listed in Appendix I.

Microarray Analysis-

Synthesis of Labeled cDNA for Microarray-

SuperScript™ Plus Indirect cDNA Labeling System was used to create cDNA for microarray analysis. This system was used to transcribe 5-20 µg of total RNA to first strand cDNA. Approximately 5 µg of total RNA was used for cDNA synthesis. The SuperScript™ protocol was used to prepare a 50x amino-allyl-dUTP (aa-dUTP) plus dNTP mixture in lieu of using the indirect labeling kit aa-dNTP mix as shown below (SuperScript® Indirect cDNA kit, ThermoFisher Scientific). This was done to increase the frequency of incorporation (FOI) of the amino allyl dUTP for labeling. First, the following solution was prepared:

50X Amino allyl dNTP mixture:

| <u>Stock</u> | <u>Volume</u> | <u>Final Conc. (µM)</u> |
|--------------|---------------|-------------------------|
| 100mM dATP | 10 µL | 25 µM |
| 100mM dCTP | 10 µL | 25 µM |
| 100mM dGTP | 10 µL | 25 µM |
| 100mM dTTP | 2 µL | 50 µM |
| 50mM aa-dUTP | 8 µL | 10 µM |
| | <hr/> 40µL | |

The Total RNA and primer were pre-annealed in a priming reaction as follows:

Priming Reaction:

| | | |
|--------------------------------|----------------|-------------|
| Anchored Oligo dT | 2.5 µg/µL each | 2 µL |
| Total RNA (Untreated/ Treated) | 2-5 µg | x µL |
| DEPC-treated water | | x µL |
| | | <hr/> 18 µL |

The priming reaction was well mixed and heated at 70°C for 5-8 minutes. Then, immediately chilled on ice for 1-5 minutes, centrifuged 10 seconds at 10,000 rpm and stored on ice until the RT reaction mix was ready.

The RT reaction mix was prepared as follows according to the manufacturer's instructions.

RT Reaction Mix:

| | |
|-------------------------------------|------------|
| 5X First-Strand buffer | 6 µL |
| 1 M DTT | 1.5 µL |
| dNTP mix (50X amino allyl dNTP mix) | 1.5 µL |
| RNaseOUT™ (40 U/µl) | 1 µL |
| SuperScript™ III RT (400 U/µl) | 2 µL |
| | <hr/> 12µL |

The RT Reaction Mix was gently mixed with the annealing mix and then heated at 46°C for 2-3 hours. The RT was inactivated by adding 15 µL 1N NaOH followed by neutralization with 15 µL of 1N HCl. The cDNA was purified using the Wizard® SV Gel and PCR Cleanup System (Promega Corp., Madison,

WI) as described previously for the cDNA prepared for qRT-PCR. The cDNA was quantified using the Cary50 Spectrophotometer as described before.

Fluorescent Labelling of cDNA-

Prior to labeling, 2 µg of the amino allyl cDNA from above, was divided into two different light protective 1.5 mL microfuge tubes. Each tube was then vacuum dried using a Dynavap v1000 (National Labnet Co., Inc., Woodbridge, NJ) at 45°C for one hour. One fraction (1 µg) was labeled with an amino reactive Alexa Fluor™ that emits at 550 nm (green). The other fraction (1 µg) was labeled with Alexa Fluor™ emitting at 647 nm (red) (ThermoFisher Scientific Corp., Grand Island, NY). The amino allyl labeled cDNA from both untreated and treated cells was labeled as follows: The cDNA was resuspended in 5 µL of nuclease free water and 3 µL of sodium bicarbonate buffer pH 8.5. The dyes were resuspended in 2 µL of dimethylsulfoxide. The cDNA and dyes were mixed together and then vortexed. The tubes were then incubated in the dark at room temperature for 1 hour. Hydroxylamine (4M) was added to a final concentration of 0.06 M to quench the unreacted dyes. The cDNA was neutralized by adding sodium acetate (NaOAc) pH 3.5 to a final concentration of 10mM. The labeled cDNA was purified from the unreacted dye and salts using a Wizard® SV Gel and PCR Cleanup System according to the manufacturer's protocol (Promega Corp., Madison, WI).

The amount of cDNA (ng) and dye incorporated was calculated using the following equations provided in the SuperScript® Indirect cDNA manual (ThermoFisher Scientific):

$$\text{Amount of cDNA (ng)} = A_{260} \times 37 \text{ ng/}\mu\text{L} \times \text{path length} \times \text{dilution factor} \times \text{total volume (}\mu\text{L)} \quad (7)$$

$$\text{pmole of Cy3 Alexa Fluor® 555 dye incorporated} = (A_{555} \times \text{Total Volume (}\mu\text{L)}) / 0.15 \quad (8)$$

$$\text{pmole of Cy5 Alexa Fluor® 647 dye incorporated} = (A_{647} \times \text{Total Volume (}\mu\text{L)}) / 0.25 \quad (9)$$

The above equation used an absorption coefficient of $150,000 \text{ M}^{-1}\text{cm}^{-1}$ at 555 nm for the Alexa Fluor® 555 and an absorption coefficient of $250,000 \text{ M}^{-1}\text{cm}^{-1}$ at 647 nm for Alexa Fluor® 647 (Thermo Fisher Scientific Corp., Grand Island, NY). The Frequency of Incorporation (FOI) is the number of dye labeled nucleotides in the cDNA per 1000 nucleotides of total cDNA. The FOI was calculated using the following equation:

$$\text{FOI} = (\text{pmole of dye Incorporated}) \times 324.5 \text{ g/mole/ng of cDNA} \quad (10)$$

Microarray Assay-

The microarray assay was a dye swap assay using the Human OneArray®v7 (OneArray Corp., San Diego, CA) and therefore, two arrays were prepared for hybridization for each analysis.

Hybridization-

The experimental design consisted of a dye swap where one array was hybridized with 1 µg of cDNA from untreated cells labeled with a 550 nm emitting Alexa Fluor™ (green) and 1 µg of cDNA from treated cells labeled with a Alexa Fluor™ that emits at 647 nm (red). The second array was hybridized with the Alexa Fluor™ labeled cDNAs swapped; the cDNA from the untreated cells was labeled with the 647 nm Alexa Fluor™ and the cDNA of the treated cells labeled with the 550 nm fluor. Each mixture was prepared in a 1.5 mL microfuge tube and vacuum dried in the dark, 45°C, using a Labnet DyNA Vap Centrifugal Evaporator V-1000 (Labnet International Corp., Edison, NJ).

The hybridization buffer consisting of freshly prepared 50% formamide, 5X saline sodium citrate (SSC), 0.1% SDS, and Sheared Salmon Sperm DNA (10 µg/ml) was preheated at 60°C. The labeled dry cDNA was resuspended in 200 µL of hybridization buffer and mixed well. Before hybridization, the array was preheated at 50°C for less than 15 minutes. The Human Array slide and cover slip were sealed together by the manufacturer with a plastic cover with one side open. The mixture of cDNA and hybridization buffer was loaded within the space between the cover slip and array on one end of the slide assembly. A plastic sleeve that was provided with the array kit was slipped over the opening to encase the array. The array was then placed and sealed in an array cassette (Sigma-Aldrich, St.

Louis, MO, USA). The hybridization sandwich was heated at 95°C for 5 minutes and then placed in a water bath at 50°C overnight.

Post Hybridization-

The hybridization chamber was unsealed and gently wiped dry. The array coverslip was removed with a sterile blade. The array was placed in a slide rack that was submerged into a low stringency buffer wash buffer, buffer A (2X SSC, 1% SDS) pre-warmed at 55°C. A magnetic stir bar was added to the bottom of the chamber to stir the buffer during the wash for 5 minutes. The array was then transferred to a medium stringency buffer, buffer B (0.1x SSC, 0.1% SDS) at 55°C for 5 minutes. The array was then transferred to the high stringency buffer, buffer C (0.1x SSC) at room temperature for 5 min. The slides were then rinsed with deionized water and dried with the use of a high-speed microarray centrifuge (ArrayIt Corp., Sunnyvale, CA) for 1 minute.

Image Acquisition and Data Analysis-

Scanning the Arrays- The arrays were scanned using a Typhoon FLA 9500 (GE Health Science, Pittsburgh, PA) scanner. The arrays were placed face down. The parameters for the scan consisted of a 10-micron resolution setting

with the Cy3 setting (555 nm) on channel 1 and the Cy5 setting (647 nm) on channel 2. The images were saved in a 16-bit TIF file format.

Quantification Using SpotXel- SpotXel (Sicasys Software for Life Sciences, Heidelberg, Germany) was used to align the grid obtained from the array manufacturer using the .gal file provided and the control corner spots on the array. The gal file defined the grid as 16 x 50 mm, the spot layout was 112 spots per column x 350 spots per row in one block. The horizontal and vertical spacing for each spot was 143 μm with a spot diameter of 71 μm . Spot detection was set to Flex-spot with border. The spot intensities were quantified for both the green and red channel once the grid was aligned. Background was subtracted to provide corrected spot intensities in an output .gpr file. The local method was used for background correction. The noise was processed using 50% of the spot size and 30 was selected for largest size defect.

Creation of MEV files with ExpressConverter- The .gpr file resulting from SpotXel was converted to a .mev (MultiExperiment Viewer) file using Express Converter version 2.1 (Saeed et al., 2006) for use in MIDAS version 2.22-b0 (Microarray Data Analysis System). Both MIDAS and ExpressConverter are part of the TM4 Software created by the J. Craig Venter Institute (Rockville, MD). In ExpressConverter, the gpr file from SpotXel was uploaded by choosing the custom input format followed by opening the .gpr file. The corresponding gene annotations

were uploaded by selecting the GAL option and inputting the .gal file provided by the Onearray manufacturer. The header of the data file was identified by selecting the row showing the headers in the file: "Block" "Column" "Row" "Name" "ID" "X" "Y", etc. The headings "Forward Mean" for each channel were dragged to IA and IB headers, respectively. The files were converted to .mev files upon pressing the green "C" option in the menu bar.

Dye Swap Normalization Using MIDAS- MIDAS was used to normalize the intensities within an array, as well as between the dye swap pair of arrays, to remove any bias attributable to the different dyes. Each dye swap array pair was processed in MIDAS using the following parameters:

Data file pair- Two quantified arrays in .mev format

One Bad Channel Tolerance Policy- Generous

No flag used for either channel A or B

No background checking for either channel

A Signal/Noise Threshold of 2.0

Total intensity was selected with Cy3 chosen as Reference. A Lowess fit was selected with the following parameters: block mode 0.33, smoothing parameter (default) and reference as N/A. An Iterative Log Mean Centering Normalization was selected with $\pm 3.0\sigma$ and reference as Cy3. Flip Dye Replicate

Consistency Checking was performed with SD Cut as Data Trim Option and $\pm 2.0\sigma$ for Cross Log Ratio Data Keep Range. The last selection in the pipeline was a Virtual Trim selection and Output of Trimmed data. Both text and PDF files were produced to visualize the results.

BRB-ARRAY Tools (Zhao & Simon, 2008) were used to obtain average fold changes in gene expression, p-values and gene families. A spreadsheet was generated from the IA and IB channel intensities from each dye swap replicate into columns as pairs. Each replicate dye swap was averaged to give one IA and one IB for each of the three time points analyzed. The spreadsheet consisted of the 6 hr IA and IB, 8 hr IA and IB and 12 hr IA and IB. BRB-ArrayTools was then used to obtain the log-ratio for each time point, the p-value for the significance of change over the three time points for each gene and the gene ID for the genes hybridized on the array. These genes were then matched to available BRBarray online databases to obtain the defined gene lists. Files were saved in GCT format. Based on Excel's final normalization, a 1-way analysis of variance (ANOVA) was used to compare response values between the 6, 8, and 12 hr time intervals. The gene expression results for the arrays will be uploaded into the public GEO database.

RESULTS

Accelerated Solvent Extraction (ASE)

ASE (Accelerated Solvent Extraction) was used to extract water soluble compounds from *Rumix crispus* leaves. Each tube produced 50-100 mg dry sample weight which was used for HPLC fractionation.

High Performance Liquid Chromatography (HPLC)

Figure 7 shows a typical chromatogram with all peak fractions that were separated and collected. Fraction number 19 (L19; in the red rectangle, Figure 7), from the leaf extract was collected between 19 minutes and 14 seconds to 20 minutes and 14 seconds after injection of 10 μ L of lyophilized ASE sample at a final concentration of 100 mg/mL in acidified H₂O with 5% ACN. The fractions shown were collected in 1 mL aliquots at 1 mL/min.

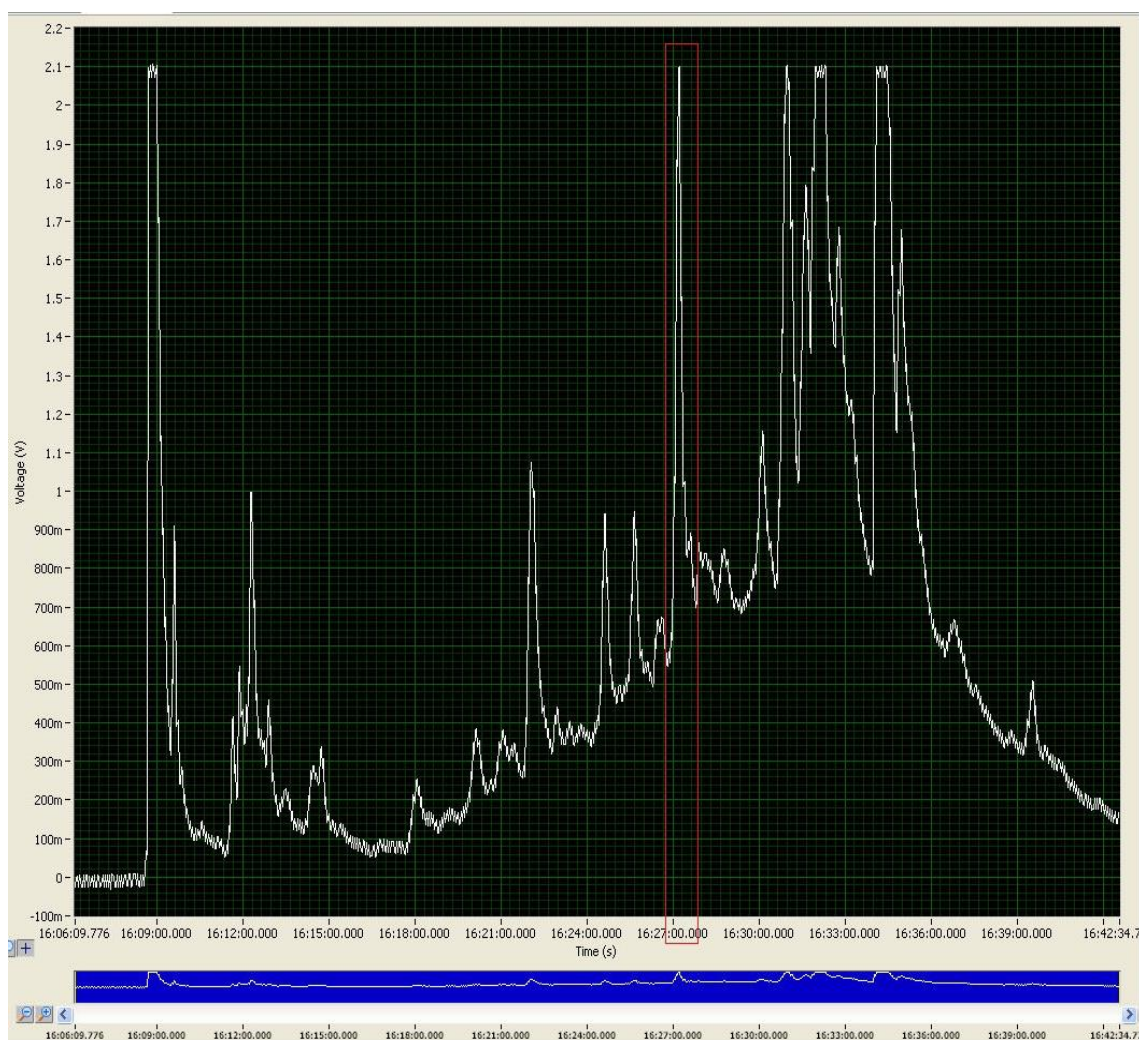


Figure 7. HPLC chromatograph of leaf ASE extract. Fifty milligrams of dry leaf extract were suspended in 0.5 mL 95% acidified water (pH 2.2) plus 5% ACN and filtered. Ten microliters of sample mix were injected onto the column. Compounds were detected at 210 nm. A Zorbax Eclipse Plus 18 column with an Alpha Bond C18 10 μ m guard column (Agilent Corp.) was used as the stationary phase. The mobile phase was a gradient of acidified water (pH 2.2) plus 5% v/v ACN to 60% ACN over 60 min. with a flow rate of 1 mL/min.

Gas Chromatography-Mass Spectrometry

Samples were outsourced to the Moore Analytical Lab (Houston, Texas). Four different samples were sent for 4 replicate analyses using mass spectrometry (MS). Acetonitrile was used as buffer with 10 μ L of sample injected. L19 was collected at 5.538-5.637 minutes and 61 seconds. L19 was found to be a Tetrahydrofuran at 94.4% purity for each isolation (Figure 8) with a molecular weight of 72.11 g/mole.

Optimization of Cell Viability Assay and Confirmation of Cytotoxicity of L19

Cell viability assays were performed to verify that the purified L19 was cytotoxic to DLD-1 cells. The number of untreated cells per well in a 96 well plate was optimized to provide linear changes in the absorbance after incubating the cells in the Aqueous One reagent. Figure 9 shows 1×10^3 , 1×10^4 , 2×10^4 , and 1×10^5 DLD-1 cells/well in a 96 well plate incubated over 4 hrs measuring the absorbance at 490 nm each hour. The optimum cell number was determined to be 1×10^4 cells/well measured after 3 hrs incubation in Aqueous One reagent; the absorbance was 0.81 ± 0.06 thus providing a high enough absorbance to observe linear changes in absorbance as cells decreased in viability in response to L19 or Dox treatment.

| Compound Label | Name | RT | Algorithm |
|------------------------|------------------------|-------|---------------------|
| Cpd 1: Tetrahydrofuran | Tetrahydrofuran | 5.582 | Find by Integration |

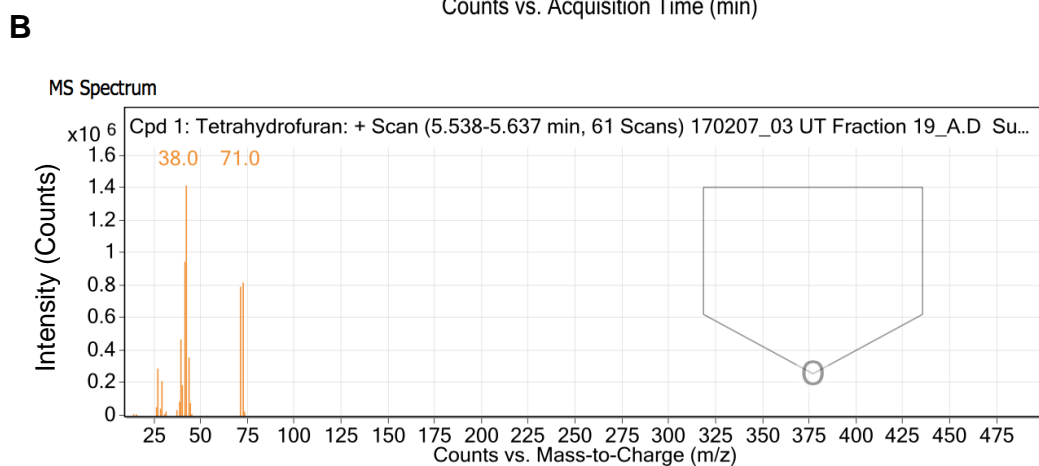
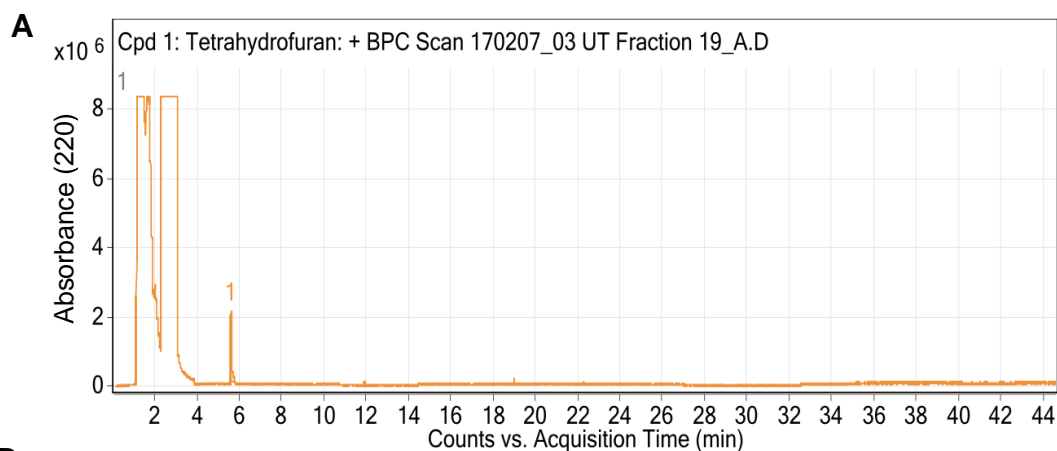


Figure 8. GC-MS chromatograph of L19 compound (A) and Tetrahydrofuran molecular mass and structure (B). Peak labeled 1 in (A) was isolated using GC followed by mass spectroscopy of peak 1 to obtain corresponding mass fragments of L19 in (B).

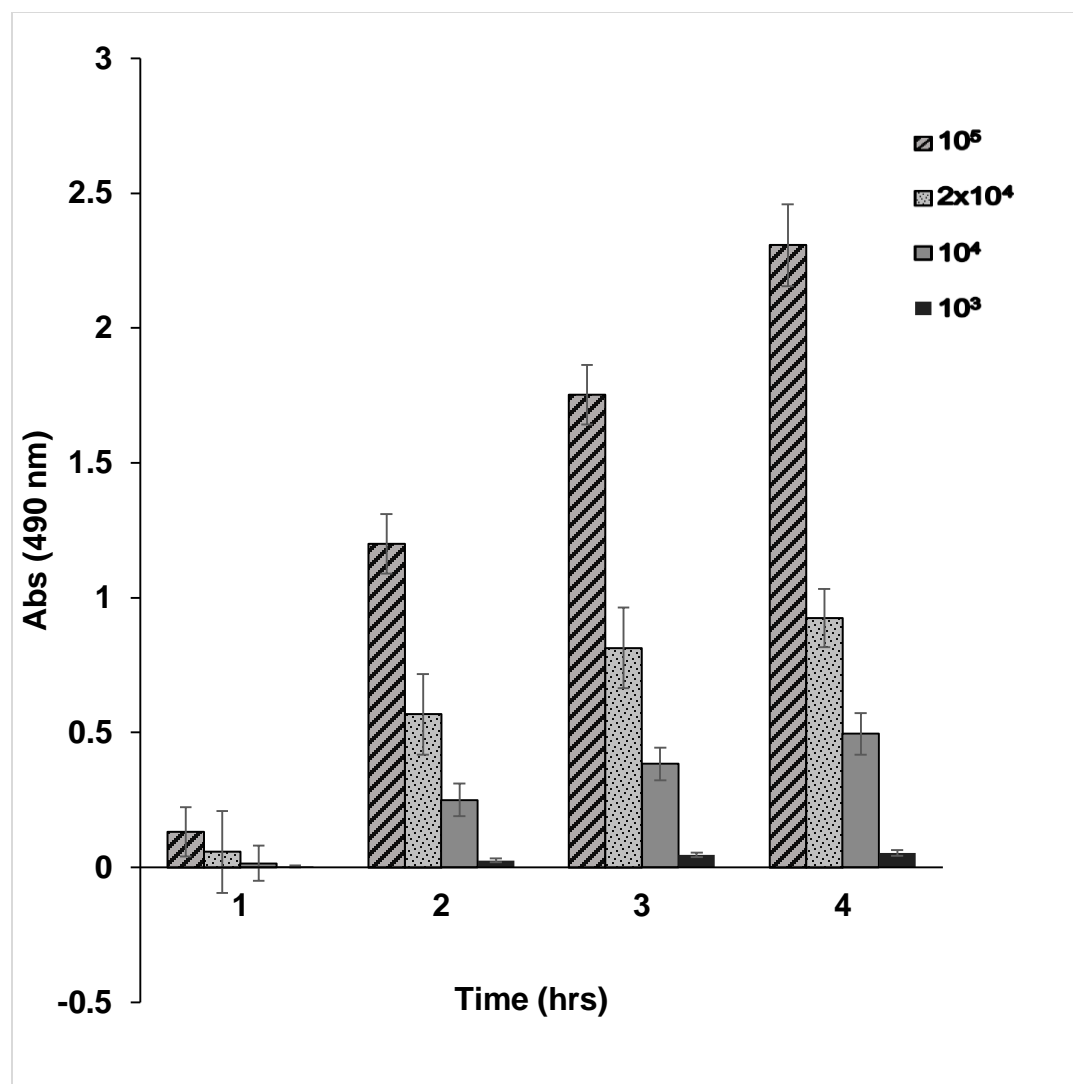


Figure 9. Cell viability of untreated DLD-1 Cells for optimizing the Aqueous One Assay. DLD-1 cells were seeded with different number of cells in wells of a 96 well plate and incubated overnight. Reagent for the Cell Titer 96® Aqueous One Reagent was added according to the manufacturer's protocol.

All of the HPLC fractions were applied to the DLD-1 cells (1×10^4 cells/well) for 0, 1, 2 and 3 hrs exposure to ensure that fraction L19 collected in this study exhibited the greatest cell toxicity as compared to the other fractions as previously seen (Bahandari, 2015). The untreated cells were used as the 100% cell viability comparison in the normalization to determine the percent viability (Figure 10). L19 was confirmed to exhibit the highest cell toxicity as compared to the other HPLC fractions that were collected in the same volume (1 mL) per fraction from 100 mg/mL of dried plant extract. The positive control for cell toxicity, Dox, showed the expected decrease in cell viability for increased concentrations of DOX consistent with previous studies (Bahandari, 2015); concentrations of the cytotoxic compounds in the HPLC fractions were not known.

Dose-Response Assay

Cells treated with a log dilution of L19 showed a sigmoidal decrease in cell viability with increasing L19 consistent with a cell death mechanism other than simple toxicity as evidenced by the dose response curve (Figure 11). Dox was used as a positive control because it has been well documented to show a sigmoidal dose response curve (Figure 12; Bhardwaj et al., 2016). The concentration of L19 varied between 27.73 and 30.5 μM for each isolation used as the zero-dilution treatment at $27.73 \pm 1.96 \mu\text{M}$. From the dose response curve, the LC_{50} for L19 was $2.73 \pm 1.96 \mu\text{M}$ on 1×10^4 DLD-1 cells. The concentration that was used to treat the cells

for the Apo-Assays, qRT-PCR, RT-Profiler and Microarray was the $2.73 \pm 1.96 \mu\text{M}$ (Figure 11). The LC_{50} of Dox was $100 \mu\text{M}$ (Figure 12).

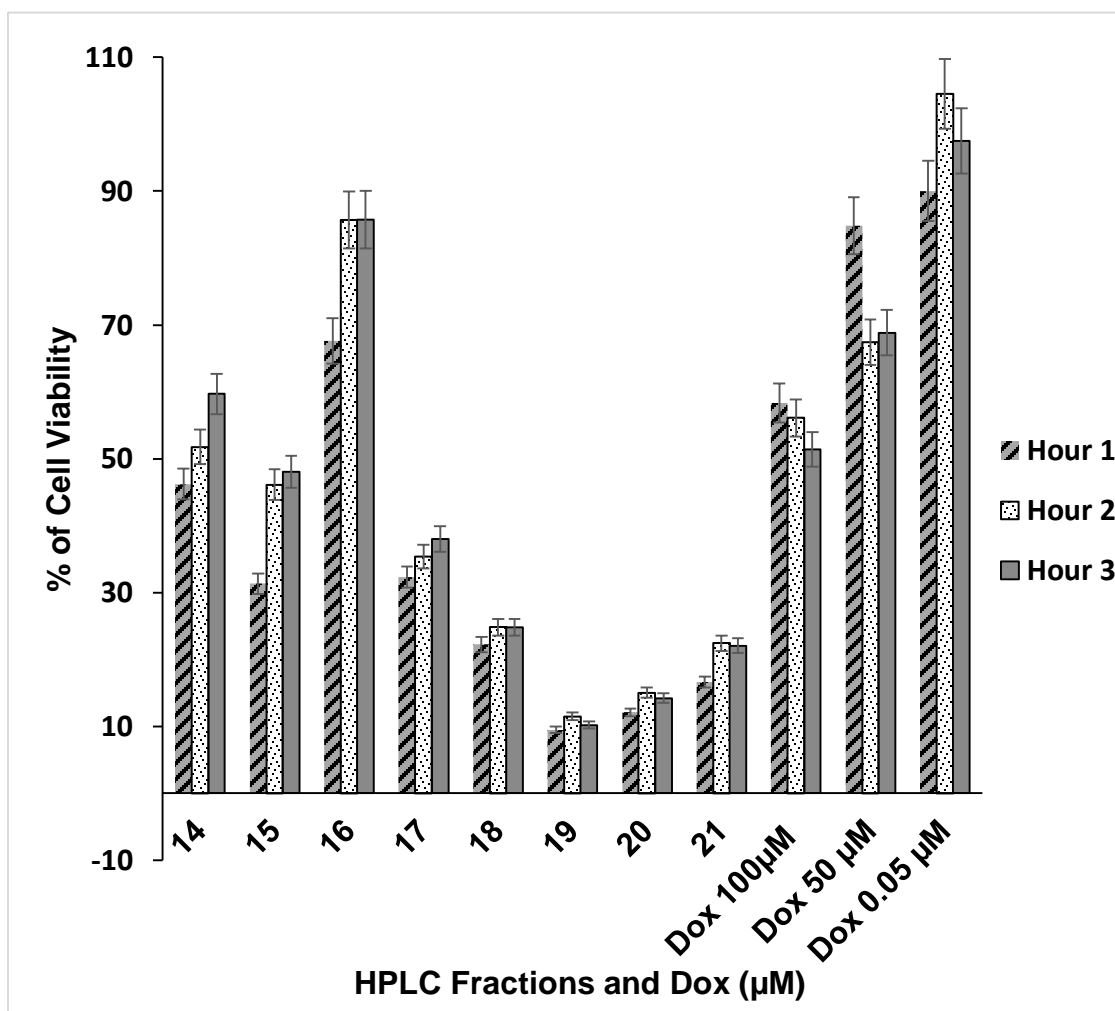


Figure 10. Cell viability for treated DLD-1 Cells treated with different HPLC fractions. HPLC Fractions, each 1mL, were lyophilized, suspended in 1 mL RPMI-plus, neutralized with 15 μ L 1N NaOH. Then, 100 μ L of neutralized suspended fraction transferred to 1×10^4 DLD1 cells in a 96 well plate. Treated and untreated was determined to be 100 μ M in this study consistent with that determined previously by Lee (2015). Cells were incubated overnight at 37°C, in humidified 6% CO₂. Absorbance readings were measured at 1, 2, and 3 hours after adding reagent. The percent cell viability was calculated by $(CV\%) = (A_T/A_{UT}) \times 100\%$.

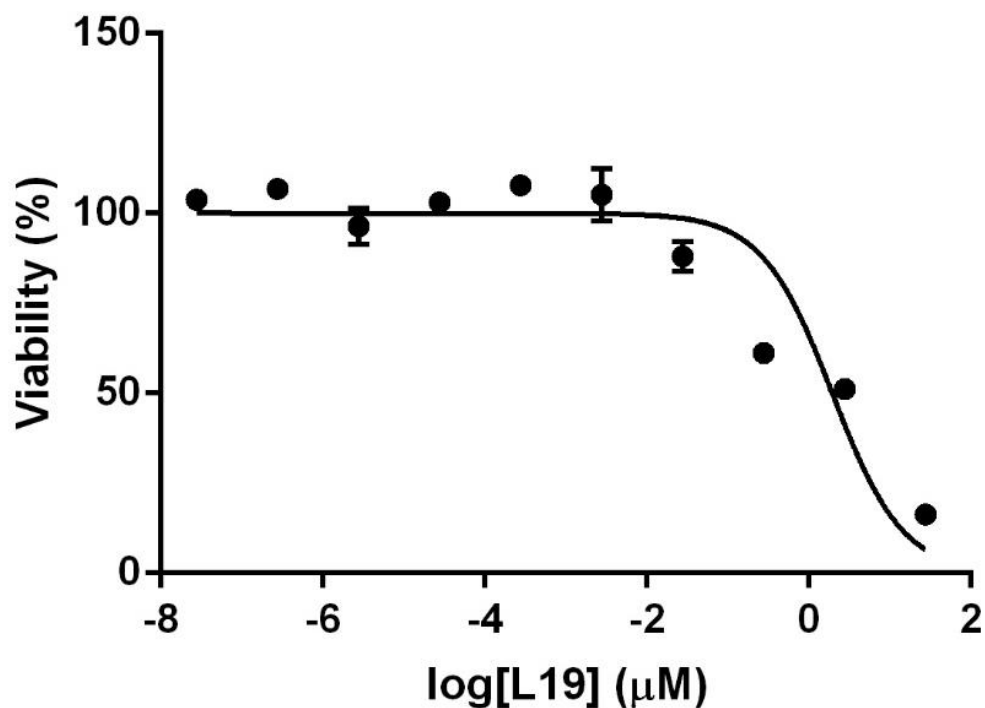


Figure 11. Dose-response curve for L19. Synchronized cells were seeded 1×10^4 cells per well of a 96 well plate and incubated overnight. Cells were treated with 100 μ L of log dilutions of L19 for 24 hours at 37°C. Cell Titer 96® Aqueous One Reagent was used to determine the percent cell viability. The standard deviation represents experiments repeated more than three times and measured in triplicate.

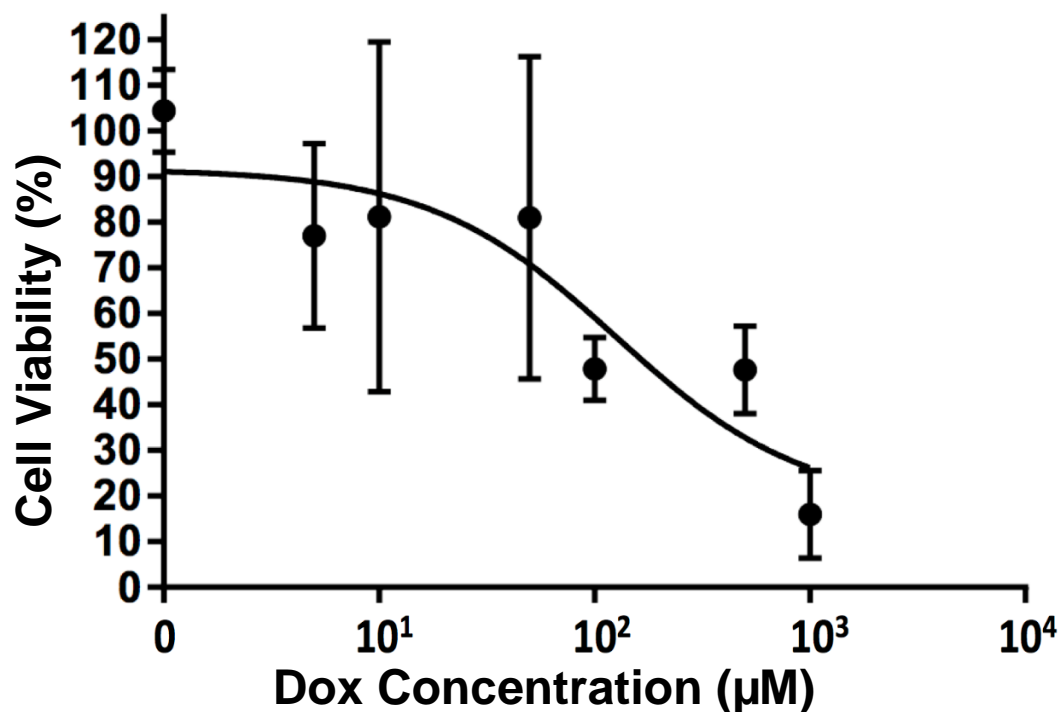


Figure 12. Dose-response curve for Doxorubicin. Synchronized cells were seeded 1×10^4 cells per well of a 96 well plate. Cells were treated with 10-fold serial dilution of 26.8 mM dox for 24 hours incubation. Cell viability was determined using the Cell Titer 96® Aqueous One Reagent. Percent viability was determined relative to the absorbance at 490 nm of untreated cells. Error bars represent values from experiments that were repeated more than three times and done in triplicate.

Induction of Caspase 3 and 7 and Cell viability of DLD-1 Cells Treated with Different HPLC Fractions

The Apo-ONE™ Homogeneous Caspase-3/7 Assay (Promega Corp.) was used to detect levels of caspase 3/7 induction from exposure to HPLC fractions 14 through 21 of ASE extract to confirm the findings of Bhandari (2015) (Figure 13); DOX was used as the positive control (Figure 14). Fraction L19 exhibited the lowest cell viability with highest caspase 3/7 activity (Figure 13). Fraction 20 also showed low cell viability with induced caspase 3/7 activity, however it was less than L19 and most likely some L19 was present in fraction 20. L19 was used for further study.

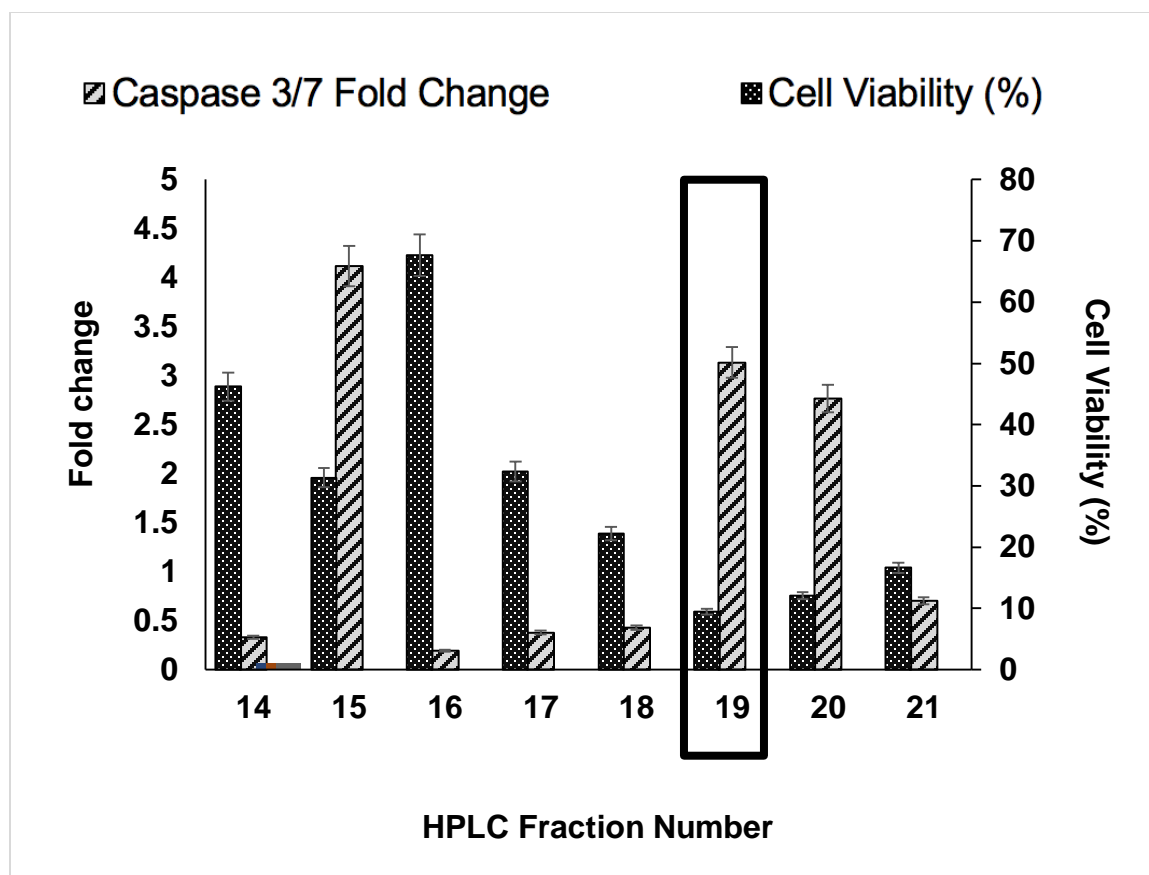


Figure 13. Histogram of Caspase 3/7-fold change and percentage of cell viability by induction of HPLC Fractions DLD-1 cell line. The 96 well cell culture plate was seeded with 1×10^4 DLD-1 cells/100 μ L/well and was incubated in 6% CO₂ at 37°C overnight. The media was then removed. The 1 mL HPLC fractions were evaporated to dryness and suspended in 100 μ L of RPMI-plus. The fluorescence was measured using an excitation at 499 nm and an emission at 521 nm. The viability was detected using the Aqueous One reagent and measuring the A₄₉₀. Both the Fold Change in caspase 3/7 activity and the percent viability were normalized to the respective treatment of untreated cells.

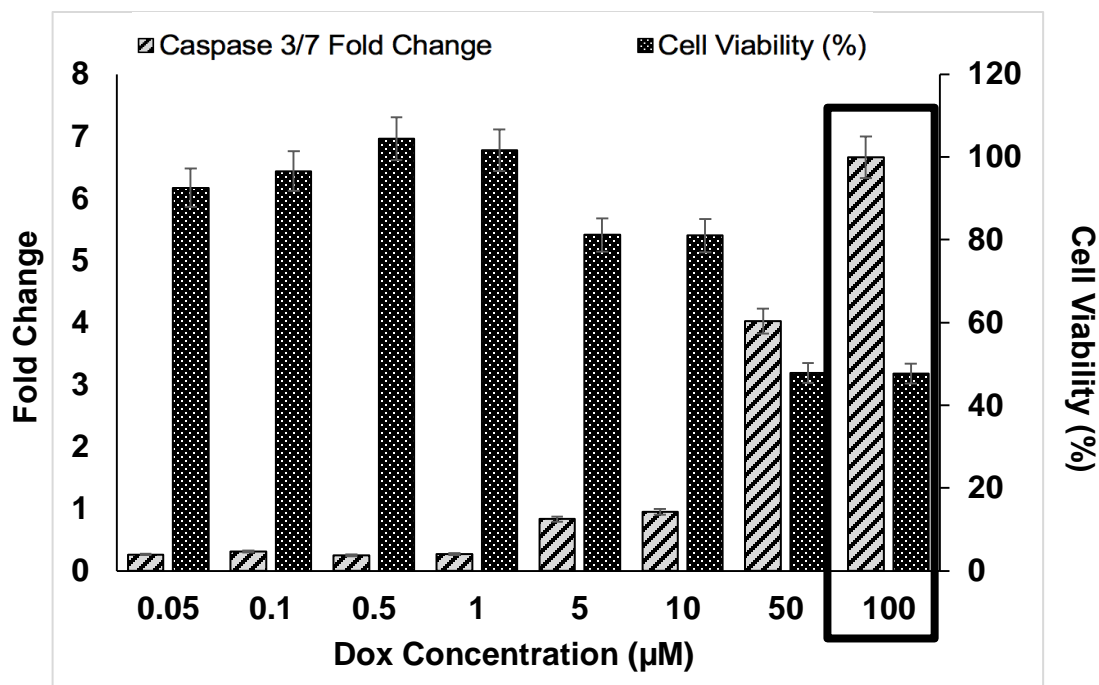


Figure 14. Histogram of Caspase 3/7-fold change and percent cell viability in DLD-1 cells in response to different Dox concentrations. Synchronized DLD-1 cells were seeded 1×10^4 cells/100 μ L/well and incubated in 6% CO_2 at 37°C overnight. The media was then removed. The different Dox concentrations were suspended in 100 μ L of RPMI-plus and added to the cells followed by incubation in 6% CO_2 at 37°C for 24 hours. The media containing Dox was removed and replaced with 25 μ L of fresh RPMI-plus media. A working solution of Apo-ONE homogenous caspase-3/7 reagent was added, mixed and incubated in the dark for one hour at room temperature. The fluorescence was measured at 521nm (excitation at 499nm) to determine the fold change in caspase 3/7 as compared to untreated cells. Percent viability was determined as described in Figure 12.

Induction of Caspase 3 and 7 and Cell Viability on DLD-1 by L19

DLD1 cells treated with serial dilutions of L19 showed a dose dependent decrease in cell viability and an increase in caspase 3/7 activity as L19 concentrations increased from $27.73 \times 10^{-5} \pm 1.96 \mu\text{M}$ to $27.73 \pm 1.96 \mu\text{M}$ (Figure 15). The $2.77 \pm 1.96 \mu\text{M}$ resulted in killing 52.4 ± 1.32 percent of the cells and exhibited a 1.4 ± 0.38 fold increase in caspase 3/7 activity. The undiluted L19 and L20 showed the lowest percent viability at $9.49 \pm 0.07\%$ and $12.09 \pm 0.11\%$ viability and 3.13 ± 0.08 and 2.76 ± 0.098 fold increase in caspase 3/7 activity respectively. L19 at a concentration of $2.76 \pm 1.96 \mu\text{M}$ concentration used for treating the DLD-1 cells for the following experiments.

Isolation of RNA

Figure 16 shows a representative native agarose gel of total RNA isolated from the untreated and treated cells after exposure to L19 for different exposure times. The quality of total RNA was determined by examining the 28S and 18S rRNA on a 1% native agarose gel. Total RNA for two different samples isolated from untreated cells, UT1 and UT2 are shown in lanes 1 and 2. Lane 3 contains the All Purpose HI-LO™ DNA marker (50–10,000 bp) and the lanes labeled T1 and T2 contain total RNA isolated from treated cells. Each lane contained 5 μL total RNA and 5 μL bromophenol blue loading dye. Based on the presence of two

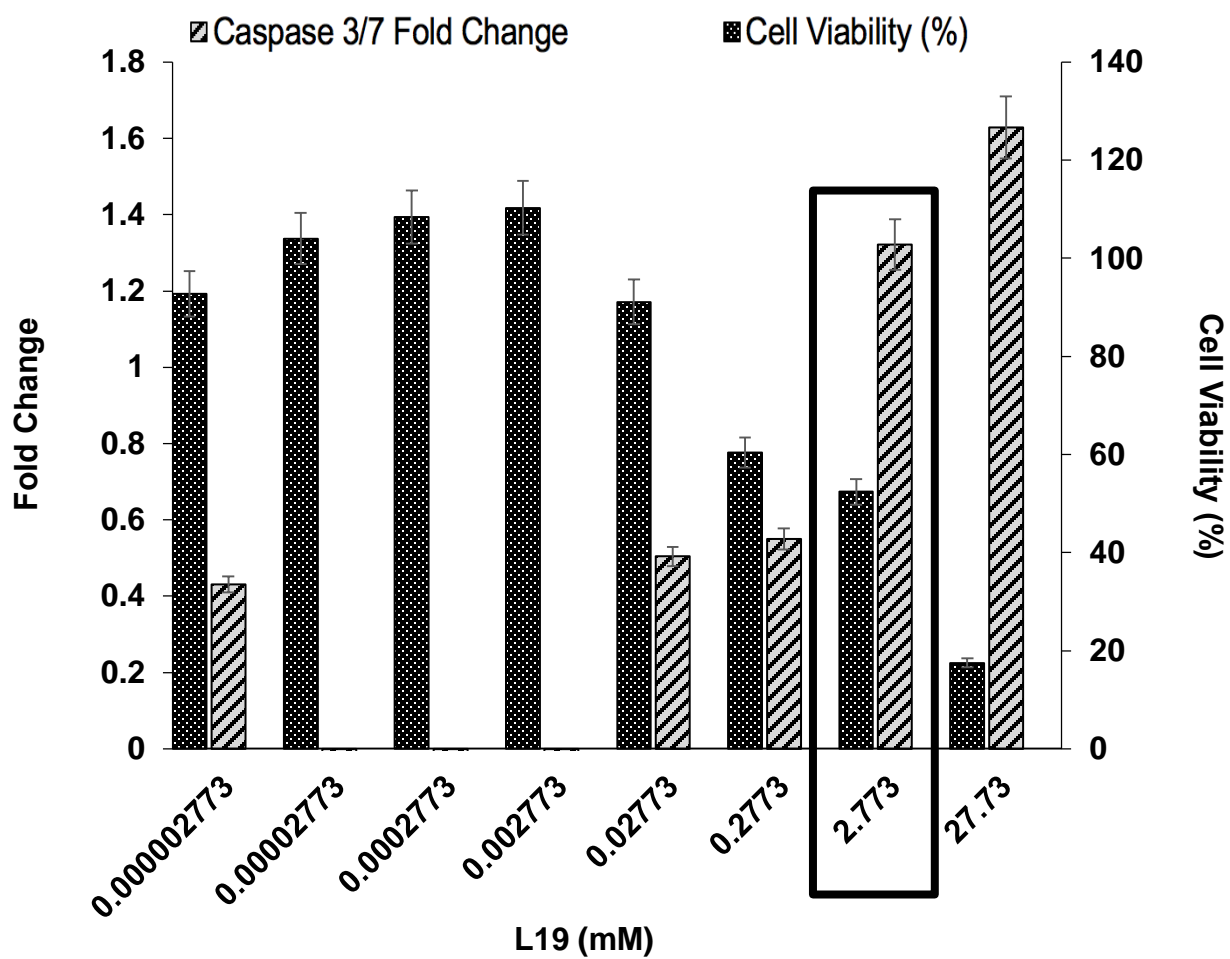


Figure 15. Caspase 3/7-fold change and percentage of cell viability by induction of L19 on DLD-1 cell line. Cells were prepared and treated with L19 as described previously in Figure 12 and 13.

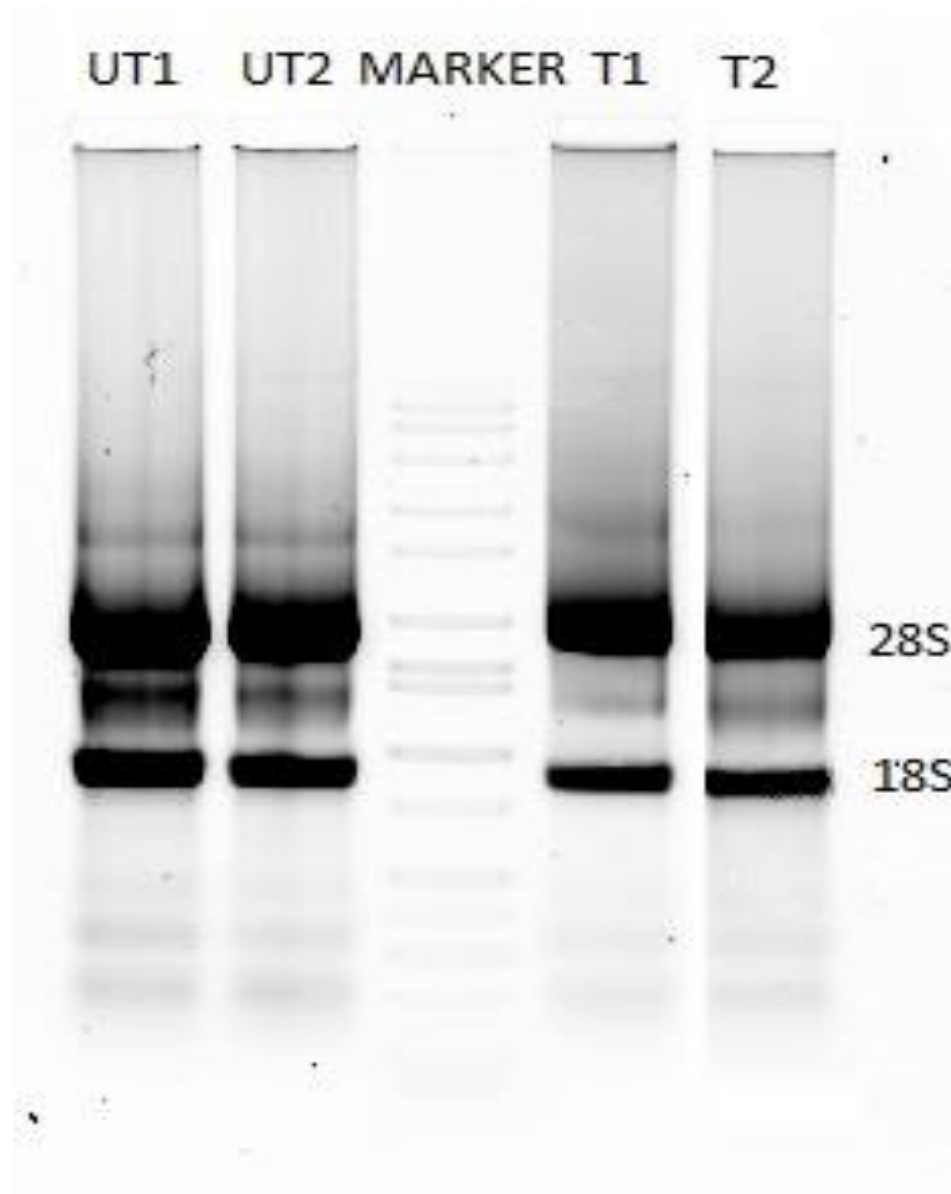


Figure 16. Quality assessment of total RNA by 1% native agarose gel. A total of 5 μ L of RNA plus 5 μ L of bromophenol blue dye were loaded in each well. The gel was run in 1X TAE buffer at 100 volts for 30 minutes. Lane UT1 and UT2 = Untreated cells, MARKER= All Purpose HI-LO™ DNA marker (50bp-10,000bp), T1 and T2 = L19 treated cells.

sharp prominent bands for the 28S and 18S rRNA (Figure 16), samples were assumed to contain high quality mRNA. The purity of the RNA was determined by measuring the $A_{260}:A_{280}$ ratio which should be between 1.8 and 2 (Table 2) (Lucena-Aguilar et al., 2016); a ratio less than 1.6 indicates protein contamination.

cDNA Synthesis for qRT PCR

The concentration of cDNA was measured using the conversion factor of 37 $\mu\text{g/mL}$ of cDNA for an A_{260} of 1. The measured A_{260} was multiplied by a path length of 0.1 cm and any dilution factors if it was diluted. The quality of RNA was measured (Table 3).

Determination of Changes in Caspase Gene Expression Using Quantitative Real Time PCR.

Quantitative Real Time PCR was used to confirm microarray data and to determine the level of gene expression of different human caspases, *CASP1*, 3, 4, 5, 6, 7, 8, 9, 10, 12. The qRT-PCR experiment was performed in triplicate for the different L19 exposure times with *GAPDH* as the housekeeping gene. The $\Delta\Delta C_t$ is a measure of the fold change (Figure 17). The error bars for each of the caspase measurements are large and most likely attributable to the variation in the cell number per well. *CASP12* gene expression increased by 6 hours as evidenced by

a 25.13 ± 4.8 fold increase showing a quick response to L19 (Figure 17). *CASP1*, 6, and 10 exhibited smaller fold changes of 1.84 ± 2.54 , 1.6 ± 1.82 , and 1.53 ± 0.73 , respectively at the 6-hour exposure time. The fold changes were relatively small in these samples, and the large standard error indicates very little change in *CASP 1*, 6 and 10 gene expressions at 6 hours.

CASP5 gene expression exhibited a maximum level in 8 hours of 2.23 ± 0.96 fold change. *CASP5* has been shown to have an inflammatory role (McIlwaine et al., 2017). *CASP 12* dropped to little to no expression. After 12 hours, *CASP1* increased 2.57 ± 0.87 while. *CASP3*, 6, and 12 increased to 1.92 ± 0.66 , 2.12 ± 0.70 , and 2.15 ± 1.28 , respectively. *CASP7* displayed down regulated by fold change 0.4 ± 0.72 or a -2.5 decrease as compared to the untreated cells and the *GAPDH* housekeeping gene. After 24 hours of exposure to the L19, *CASP 1* increased to 5.85 ± 1.8 . All of the other *CASP* genes showed no significant expression at 24 hours. *CASP3* showed only a small increase by 8 hours then it returned to the same as untreated. *CASP4* was unaffected throughout the 24-hour period measured. *CASP6* shows only a slight increase by 12 hours, then goes to no change. *CASP7* displayed a steady decrease through the 24-hour exposure of L19. *CASP8* and 9 were down regulated by 24 hours with no change before that. Same with *CASP10* except at 12 hours it showed upregulation as mentioned before. *CASP12* has a huge positive increase by 6 hours and then decreased to same as untreated by 8 hours.

Table 2. Quality and total concentration of total RNA for representative L19 treated and untreated DLD-1 cells at 6, 8, 12, and 24 hour exposure times. The concentration of RNA was measured using the conversion factor of 40 µg/mL of RNA for an A₂₆₀ of 1. The measured A₂₆₀ was multiplied by a path length of 0.1 cm and any dilution factors (if it was diluted). Purity of RNA was measured by the A_{260nm}/A_{280 nm} ratio.

| Time Points | A ₂₈₀ | A ₂₆₀ | A ₂₆₀ /A ₂₈₀ | Concentration (µg/mL) |
|-------------|------------------|------------------|------------------------------------|--------------------------|
| T6 | 0.351 | 0.641 | 1.826 | 2564 |
| T8 | 0.105 | 0.21 | 2.000 | 840 |
| T12 | 0.219 | 0.407 | 1.858 | 1628 |
| T24 | 0.553 | 0.997 | 1.803 | 3988 |
| UT6 | 0.347 | 0.703 | 2.026 | 2812 |
| UT8 | 0.084 | 0.174 | 2.071 | 696 |
| UT12 | 0.173 | 0.355 | 2.052 | 1420 |
| UT24 | 0.173 | 0.298 | 1.723 | 1192 |

Table 3. cDNA isolated from L19 treated and untreated DLD-1 cells at different time points of exposure for qRT-PCR.

| Time Points | A₂₈₀ | A₂₆₀ | A₂₆₀/A₂₈₀ | Concentration (µg/mL) |
|--------------------|------------------------|------------------------|--|----------------------------------|
| T6 | 0.632 | 1.166 | 1.845 | 43.142 |
| T8 | 0.18 | 0.328 | 1.822 | 12.136 |
| T12 | 0.396 | 0.694 | 1.753 | 25.678 |
| T24 | 0.357 | 0.663 | 1.857 | 24.531 |
| UT6 | 0.55 | 0.991 | 1.802 | 36.667 |
| UT8 | 0.19 | 0.372 | 1.958 | 13.764 |
| UT12 | 0.425 | 0.739 | 1.739 | 27.343 |
| UT24 | 0.328 | 0.586 | 1.787 | 21.682 |

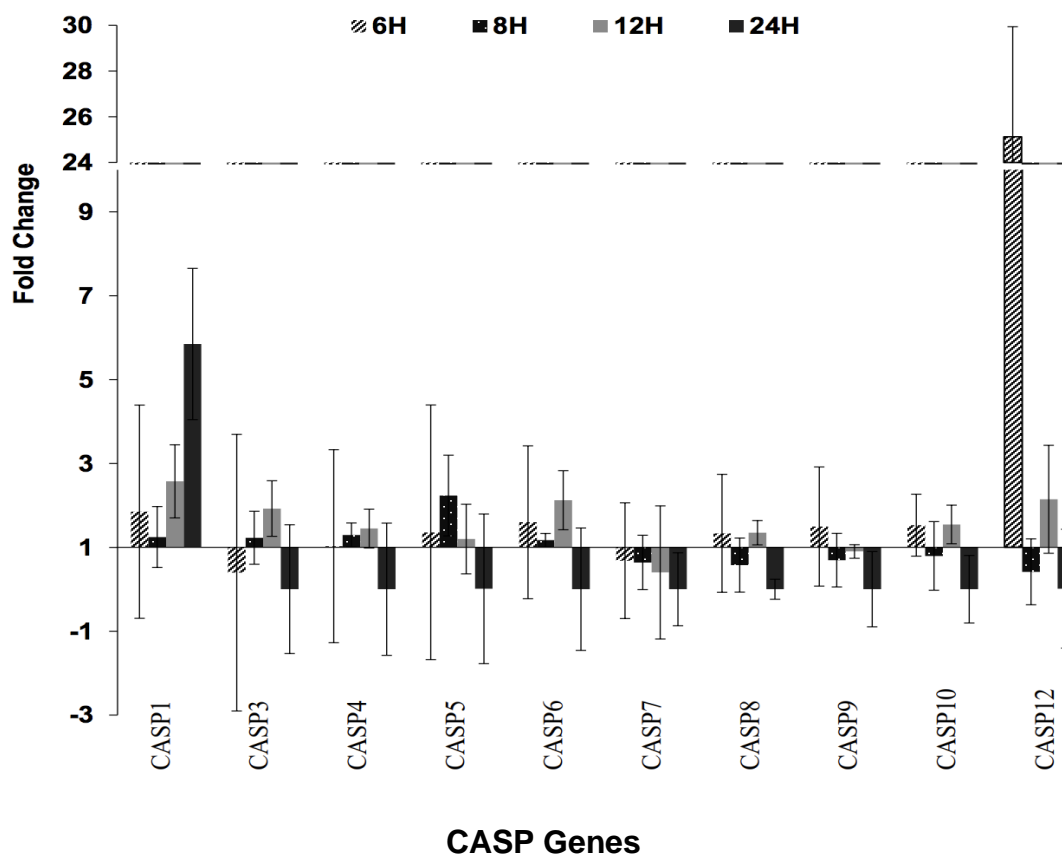


Figure 17. qRT-PCR of *CASP* gene expression in response to L19 exposure. DLD-1 passage 18 cells were treated with L19 for different exposure times (6, 8, 12, 24 hours). Caspase primer sequences (table. 1) were obtained from the NCBI primer data base. Primers were designed to give a PCR product of 200bp \pm 10. *GAPDH* was used as a house keeping gene control. The annealing temperature was 60°C. Template was 20 ng of purified cDNA added to qRT SYBR Green master mix. The normalized Ct value for each caspase was relative to the Ct value of *GAPDH* cDNA present. The $\Delta\Delta Ct$ value was calculated by subtracting the ΔCt of untreated cells from the ΔCt value of treated cells. The fold change was determined as $2^{-\Delta\Delta Ct}$. Hashes, dots, gray and black bars showed 6, 8, 12 and 24 hours, respectively.

RT² Profiler™ PCR Human Apoptosis Array

The RT² Profiler™ PCR Human Apoptosis Array (SA Biosciences, Cat no: PAHS-012Z) was used to analyze the expression of 84 apoptotic and anti-apoptotic genes of DLD-1 cells treated by L19 at the different time points. This array was utilized to confirm the qRT-PCR results above and to determine the apoptosis mechanism/s for the L19 effect on DLD-1 cells. Equal amounts of treated and untreated cDNA (20ng/well) were used per reaction. The average Ct of two housekeeping genes (HK), Glyceraldehyde-3-phosphate dehydrogenase (*GAPDH*) and beta actin (*ACTB*), were chosen for normalizing the Ct values because they both showed no change at different time points in response to the L19 treatment or as compared to the untreated cells; the fold changes were 1.03 ± 0.18 and 0.85 ± 0.06 , respectively. The Ct values were analyzed using the online SABiosciences software (SA Biosciences Corp.) to determine any changes in gene expression (Table 4). Column 1 lists the gene abbreviation, column 2 shows fold change ($2^{-\Delta\Delta Ct}$) at each time of exposure to L19. A fold change greater than 1.5 is up-regulated, whereas a fold change less than 0.7 is down-regulated. In other words, if $\Delta\Delta Ct$ ($\Delta Ct_{\text{Treated}} - \Delta Ct_{\text{Untreated}} = \Delta\Delta Ct$) is equal zero, then $\Delta Ct_{\text{Treated}} = \Delta Ct_{\text{Untreated}}$ and there is no up or down-regulation. If $\Delta\Delta Ct = -1$; then $2^{-(-1)} = 2$ which means the gene of interest is expressed two times more than the control genes (*ACTB* and *GAPDH*). Thus, genes showed significant upregulation. On the other

hand, if $\Delta\Delta Ct=1$, $2^{-(\Delta\Delta Ct)} = \frac{1}{2} = 0.5$ the gene regulation was two times less than the control which shows a significant down regulation.

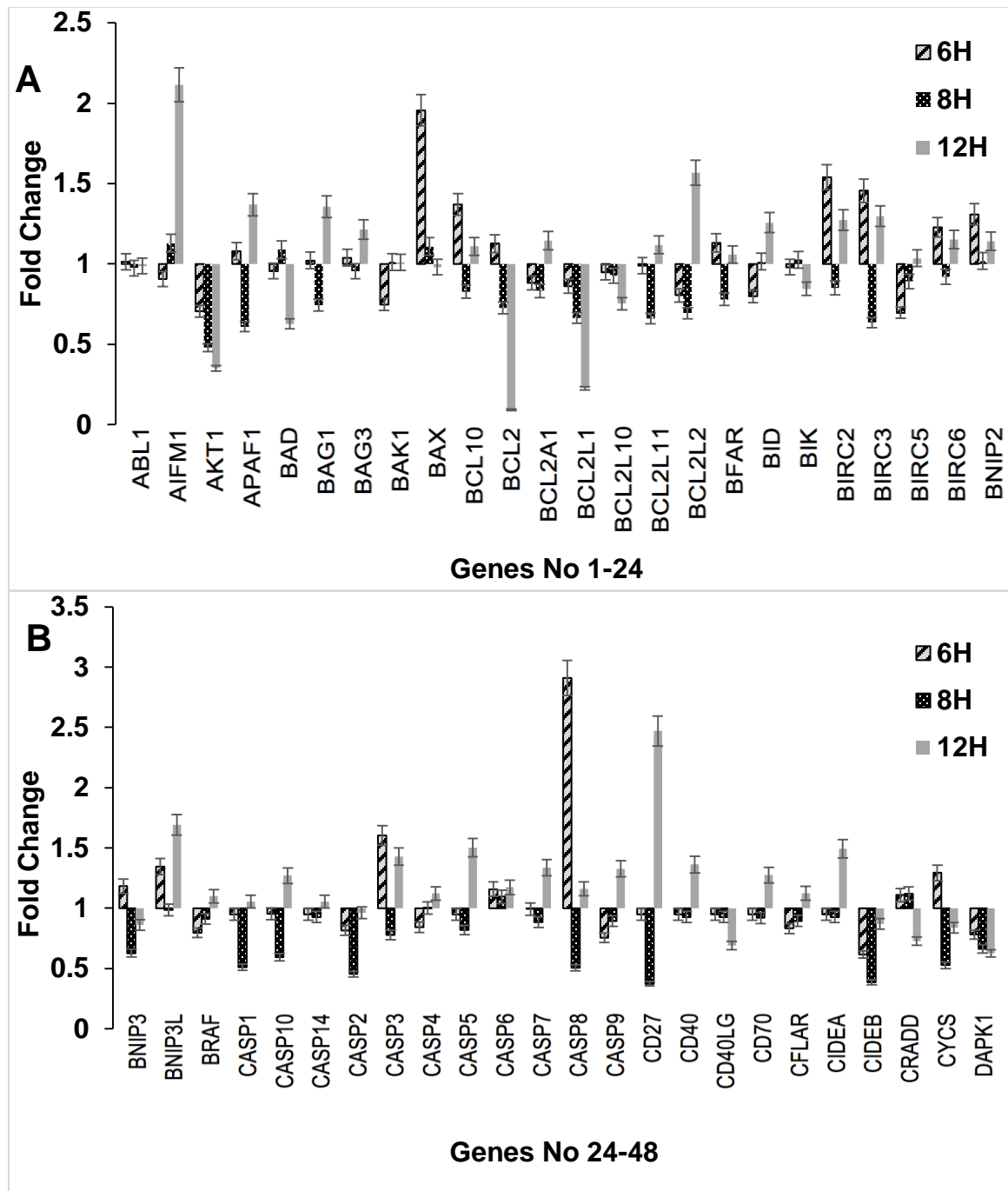
Based on Table 4 (A) and figure 18 (B). *CASP1* showed no changes in 6 and 12 hours and significant down-regulated in 8 hours (0.51-fold change). *CASP3*, an executioner caspase, was marginally up-regulated at 1.61 and 1.43-fold by 6 and 12 hours, respectively. *CASP5* (0.95, 0.82-fold change) and *CASP4* (0.84, 1.00-fold change) (inflammatory CASPs) showed no significant changes in 6 and 8 hours, respectively; however *CASP5* showed up regulation at 12 hours (1.5 fold change). *CASP6* and *CASP7*, both executioner caspases, did not show remarkable changes at any of the time points. *CASP8* showed significant up-regulated in 6, hours to a fold change of 2.91 and down regulated at 8 hours (0.51-fold change), then showed no changes at 12 hours (1.16). *CASP9* showed to be unchanged at 8 and 12 time points in RT² Profiler™; while it showed minimally downregulation in 6 hours (0.75). *CASP10* showed down-regulated by 0.59 at 8 hours but returned to no significant change relative to untreated at 12 hours (1.27-fold change). *CASP14*, which encodes an anti-apoptotic protein showed no up or down regulation. *CASP2* had significant down-regulated in 8 hours by fold change 0.45, *CRADD* (*CASP2* and *RIPK1* domain containing adaptor with death domain) was up-regulated (1.87) at 6 hours.

Table 4. RT² Profiler™ PCR Human Apoptosis Array (SA Biosciences, Cat no: PAHS-012Z) fold change ($2^{-\Delta\Delta C_t}$) for 6, 8, and 12 hours. Column 1 (from left to right): gene abbreviation; column 2: fold change. For normalizing the Ct values, two housekeeping genes (HK) were chosen, Glyceraldehyde-3-phosphate dehydrogenase (*GAPDH*) and beta Actin, (*ACTB*), with 1.03 ± 1.79 and 0.85 ± 0.06 , respectively, because they showed no change in response to L19 treatment as compared to untreated at the different time points. Parts A and B represent up- and down-regulated genes, respectively. Greater than 1.5-fold change and less than 0.7 were considered significant.

| A: Upregulated genes | | | | | |
|-----------------------------|----------------|-------------|----------------|-------------|-----------------|
| Gene | 6 Hours | Gene | 8 Hours | Gene | 12 Hours |
| CASP8 | 2.9099 | | | CD27 | 2.469 |
| XIAP | 2.6871 | | | AIFM1 | 2.1145 |
| TNFRSF9 | 2.1078 | | | PYCARD | 1.8368 |
| BAX | 1.9568 | | | DIABLO | 1.7717 |
| TNFSF10 | 1.8715 | | | FAS | 1.6986 |
| CASP3 | 1.6055 | | | BNIP3L | 1.6921 |
| BIRC2 | 1.5394 | | | FASLG | 1.6321 |
| IGF1R | 1.5254 | | | IL10 | 1.6161 |
| | | | | BCL2L2 | 1.5668 |
| | | | | CASP5 | 1.5017 |
| | | | | CIDEA | 1.4933 |
| | | | | NAIP | 1.4817 |

| B: Downregulated genes | | | | | |
|-------------------------------|----------------|-------------|----------------|-------------|-----------------|
| Gene | 6 Hours | Gene | 8 Hours | Gene | 12 Hours |
| BID | 0.7983 | BFAR | 0.7789 | NOD1 | 0.7876 |
| BRAF | 0.7967 | CASP3 | 0.778 | BCL2L10 | 0.7531 |
| MCL1 | 0.7955 | TRADD | 0.7567 | LTBR | 0.7523 |
| LTBR | 0.7952 | TNFRSF10 A | 0.7566 | TP53 | 0.7519 |
| DAPK1 | 0.7804 | FADD | 0.7493 | TNFSF8 | 0.7484 |
| CASP9 | 0.7547 | BAG1 | 0.7439 | CRADD | 0.7274 |
| TNFRSF10 B | 0.7498 | TRAF3 | 0.7395 | CD40LG | 0.6924 |

| | | | | | |
|----------|--------|---------------|--------|-----------|--------|
| BAK1 | 0.7479 | BCL2 | 0.7244 | LTA | 0.6831 |
| TP53 | 0.742 | BCL2L2 | 0.6946 | TNFRSF10A | 0.6402 |
| AKT1 | 0.7054 | TP73 | 0.6663 | BAD | 0.6262 |
| GADD45A | 0.6983 | BCL2L1 | 0.6639 | DAPK1 | 0.625 |
| BIRC5 | 0.6959 | DAPK1 | 0.6629 | TNFRSF1A | 0.5126 |
| TNFRSF25 | 0.6885 | BCL2L11 | 0.6608 | TRADD | 0.4627 |
| NFKB1 | 0.6761 | BIRC3 | 0.6343 | AKT1 | 0.3506 |
| TNFRSF1A | 0.6563 | NOD1 | 0.6333 | TRAF2 | 0.3419 |
| FADD | 0.6441 | BNIP3 | 0.6274 | BCL2L1 | 0.2263 |
| HRK | 0.6242 | TP53 | 0.6274 | BCL2 | 0.0931 |
| CIDEB | 0.6169 | TNFRSF10 B | 0.6117 | | |
| TP73 | 0.6139 | XIAP | 0.6105 | | |
| NOL3 | 0.5687 | APAF1 | 0.6095 | | |
| | | CASP10 | 0.5932 | | |
| | | LTA | 0.563 | | |
| | | TNFRSF1B | 0.5401 | | |
| | | CYCS | 0.5273 | | |
| | | IGF1R | 0.5244 | | |
| | | TRAF2 | 0.5219 | | |
| | | CASP1 | 0.5103 | | |
| | | CASP8 | 0.5055 | | |
| | | AKT1 | 0.4791 | | |
| | | CASP2 | 0.4535 | | |
| | | NAIP | 0.3963 | | |
| | | CIDEB | 0.3865 | | |
| | | CD27 | 0.3737 | | |
| | | TNFRSF25 | 0.3262 | | |
| | | PYCARD | 0.2119 | | |



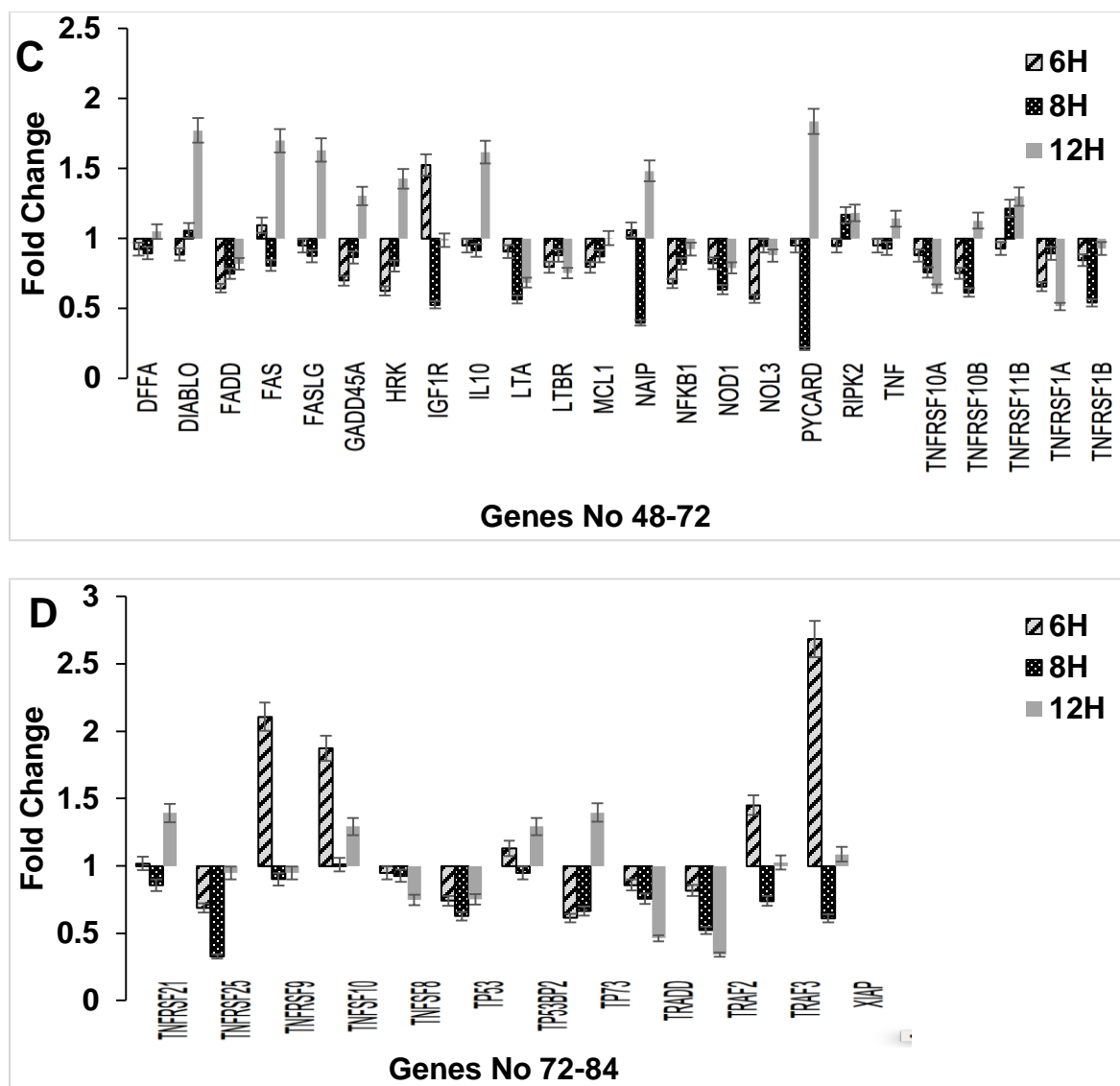


Figure 18. qRT-PCR of DLD1 cells exposed to L19 at 6, 8, and 12 hours (legend) using the RT² Profiler Human Apoptosis PCR Array (Cat no: PAHS-01Z). The fold change was calculated using $2^{-\Delta\Delta C_t}$ where the ΔC_t of L19 treated cells were normalized to the ΔC_t of untreated cells using the online software available at the manufacture's website. Panels A, B, C and D display the results for 84 genes involved in apoptosis regulation. The standard deviation represents the variance between triplicates within each experiment as well as replicate experiments.

TNF (Tumor necrosis factor) which activates *TNF-R1* (Tumor necrosis factor receptor superfamily, member 10a) showed no significant changes at 6, 8 and 12 hours by 0.94, 0.93 and 1.14-fold changes respectively (Table 4B; Figure 18C). *TRAF2* (TNF receptor-associated factor 2), which can activate *TRADD* (TNFRSF1A-associated via death domain) directly, was down-regulated after 8 hours at 0.52 and 12 hours at 0.34 fold change. *FADD* (Fas (TNFRSF6)-associated via death domain) was minimally down-regulation at each time point by 0.7-fold. *BAD* (BCL2-associated agonist of cell death) was down-regulated at 12 hours by 0.62. Neither *BID* nor *CYCS* showed any significant changes at 6 or 12 hours respectively by 1.29 (*CYCS* fold change at 6 hours) or 1.26 (*BID* fold change at 12 hours) (Figure 18B). *AIF* (Apoptosis Inducing Factor) was up-regulated at 12 hours by 2.11-fold changes, exhibiting no changes at 6 or 8 hours (0.91 and 1.13-fold change, respectively).

Comparison of The Two qRT-PCR Results

Ideally the two methods, qRT-PCR and the RT² Profiler™, should show similar results or at least similar trends. Differences observed might be attributable to the fact that the primers used in the qRT-PCR designed from the NCI primer database may not be the same as the primers used in the RT² Profiler™ which are proprietary. Table 5 lists the fold changes of key apoptotic genes to compare the results between the two methods. *CASP3* was down-regulated by 6 hours to a

0.41 \pm 3.3 fold change as indicated by qRT-PCR and by 1.61 from RT² Profiler™. By 12 hours, *CASP3* was up-regulation to a 1.92 \pm 0.66 fold change as indicated by qRT-PCR and by 1.43 from RT² Profiler™. Up regulation of *CASP3* is supportive of apoptosis. *CASP1*, 9 and 10 were up-regulated at 6 hours in qRT-PCR (1.85 \pm 2.54, 1.49 \pm 1.42, and 1.53 \pm 0.74, respectively) but showed to be unchanged in RT² Profiler™. The standard deviations for the qRT-PCR results are high, and there was no significant change in the qRT-PCR consistent with the RT² Profiler™. *CASP1* showed to be up-regulated by 2.57 \pm 0.87 in 12 hours using qRT-PCR but no significant change using the RT² Profiler (1.05-fold change). *CASP4*, at 12 hours and *CASP5* at 8 hours, were up-regulated in the qRT-PCR data (1.45 \pm 0.46 and 2.23 \pm 0.96, respectively); while *CASP5* and *CASP4* stayed the same in RT² Profiler data (Table 5). *CASP7* was down-regulated in qRT-PCR results, with only marginal up regulation (1.34-fold change) at 12 hours (Table 5). *CASP8* showed significant up-regulation in 6 hours (2.91-fold change) and no changes in 8 and 12 hours. The qRT-PCR data indicated marginal up-regulation of 1.33 \pm 1.41, 0.58 \pm 0.68 and 1.35 \pm 0.29, respectively, indicating no changes in 6 and 12 hours and significant down regulated in 8 hours (Table 5).

Table 5. Comparison of fold changes for CASP genes over different time intervals using RT² Profiler™ PCR Human Apoptosis Array (SA) and qRT-PCR results (reported as means \pm 1 SD).

| Gene | Treatment Time | | | | | |
|----------------------|----------------|-----------------|-------|-----------------|--------|-----------------|
| | 6 hrs | | 8 hrs | | 12 hrs | |
| | SA | qRT-PCR | SA | qRT-PCR | SA | qRT-PCR |
| <i>CASP1</i> | 0.95 | 1.85 \pm 2.54 | 0.51 | 1.24 \pm 0.73 | 1.05 | 2.57 \pm 0.87 |
| <i>CASP3</i> | 1.61 | 0.40 \pm 3.30 | 0.78 | 1.23 \pm 0.63 | 1.43 | 1.92 \pm 0.66 |
| <i>CASP4</i> | 0.84 | 1.03 \pm 2.30 | 1.00 | 1.29 \pm 0.29 | 1.12 | 1.45 \pm 0.46 |
| <i>CASP5</i> | 0.95 | 1.36 \pm 3.04 | 0.82 | 2.23 \pm 0.96 | 1.50 | 1.20 \pm 0.83 |
| <i>CASP6</i> | 1.16 | 1.60 \pm 1.82 | 1.09 | 1.17 \pm 0.16 | 1.17 | 2.12 \pm 0.70 |
| <i>CASP7</i> | 0.99 | 0.68 \pm 1.38 | 0.88 | 0.64 \pm 0.65 | 1.34 | 0.40 \pm 1.59 |
| <i>CASP8</i> | 2.91 | 1.33 \pm 1.41 | 0.51 | 0.58 \pm 0.64 | 1.16 | 1.35 \pm 0.29 |
| <i>CASP9</i> | 0.75 | 1.49 \pm 1.42 | 0.89 | 0.69 \pm 0.64 | 1.33 | 0.90 \pm 0.16 |
| <i>CASP10</i> | 0.95 | 1.53 \pm 0.74 | 0.59 | 0.79 \pm 0.82 | 1.27 | 1.54 \pm 0.46 |

The ANOVA results indicated that the hypothesis (H_1) in the RT² Profiler™ assay was that all three time points (6, 8, and 12 hours) were statistically different for mean values of gene expression (dependent variable). The p-value of mean differences between time treatments rejected H_0 ($F_2 = 18.99$, $p < 0.0001$); however, the mean for different genes, rejected H_1 ($F_{83} = 1.17$, $p = 0.19$). Thus, the difference between the 3-time points were statistically different but at least one gene showed no changes during the different times.

Table 6. Summary of gene expression for three independent time points (Group) across genes for RT² Profiler Human Apoptosis PCR array results. The number of genes assayed were 84 (Count).

| Group | Count | Sum | Average | Variance |
|--------------|--------------|------------|----------------|-----------------|
| 6H | 84 | 86.85 | 1.03 | 0.16 |
| 8H | 84 | 67.03 | 0.80 | 0.04 |
| 12H | 84 | 92.77 | 1.10 | 0.15 |

Table 7. A two-factor analysis of variance for three independent time point groups (across genes) for RT² Profiler Human Apoptosis PCR array results, that indicates F and P-value for total intensities of different time points and genes of RT² Profiler Human Apoptosis PCR array results. The groups were defined as 84 genes in three different time intervals (6, 8, 12 hours).

| Source of Variation | SS | df | MS | F | P-value |
|----------------------------|-----------|-----------|-----------|----------|----------------|
| Genes | 11.10 | 83.00 | 0.13 | 1.17 | 0.19 |
| Hours | 4.33 | 2.00 | 2.16 | 18.99 | 3.73492E-08 |
| Error | 18.91 | 166.00 | 0.11 | | |
| Total | 34.34 | 251.00 | | | |

Microarray cDNA Quantification

The concentration of labeled cDNA was quantified from the absorbance at

260 nm for each of the purified samples (Table 8). The Frequency of Incorporation (FOI) for each dye was calculated using the absorption at 555nm and 647 nm for Alexa Fluor® 555 and Alexa Fluor® 647, which had absorption coefficients of 150,000 L·mol⁻¹·cm⁻¹ (555 nm) and 250,000 L·mol⁻¹·cm⁻¹ (647 nm), respectively (Invitrogen; Carlsbad, CA). The measured absorption spectrum for each dye labeled cDNA in a 1mm path length is shown in Figure 19. The yield of cDNA and the FOI are listed in Table 8. The FOI range was 17.4 ± 1.43 to 20.76 ± 2.93 consistent with the recommended minimum FOI by the manufacturer (Qiagen Corp.).

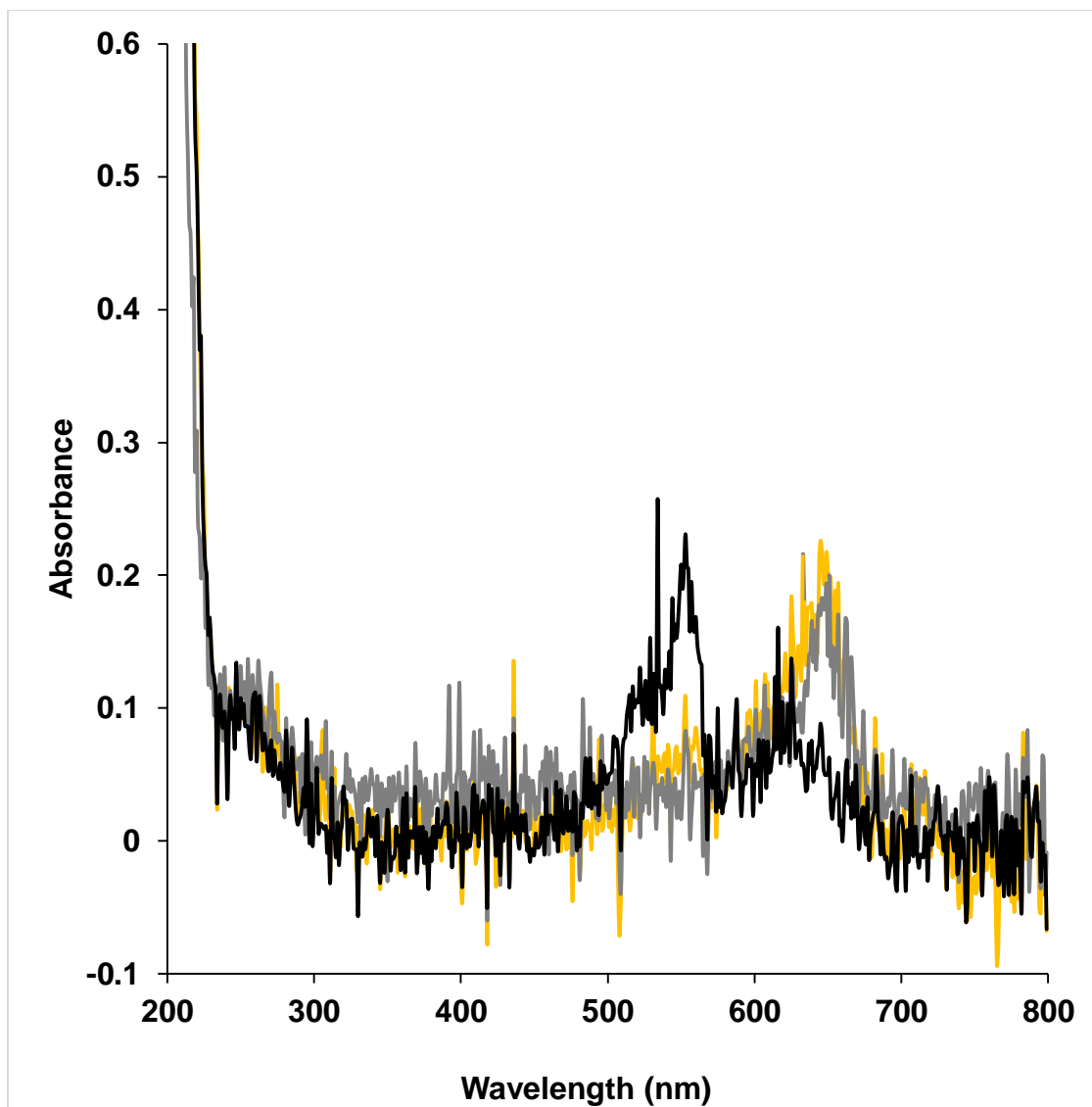


Figure 19. Absorption spectra of Alexa Fluor® 555 labeled cDNA and Alexa Fluor® 647. Amount of cDNA and dye incorporation was quantified using the A_{260} and A_{555} or A_{647} respectively. The path length was 1 mm. The gray and yellow spectra are the Alexa Fluor 647 labeled cDNA with a maximum absorption at 647 nm. The black spectrum is the absorption for the Alexa Fluor 555 labeled cDNA with a maximum absorption at 555 nm.

Table 8. Yield of labeled cDNA for both Alexa Fluor 555 and Alexa Fluor 647, amount of dye incorporation and frequency of incorporation (FOI) for two samples of treated and untreated cells.

| | | Alexa Fluor® 555 Labeled cDNA Yield (µg) | Alexa Fluor® 555 Incorporation (pmole) | FOI for Alexa Fluor® 555 | Alexa Fluor® 647 Labeled cDNA Yield (µg) | Alexa Fluor® 647 Incorporation (pmole) | FOI for Alexa Fluor® 647 |
|------------------|----------|--|--|--------------------------|--|--|--------------------------|
| Treated | Sample 1 | 1.55 | 70 | 17.5 | 1.44 | 75 | 17.67 |
| | Sample 2 | 1.44 | 80 | 18.88 | 1.43 | 100 | 23.56 |
| Untreated | Sample 1 | 1.83 | 80 | 17.77 | 1.11 | 75 | 22.97 |
| | Sample 2 | 2.2 | 100 | 15.45 | 1.24 | 68.75 | 18.85 |

Microarray Data Normalization Analysis

After preprocessing fluorescent intensity of each individual spot using the SpotXel software, data were normalized and filtered using MIDAS as described in Materials and Methods. The average of the raw intensities of all replicate dye-swap experiments for each time point was plotted with the different Alexa 555 raw intensity versus the Alexa 647 raw intensity (Figure 20). The log of raw intensities of Alexa 555 versus Alexa 647 were scattered in a Gaussian distribution and most of them had equal variability (Figure 20). Each individual point (each raw intensity) represents a positive hybridization of the respective labeled cDNA on the array slide after the background subtraction.

When the log of the raw intensities of B vs the log intensities of A were plotted, the majority of the ratios (Alexa 647 intensity divided by the Alexa 555 intensity) for the 6-hour time point clustered at the bottom left corner of the graph at minimal to no difference in intensity between the two different dye-labeled cDNAs (Figure 21). Many of these spots were control spots for hybridization and normalization which showed no difference post-normalization using SpotXel and MIDAS software (Figure 21). However, the normalization process also brought the target genes out from the clustered origin as illustrated at the 8-hour time interval (Figure 21C and D).

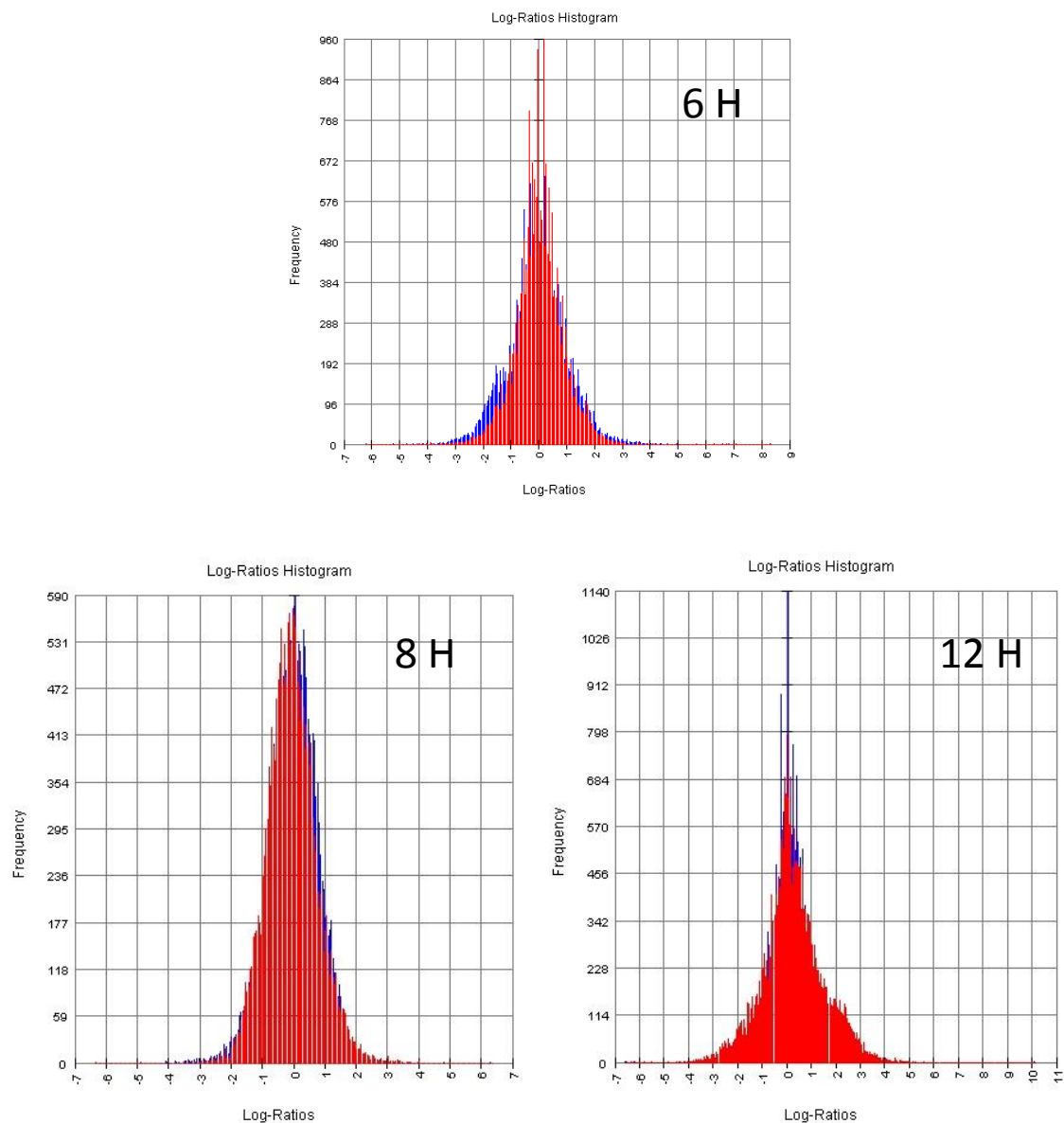


Figure 20. Flip dye histogram of distribution Alexa 555 vs Alexa 647 at different time points. Flip dye histograms are for 6H, 8 H and 12H of untreated and treated DLD-1 cell's labeled cDNA. X and Y axis represent the average frequency and log ratios of gene expression, respectively. Graphs after data normalization and filtering with SpotXel and MIDAS were plotted using the MIDAS software.

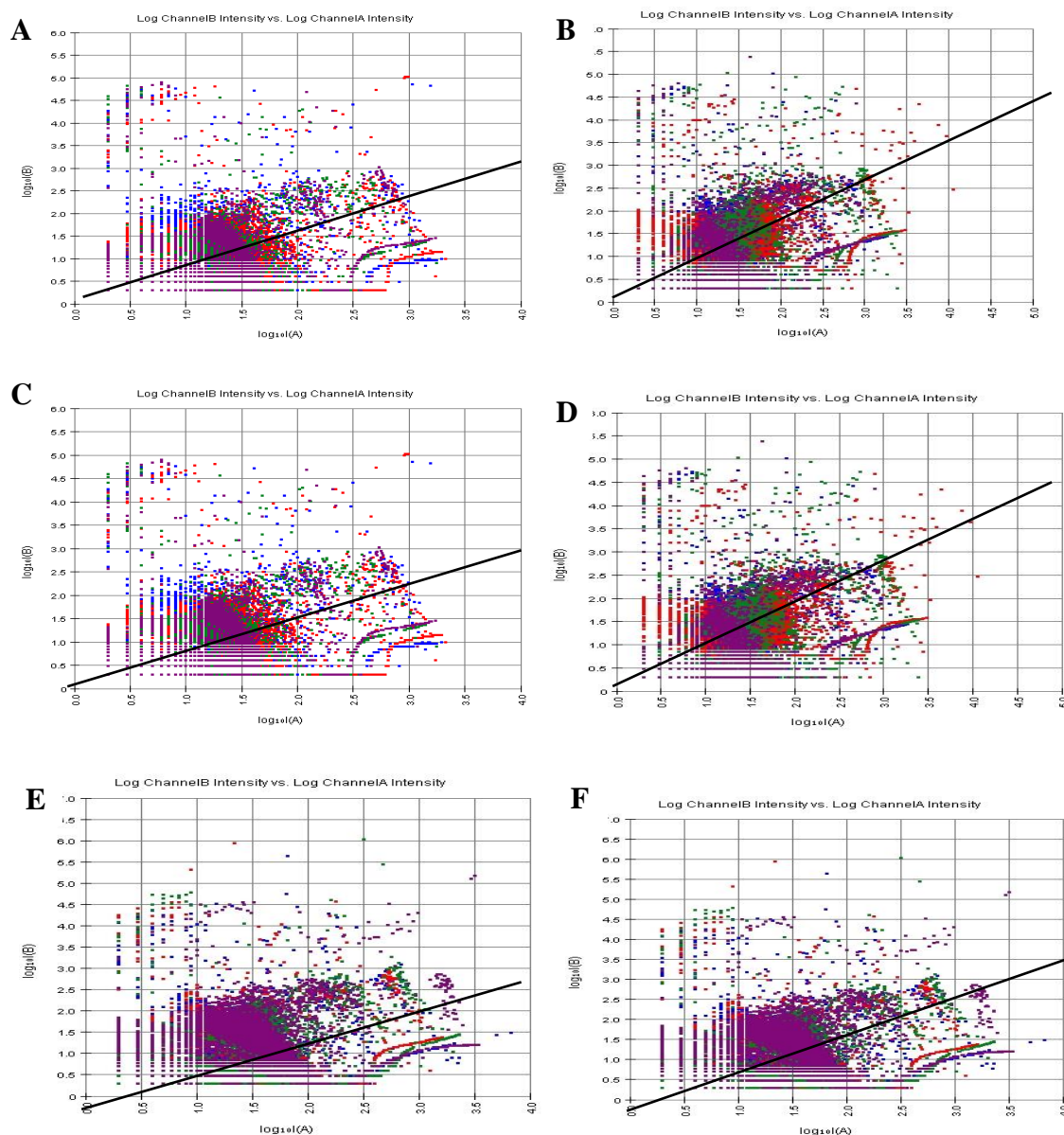


Figure 21. Scatter plots of the average distribution Alexa 555 vs Alexa 647 for raw intensity and log intensity at different time points in dye-swap experiment. $\log_{10}(IA)$ vs $\log_{10}(IB)$ scatter plots are for 6H (A), 8 H (C) and 12H (E) of untreated and treated DLD-1 cell's labeled cDNA. X and Y coordinates represented average Alexa 647 (IA) and Alexa 555 (IB) log intensities respectively. Plots B, D, and F corresponded to the log vs log for 6, 8 and 12 hour intervals, respectively. Graphs after data normalization and filtering with SpotXel and MIDAS were plotted using the MIDAS software.

If the two intensities are equal to each other the spots will follow the trend line. The spot intensities higher than this line represent upregulated genes. The spot intensities below the trend line are down regulated in response to L19 treatment. Based on Stekel (2003), if the log intensities behaved equally, all points should show the bell shape in the histogram which is evident for these experiments (Figure 20) and be scattered across the regression line (Figure 21B, D and F).

The ratio to Intensity plots (R-I plots) remove dye bias and low quality data or noise (Quackenbush, 2002; Figure 22). RI plot normalization was chosen to disclose specific intensities dependent on $\text{Log}_2(\text{IB}/\text{IA})$. Locally Weighted Linear Regression (Lowess) normalization was displayed as $\text{Log}_2(\text{IB}/\text{IA})$ expression versus the log_{10} of the Alexa 555 times the Alexa 647 intensities ($\text{Log}_{10}(\text{IA} \cdot \text{IB})$). The RI plot facilitates data comparison and correct spatial and symmetric variation (Quackenbush, 2002). Most of the total intensity spots were located near the lower left of each panel especially for 6 hr (Figure 22A), indicating that the majority or genes were not affected by L19. The 8 hr exposure showed the most dispersed set of genes in response to L19 (Figure 22B). After 12 hours, fewer genes were visible (Figure 22C). The genes that showed differential expression are listed in Table 11.

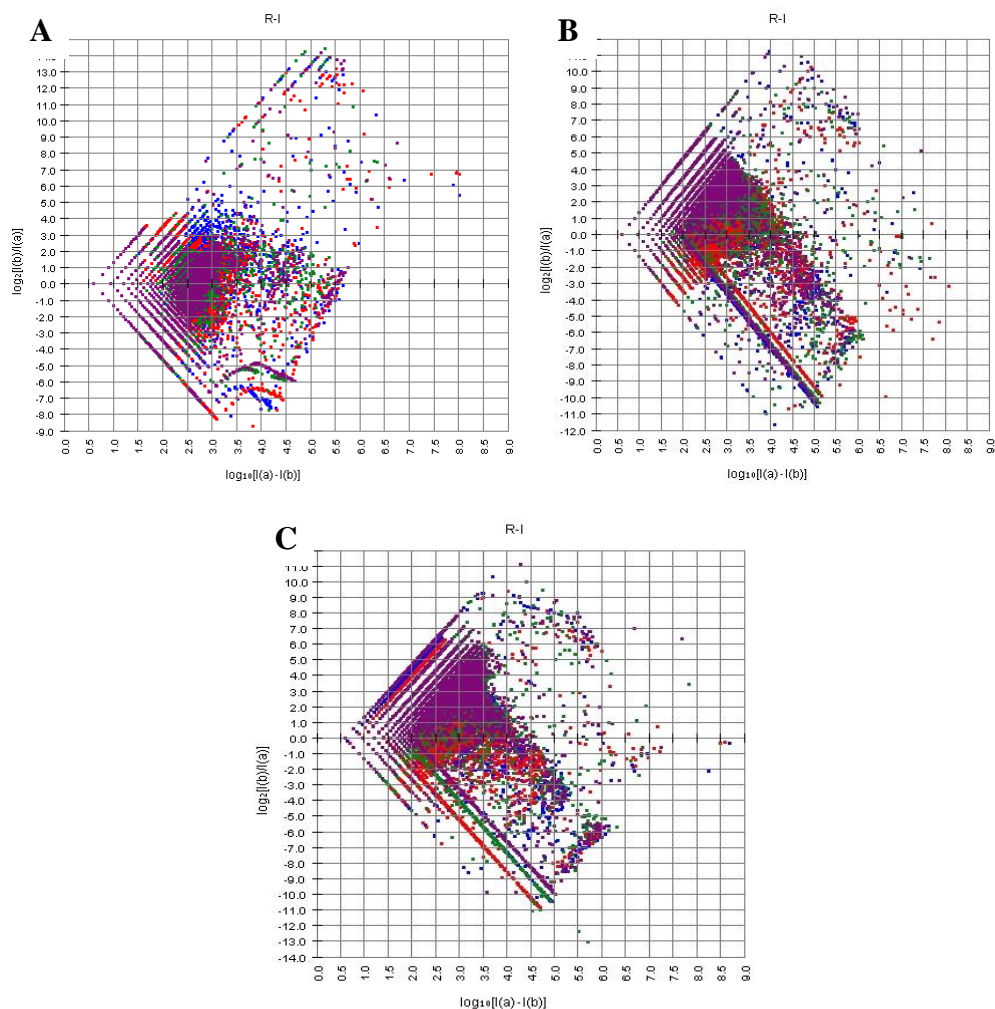


Figure 22. Specific intensity-dependent log (IB/A) plot (R-I plot). Lowess data normalization analysis has been applied for average total intensity of Labelled cDNA of treated and untreated DLD-1 cells. IA and IB are defined as channel A and channel B spot intensity respectively. R-I graphs were plotted for each of 6H (A), 8H (B) and 12H (C). Data were normalized and visualized using MIDAS.

Flip-dye Diagnostic normalization was used to remove inconsistent or questionable data as compared to the two dye swapped arrays. Figure 23 shows the results for the dye-swap experiments, blue scatter plots denoted treated cDNA labeled with Alexa Fluor 555 and untreated cDNA labeled with Alexa Fluor 647. The red scatter plot showed opposite labeling of blue plot (Alexa Fluor 555 labeled untreated with Alexa Fluor 647 labeled treated). Most of the total intensities spots in plots C and D were widely distributed which showed more gene expression in 8 hours in comparison to 6 and 12 hours (Figure 23).

The ANOVA compared all three independent time points of the microarray gene expression (Tables 9, 10). The one-way ANOVA showed a large difference between the mean of each of the three-time point groups ($F_{2,32776} = 8.77$, $p < 0.001$; Table 10) and therefore, the null hypothesis was rejected.

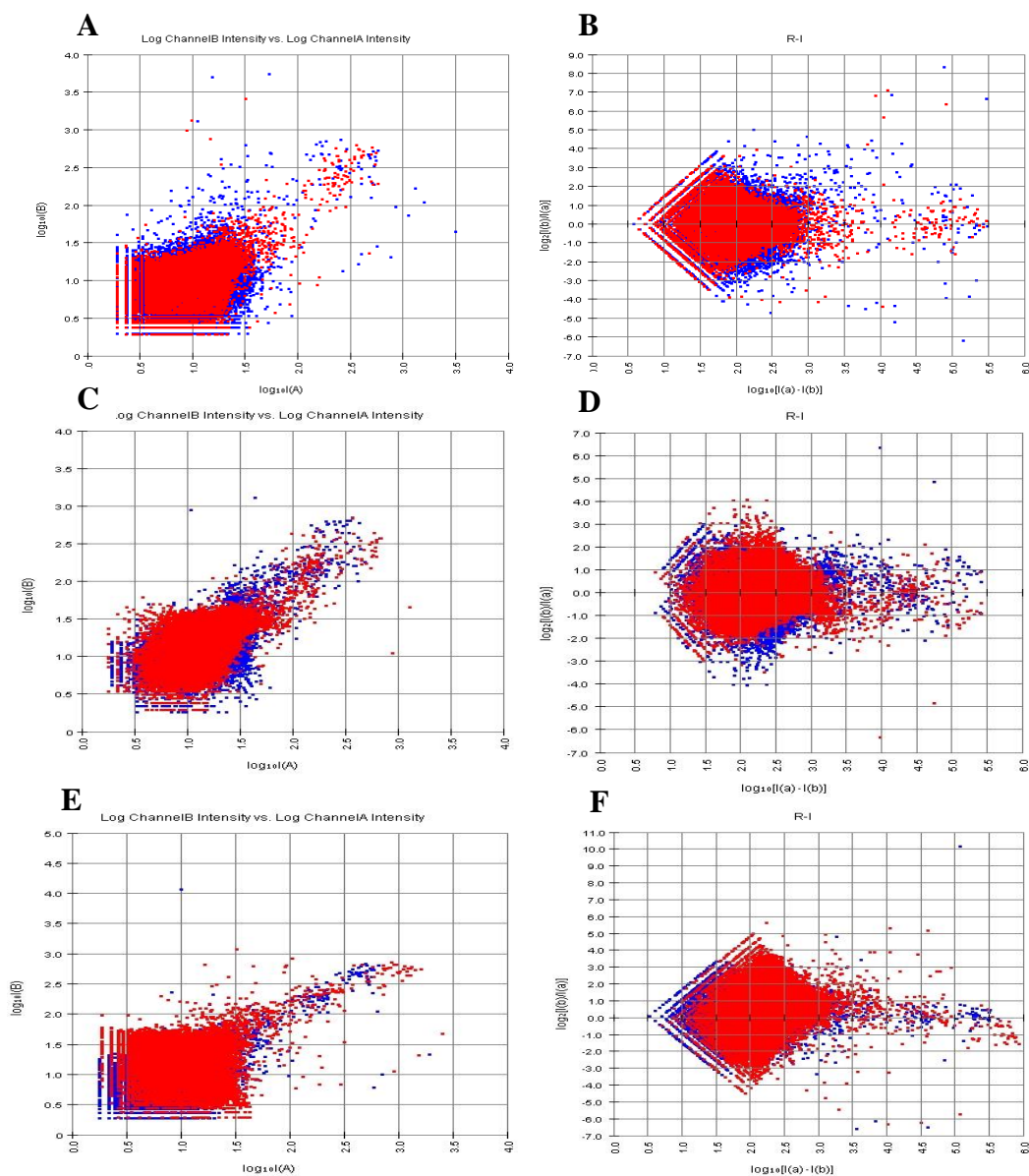


Figure 23. Diagnostic plots for two different arrays in the dye-swap experiments. Blue scatter plots denoted Alexa 555 treated and Alexa 647 untreated and red plots represented Alexa 647 treated and Alexa 555 untreated DLD-1 cells. Panels A & B (6 hour), C & D (8 hour) and E & F (12 hour) represent each of the treatment time intervals. These plots were normalized by Spotxel and plotted by Tiger MIDAS.

Table 9. Results of an analysis of variance for three independent time points groups for microarray gene expression results.

| Groups | Count | Sum | Average \pm variance |
|--------------------|--------------|------------|--|
| 6hr IB ave | 7794 | 275.105 | 0.035 \pm 0.177 |
| 8hr IB ave | 11850 | 41.508 | 0.003 \pm 0.222 |
| 12hr IB ave | 13135 | 248.499 | 0.018 \pm 0.378 |

Table 10. Results of a one-way analysis of variance of three independent time points groups for Microarray gene expression results, F and P-value for total intensities of different time points for Microarray fold change results.

| Source of Variation | SS | df | MS | F | P-value |
|----------------------------|-----------|-----------|-----------|----------|----------------|
| Between Groups | 4.814 | 2 | 2.407 | 8.772 | 0.000 |
| Within Groups | 8993.627 | 32776 | 0.274 | | |
| Total | 8998.442 | 32778 | | | |

Genes Affected by L19

BRB Array tools was used to match the gene IDs to their function in order to determine other cellular processes that were affected by exposure to L19. Some genes had their respective functions up- or down-regulated (Table 11). There are several cancer genes in key signaling pathways that have players both-up and down-regulated such as: MAPKinsase pathway, Interleukin (IL) cytokine pathway, Cell death (CD), and p53. Additionally, there are numerous neurological, olfactory, and metabolic pathways affected, suggesting that L19 could be applied against diseases other than cancer, but could also have detrimental side effects.

Table 11. Microarray genes affected by L19 at 6, 8, and 12 hours. Greater than 1.5-fold change and lower than 0.5 were considered significant. BRB-Array Tools was used to generate the Defined Genelists.

A: Upregulated genes

| 6 Hours | | |
|-----------------|---|--------------------|
| Symbol | Defined Gene Lists | Fold Change |
| OR2C1 | Olfactory transduction | 3.573 |
| TAOK1 | MAPK signaling pathway | 2.485 |
| EFNA2 | Axon guidance | 1.447 |
| 8 Hours | | |
| PTH1R | Neuroactive ligand-receptor interaction | 2.193 |
| RANBP2 | Cycling of Ran in nucleocytoplasmic transport, Mechanism of Protein Import into the Nucleus, Sumoylation by RanBP2 Regulates Transcriptional Repression, RNA transport | 1.655 |
| PRCP | Protein digestion and absorption | 1.406 |
| 12 Hours | | |
| SLC16A10 | Protein digestion and absorption | 2.276 |
| PRLHR | Neuroactive ligand-receptor interaction | 2.155 |
| NUDT12 | Nicotinate and nicotinamide metabolism, Peroxisome | 2.036 |
| CD74 | Antigen Processing and Presentation, Antigen processing and presentation | 1.944 |
| RAP2B | Phospholipase C-epsilon pathway | 1.892 |
| OR1D5 | Olfactory transduction | 1.814 |
| PEX13 | Peroxisome | 1.662 |
| DLST | Citrate cycle (TCA cycle), Lysine degradation, Metabolic pathways | 1.551 |
| DCTN1 | Lissencephaly gene (LIS1) in neuronal migration and development, Huntington's disease, Vasopressin-regulated water reabsorption | 1.551 |
| SNF8 | Endocytosis | 1.512 |

| B: Downregulated genes | | |
|-------------------------------|--|--------------------|
| 6 Hours | | |
| Symbol | Defined Gene Lists | Fold Change |
| FZD9FZD9+S18:US20:U183 | Basal cell carcinoma, Melanogenesis, Pathways in cancer, Wnt signaling pathway | 0.791 |
| GRIN3A | Neuroactive ligand-receptor interaction | 0.788 |
| FOLH1 | Vitamin digestion and absorption | 0.778 |
| SLC1A5 | Protein digestion and absorption | 0.766 |
| NPC1L1 | Fat digestion and absorption | 0.766 |
| POGLUT1 | Other types of O-glycan biosynthesis | 0.766 |
| GSTK1 | Drug metabolism - cytochrome P450, Glutathione metabolism, Metabolism of xenobiotics by cytochrome P450, Peroxisome | 0.762 |
| NNT | Metabolic pathways, Nicotinate and nicotinamide metabolism | 0.762 |
| NR0B1 | CARM1 and Regulation of the Estrogen Receptor | 0.748 |
| RAD9A | Role of BRCA1, BRCA2 and ATR in Cancer Susceptibility | 0.724 |
| PLA2G2A | alpha-Linolenic acid metabolism, Arachidonic acid metabolism, Ether lipid metabolism, Fat digestion and absorption, Fc epsilon RI signaling pathway, Glycerophospholipid metabolism, GnRH signaling pathway, Linoleic acid metabolism, Long-term depression, MAPK signaling pathway, Metabolic pathways, Pancreatic secretion, Toxoplasmosis, Vascular smooth muscle contraction, VEGF signaling pathway | 0.722 |
| GNAT1 | Phototransduction | 0.722 |
| SNAP29 | SNARE interactions in vesicular transport | 0.722 |
| PPP2R1B | Chagas disease (American trypanosomiasis), Hepatitis C, Long-term depression, mRNA surveillance pathway, Oocyte meiosis, TGF-beta signaling pathway, Tight junction, Wnt signaling pathway | 0.722 |
| MAP3K8 | MAPKinase Signaling Pathway, MAPK signaling pathway, T cell receptor signaling pathway, Toll-like receptor signaling pathway | 0.722 |
| NUTF2 | Mechanism of Protein Import into the Nucleus | 0.700 |
| DPYD | beta-Alanine metabolism, Drug metabolism - other enzymes, Metabolic pathways, Pantothenate and CoA biosynthesis, Pyrimidine metabolism | 0.678 |
| ENTPD4 | Lysosome, Purine metabolism, Pyrimidine metabolism | 0.678 |

| | | |
|--------|--|-------|
| PCNA | p53 Signaling Pathway, Base excision repair, Cell cycle, DNA replication, Mismatch repair, Nucleotide excision repair | 0.678 |
| B3GAT1 | Glycosaminoglycan biosynthesis - chondroitin sulfate / dermatan sulfate, Glycosaminoglycan biosynthesis - heparan sulfate / heparin, Metabolic pathways | 0.678 |
| ABCC6 | ABC transporters | 0.678 |
| IRF7 | The information-processing pathway at the IFN-beta enhancer, Cytosolic DNA-sensing pathway, Hepatitis C, RIG-I-like receptor signaling pathway, Toll-like receptor signaling pathway | 0.678 |
| IL3 | Cytokine Network, Cytokines and Inflammatory Response, Dendritic cells in regulating TH1 and TH2 Development, Erythrocyte Differentiation Pathway, IL 17 Signaling Pathway, IL 3 signaling pathway, Regulation of BAD phosphorylation, Regulation of hematopoiesis by cytokines, The Role of Eosinophils in the Chemokine Network of Allergy, Apoptosis, Asthma, Cytokine-cytokine receptor interaction, Fc epsilon RI signaling pathway, Hematopoietic cell lineage, Jak-STAT signaling pathway | 0.670 |
| OR52H1 | Olfactory transduction | 0.637 |
| MYL5 | Focal adhesion, Leukocyte transendothelial migration, Regulation of actin cytoskeleton, Tight junction | 0.632 |
| SESN3 | p53 signaling pathway | 0.632 |
| DLG4 | Nitric Oxide Signaling Pathway, Synaptic Proteins at the Synaptic Junction, Huntington's disease | 0.632 |
| LAMB2 | Amoebiasis, ECM-receptor interaction, Focal adhesion, Pathways in cancer, Small cell lung cancer, Toxoplasmosis | 0.632 |
| PIGB | Glycosylphosphatidylinositol(GPI)-anchor biosynthesis, Metabolic pathways | 0.632 |
| ZAP70 | Activation of Csk by cAMP-dependent Protein Kinase Inhibits Signaling through the T Cell Receptor, Lck and Fyn tyrosine kinases in initiation of TCR Activation, T Cell Receptor Signaling Pathway, Natural killer cell mediated cytotoxicity, Primary immunodeficiency, T cell receptor signaling pathway | 0.632 |
| NDUFS5 | Alzheimer's disease, Huntington's disease, Metabolic pathways, Oxidative phosphorylation, Parkinson's disease | 0.632 |
| AVP | Control of skeletal myogenesis by HDAC & calcium/calmodulin-dependent kinase (CaMK), Vasopressin-regulated water reabsorption | 0.631 |
| RBKS | Pentose phosphate pathway | 0.614 |
| NDST1 | Glycosaminoglycan biosynthesis - heparan sulfate / heparin, Metabolic pathways | 0.609 |
| LILRB2 | Osteoclast differentiation | 0.601 |
| STX2 | SNARE interactions in vesicular transport | 0.585 |
| RFT1 | N-Glycan biosynthesis | 0.585 |
| RXRA | Basic mechanism of action of PPARa, PPARb(d) and PPARg and effects on gene expression, Control of Gene Expression by Vitamin D Receptor, Degradation of the RAR and RXR by the proteasome, FXR and LXR Regulation of Cholesterol Metabolism, | 0.585 |

| | | |
|---------|--|-------|
| | Map Kinase Inactivation of SMRT Corepressor, Mechanism of Gene Regulation by Peroxisome Proliferators via PPAR α (alpha), Nuclear receptors coordinate the activities of chromatin remodeling complexes and coactivators to facilitate initiation of transcription in carcinoma cells, Role of PPAR-gamma Coactivators in Obesity and Thermogenesis, Transcription Regulation by Methyltransferase of CARM1, Visceral Fat Deposits and the Metabolic Syndrome, Adipocytokine signaling pathway, Bile secretion, Hepatitis C, Non-small cell lung cancer, Pathways in cancer, PPAR signaling pathway, Small cell lung cancer, Thyroid cancer | |
| ADAM17 | g-Secretase mediated ErbB4 Signaling Pathway, Presenilin action in Notch and Wnt signaling, Proteolysis and Signaling Pathway of Notch , Alzheimer's disease, Epithelial cell signaling in Helicobacter pylori infection, Notch signaling pathway | 0.585 |
| PPP2R5B | mRNA surveillance pathway, Oocyte meiosis, Wnt signaling pathway | 0.585 |
| CUL3 | Ubiquitin mediated proteolysis | 0.585 |
| PFN3 | Regulation of actin cytoskeleton, Shigellosis | 0.585 |
| SLC1A3 | Malate-aspartate shuttle | 0.585 |
| PSMD3 | Proteasome | 0.536 |
| TSHR | Autoimmune thyroid disease, Neuroactive ligand-receptor interaction | 0.536 |
| LIN7A | Chaperones modulate interferon Signaling Pathway | 0.536 |
| CBLB | Bacterial invasion of epithelial cells, Chronic myeloid leukemia, Endocytosis, ErbB signaling pathway, Insulin signaling pathway, Jak-STAT signaling pathway, Pathways in cancer, T cell receptor signaling pathway, Ubiquitin mediated proteolysis | 0.536 |
| PDE6A | Visual Signal Transduction, Phototransduction, Purine metabolism | 0.536 |
| TSC1 | mTOR Signaling Pathway, Insulin signaling pathway, mTOR signaling pathway | 0.536 |
| TAS2R20 | Taste transduction | 0.536 |
| LIPT2 | Lipoic acid metabolism, Metabolic pathways | 0.531 |
| PARD6B | Endocytosis, Tight junction | 0.526 |
| ATP5A1 | Electron Transport Reaction in Mitochondria, Alzheimer's disease, Huntington's disease, Metabolic pathways, Oxidative phosphorylation, Parkinson's disease | 0.521 |
| TXNRD1 | Pyrimidine metabolism, Selenocompound metabolism | 0.485 |
| GNA14 | Amoebiasis, Calcium signaling pathway, Chagas disease (American trypanosomiasis) | 0.485 |
| CLDN10 | Cell adhesion molecules (CAMs), Hepatitis C, Leukocyte transendothelial migration, Tight junction | 0.485 |
| PSME3 | Antigen processing and presentation, Hepatitis C, Proteasome | 0.485 |

| | | |
|----------|--|-------|
| COX6B2 | Alzheimer's disease, Cardiac muscle contraction, Huntington's disease, Metabolic pathways, Oxidative phosphorylation, Parkinson's disease | 0.485 |
| ATF6B | Protein processing in endoplasmic reticulum | 0.485 |
| IFNW1 | Cytokine-cytokine receptor interaction, Jak-STAT signaling pathway, RIG-I-like receptor signaling pathway | 0.485 |
| HNF4G | Maturity onset diabetes of the young | 0.485 |
| IL33 | Cytosolic DNA-sensing pathway | 0.485 |
| ARSA | Lysosome, Sphingolipid metabolism | 0.485 |
| RPS11 | Ribosome | 0.485 |
| FGA | Acute Myocardial Infarction, Extrinsic Prothrombin Activation Pathway, Fibrinolysis Pathway, Intrinsic Prothrombin Activation Pathway, Complement and coagulation cascades | 0.485 |
| BMP4 | ALK in cardiac myocytes, Basal cell carcinoma, Hedgehog signaling pathway, Pathways in cancer, TGF-beta signaling pathway | 0.466 |
| DDX3Y | RIG-I-like receptor signaling pathway | 0.455 |
| EED | The PRC2 Complex Sets Long-term Gene Silencing Through Modification of Histone Tails | 0.444 |
| RELA | Acetylation and Deacetylation of RelA in The Nucleus, Activation of PKC through G protein coupled receptor, AKT Signaling Pathway, ATM Signaling Pathway, Bone Remodelling, Cadmium induces DNA synthesis and proliferation in macrophages, CD40L Signaling Pathway, Ceramide Signaling Pathway, Chaperones modulate interferon Signaling Pathway, Corticosteroids and cardioprotection, CXCR4 Signaling Pathway, Double Stranded RNA Induced Gene Expression, Erythropoietin mediated neuroprotection through NF-kB, fMLP induced chemokine gene expression in HMC-1 cells, Free Radical Induced Apoptosis, HIV-1 Nef: negative effector of Fas and TNF, Human Cytomegalovirus and Map Kinase Pathways, Inactivation of Gsk3 by AKT causes accumulation of b-catenin in Alveolar Macrophages, Induction of apoptosis through DR3 and DR4/5 Death Receptors , Influence of Ras and Rho proteins on G1 to S Transition, Keratinocyte Differentiation, MAPKinase Signaling Pathway, Mechanism of Gene Regulation by Peroxisome Proliferato ... | 0.433 |
| HS6ST2 | Glycosaminoglycan biosynthesis - heparan sulfate / heparin | 0.433 |
| PAFAH1B2 | Ether lipid metabolism, Metabolic pathways | 0.433 |
| CYP26A1 | Nuclear Receptors in Lipid Metabolism and Toxicity, Retinol metabolism | 0.433 |
| DIAPH2 | Regulation of actin cytoskeleton | 0.433 |
| PRKCQ | Keratinocyte Differentiation, Adipocytokine signaling pathway, T cell receptor signaling pathway, Tight junction, Vascular smooth muscle contraction | 0.433 |
| ATP5J | Alzheimer's disease, Huntington's disease, Metabolic pathways, Oxidative phosphorylation, Parkinson's disease | 0.433 |

| | | |
|-----------|--|-------|
| GRIK2 | Neuroactive ligand-receptor interaction | 0.433 |
| BET1L | SNARE interactions in vesicular transport | 0.433 |
| TNFRSF11B | Cytokine-cytokine receptor interaction, Osteoclast differentiation | 0.433 |
| HLA-DMB | Allograft rejection, Antigen processing and presentation, Asthma, Autoimmune thyroid disease, Cell adhesion molecules (CAMs), Graft-versus-host disease, Intestinal immune network for IgA production, Leishmaniasis, Phagosome, Rheumatoid arthritis, Staphylococcus aureus infection, Systemic lupus erythematosus, Toxoplasmosis, Type I diabetes mellitus, Viral myocarditis | 0.431 |
| MTHFR | Metabolic pathways, One carbon pool by folate | 0.415 |
| SUV420H2 | Lysine degradation | 0.415 |
| PVRL3 | Adherens junction, Cell adhesion molecules (CAMs) | 0.402 |
| PHF5A | Spliceosome | 0.399 |
| CD9 | Hematopoietic cell lineage | 0.383 |
| NAMPT | Nicotinate and nicotinamide metabolism | 0.383 |
| NKX2-2 | Maturity onset diabetes of the young | 0.379 |
| HIST1H3G | Systemic lupus erythematosus | 0.379 |
| CREB5 | Huntington's disease, Prostate cancer, Vasopressin-regulated water reabsorption | 0.379 |
| GHSR | Neuroactive ligand-receptor interaction | 0.379 |
| AGK | Glycerolipid metabolism, Metabolic pathways | 0.379 |
| FZR1 | Cell cycle, Progesterone-mediated oocyte maturation, Ubiquitin mediated proteolysis | 0.379 |
| PNLIP | Fat digestion and absorption, Glycerolipid metabolism, Metabolic pathways, Pancreatic secretion, Vitamin digestion and absorption | 0.379 |
| CR1 | B Lymphocyte Cell Surface Molecules, Complement and coagulation cascades, Hematopoietic cell lineage, Leishmaniasis, Malaria | 0.379 |
| CDC40 | Spliceosome | 0.379 |
| CARD8 | NOD-like receptor signaling pathway | 0.379 |
| AKT3 | Acute myeloid leukemia, Adipocytokine signaling pathway, Apoptosis, B cell receptor signaling pathway, Carbohydrate digestion and absorption, Chagas disease (American trypanosomiasis), Chemokine signaling pathway, Chronic myeloid leukemia, Colorectal cancer, Endometrial cancer, ErbB signaling pathway, Fc epsilon RI signaling pathway, Fc gamma R-mediated phagocytosis, Focal adhesion, Glioma, Hepatitis C, Insulin signaling pathway, Jak-STAT signaling pathway, MAPK signaling pathway, Melanoma, mTOR signaling pathway, Neurotrophin signaling pathway, Non-small cell lung cancer, Osteoclast differentiation, Pancreatic cancer, Pathways in cancer, Progesterone-mediated oocyte maturation, Prostate cancer, Renal cell carcinoma, Small cell lung cancer, T cell receptor signaling | 0.379 |

| | | |
|---------|---|-------|
| | pathway, Tight junction, Toll-like receptor signaling pathway, Toxoplasmosis, VEGF signaling pathway | |
| CRB3 | Tight junction | 0.379 |
| CDK7 | Cyclins and Cell Cycle Regulation, Degradation of the RAR and RXR by the proteasome, Estrogen-responsive protein Efp controls cell cycle and breast tumors growth, Sonic Hedgehog (SHH) Receptor Ptc1 Regulates cell cycle, Cell cycle, Nucleotide excision repair | 0.379 |
| IQSEC3 | Endocytosis | 0.379 |
| VAMP1 | SNARE interactions in vesicular transport | 0.363 |
| GUCY1A3 | Ion Channels and Their Functional Role in Vascular Endothelium, Gap junction, Long-term depression, Purine metabolism, Salivary secretion, Vascular smooth muscle contraction | 0.359 |
| COX7C | Alzheimer's disease, Cardiac muscle contraction, Huntington's disease, Metabolic pathways, Oxidative phosphorylation, Parkinson's disease | 0.348 |
| OR4A15 | Olfactory transduction | 0.334 |
| TWIST1 | Tumor Suppressor Arf Inhibits Ribosomal Biogenesis | 0.333 |
| SRSF2 | Spliceosomal Assembly, Spliceosome | 0.322 |
| PAQR7 | How Progesterone Initiates the Oocyte Maturation | 0.322 |
| RENBP | Amino sugar and nucleotide sugar metabolism | 0.322 |
| XCL1 | Chemokine signaling pathway, Cytokine-cytokine receptor interaction | 0.322 |
| KCNMA1 | Pancreatic secretion, Salivary secretion, Vascular smooth muscle contraction | 0.322 |
| TPM2 | Cardiac muscle contraction, Dilated cardiomyopathy, Hypertrophic cardiomyopathy (HCM) | 0.322 |
| FOLR2 | Endocytosis | 0.322 |
| JAK3 | IL 2 signaling pathway, IL 4 signaling pathway, IL 6 signaling pathway, IL-2 Receptor Beta Chain in T cell Activation, IL22 Soluble Receptor Signaling Pathway , IL-7 Signal Transduction, Stat3 Signaling Pathway, Chemokine signaling pathway, Jak-STAT signaling pathway, Primary immunodeficiency | 0.322 |
| OR10C1 | Olfactory transduction | 0.322 |
| SETD7 | Lysine degradation | 0.322 |
| LDHAL6B | Cysteine and methionine metabolism, Glycolysis / Gluconeogenesis, Metabolic pathways, Propanoate metabolism, Pyruvate metabolism | 0.322 |
| TAS2R60 | Taste transduction | 0.322 |
| RELT | Cytokine-cytokine receptor interaction | 0.322 |
| PRKCSH | Protein processing in endoplasmic reticulum | 0.322 |
| POLR3H | Cytosolic DNA-sensing pathway, Metabolic pathways, Purine metabolism, Pyrimidine metabolism, RNA polymerase | 0.303 |

| | | |
|---------|---|-------|
| KLK2 | Erk1/Erk2 Mapk Signaling pathway, Nerve growth factor pathway (NGF), Phosphorylation of MEK1 by cdk5/p35 down regulates the MAP kinase pathway, Trka Receptor Signaling Pathway | 0.300 |
| GABRA5 | Cardiac Protection Against ROS, Gamma-aminobutyric Acid Receptor Life Cycle, Neuroactive ligand-receptor interaction | 0.284 |
| NT5C2 | Metabolic pathways, Nicotinate and nicotinamide metabolism, Purine metabolism, Pyrimidine metabolism | 0.284 |
| SGPP2 | Sphingolipid metabolism | 0.263 |
| ARAF | Acute myeloid leukemia, Bladder cancer, Chronic myeloid leukemia, Colorectal cancer, Endometrial cancer, ErbB signaling pathway, Glioma, Hepatitis C, Insulin signaling pathway, Long-term depression, Long-term potentiation, Melanoma, Natural killer cell mediated cytotoxicity, Non-small cell lung cancer, Pancreatic cancer, Pathways in cancer, Progesterone-mediated oocyte maturation, Prostate cancer, Regulation of actin cytoskeleton, Renal cell carcinoma, Vascular smooth muscle contraction | 0.263 |
| PSMA8 | Proteasome | 0.263 |
| HRH1 | Calcium signaling pathway, Neuroactive ligand-receptor interaction | 0.263 |
| EPO | EPO Signaling Pathway, Erythrocyte Differentiation Pathway, Erythropoietin mediated neuroprotection through NF-kB, Hypoxia-Inducible Factor in the Cardiovascular System, Regulation of hematopoiesis by cytokines, Cytokine-cytokine receptor interaction, Hematopoietic cell lineage, Jak-STAT signaling pathway | 0.263 |
| CYP27A1 | Metabolic pathways, PPAR signaling pathway, Primary bile acid biosynthesis | 0.263 |
| NDUFS3 | Alzheimer's disease, Huntington's disease, Metabolic pathways, Oxidative phosphorylation, Parkinson's disease | 0.263 |
| RICTOR | mTOR signaling pathway | 0.263 |
| ATP5B | Alzheimer's disease, Huntington's disease, Metabolic pathways, Oxidative phosphorylation, Parkinson's disease | 0.263 |
| MAFK | Oxidative Stress Induced Gene Expression Via Nrf2 | 0.263 |
| SMS | Arginine and proline metabolism, beta-Alanine metabolism, Cysteine and methionine metabolism, Glutathione metabolism, Metabolic pathways | 0.263 |
| GRIN2B | Nitric Oxide Signaling Pathway, Alzheimer's disease, Amyotrophic lateral sclerosis (ALS), Huntington's disease, Long-term potentiation, Neuroactive ligand-receptor interaction, Systemic lupus erythematosus | 0.263 |
| OCLN | Cell adhesion molecules (CAMs), Hepatitis C, Leukocyte transendothelial migration, Pathogenic Escherichia coli infection, Tight junction | 0.263 |
| BMP8A | Hedgehog signaling pathway, TGF-beta signaling pathway | 0.263 |
| UTS2R | Neuroactive ligand-receptor interaction | 0.263 |
| ABCG8 | ABC transporters, Bile secretion, Fat digestion and absorption | 0.263 |

| | | |
|---------|--|-------|
| GNRH2 | GnRH signaling pathway | 0.254 |
| CLDN4 | Cell adhesion molecules (CAMs), Hepatitis C, Leukocyte transendothelial migration, Tight junction | 0.252 |
| ACTN3 | Cell to Cell Adhesion Signaling, Integrin Signaling Pathway, uCalpain and friends in Cell spread, Adherens junction, Amoebiasis, Arrhythmogenic right ventricular cardiomyopathy (ARVC), Focal adhesion, Leukocyte transendothelial migration, Regulation of actin cytoskeleton, Systemic lupus erythematosus, Tight junction | 0.241 |
| H2AFJ | Systemic lupus erythematosus | 0.222 |
| AP4E1 | Lysosome | 0.214 |
| PQBP1 | Spliceosome | 0.214 |
| CACNG1 | Arrhythmogenic right ventricular cardiomyopathy (ARVC), Cardiac muscle contraction, Dilated cardiomyopathy, Hypertrophic cardiomyopathy (HCM), MAPK signaling pathway | 0.202 |
| IDH3G | Citrate cycle (TCA cycle), Metabolic pathways | 0.202 |
| POMT1 | Other types of O-glycan biosynthesis | 0.202 |
| BDKRB1 | Calcium signaling pathway, Complement and coagulation cascades, Neuroactive ligand-receptor interaction, Regulation of actin cytoskeleton | 0.202 |
| SPCS3 | Protein export | 0.202 |
| RRBP1 | Protein processing in endoplasmic reticulum | 0.202 |
| UBE2NL | Ubiquitin mediated proteolysis | 0.202 |
| GEMIN8 | RNA transport | 0.202 |
| MSR1 | Phagosome | 0.202 |
| HERC1 | Ubiquitin mediated proteolysis | 0.202 |
| ADCY3 | Bile secretion, Calcium signaling pathway, Chemokine signaling pathway, Dilated cardiomyopathy, Gap junction, Gastric acid secretion, GnRH signaling pathway, Melanogenesis, Olfactory transduction, Oocyte meiosis, Pancreatic secretion, Progesterone-mediated oocyte maturation, Purine metabolism, Salivary secretion, Vascular smooth muscle contraction, Vasopressin-regulated water reabsorption, Vibrio cholerae infection | 0.202 |
| EIF4E1B | Insulin signaling pathway, mTOR signaling pathway, RNA transport | 0.202 |
| TIMP1 | Inhibition of Matrix Metalloproteinases | 0.202 |
| TPH1 | Metabolic pathways, Tryptophan metabolism | 0.202 |
| ORC5 | CDK Regulation of DNA Replication, Cell cycle | 0.202 |
| PIGH | Glycosylphosphatidylinositol(GPI)-anchor biosynthesis, Metabolic pathways | 0.202 |
| OR4A16 | Olfactory transduction | 0.202 |
| HNF4A | Maturity onset diabetes of the young | 0.193 |

| | | |
|---------|--|-------|
| STAT4 | IL12 and Stat4 Dependent Signaling Pathway in Th1 Development, NO2-dependent IL 12 Pathway in NK cells, Jak-STAT signaling pathway | 0.193 |
| ORC4 | CDK Regulation of DNA Replication, Cell cycle | 0.184 |
| EIF2S1 | Apoptotic Signaling in Response to DNA Damage, Double Stranded RNA Induced Gene Expression, Eukaryotic protein translation, Regulation of eIF2, Skeletal muscle hypertrophy is regulated via AKT/mTOR pathway, VEGF, Hypoxia, and Angiogenesis, Hepatitis C, Protein processing in endoplasmic reticulum, RNA transport | 0.170 |
| TAAR9 | Neuroactive ligand-receptor interaction | 0.170 |
| CYP19A1 | Metabolic pathways, Steroid hormone biosynthesis | 0.163 |
| GSK3A | Phosphoinositides and their downstream targets., Chemokine signaling pathway | 0.152 |
| F5 | Extrinsic Prothrombin Activation Pathway, Intrinsic Prothrombin Activation Pathway, Complement and coagulation cascades | 0.138 |
| CPA2 | Pancreatic secretion, Protein digestion and absorption | 0.138 |
| SLIT1 | Axon guidance | 0.138 |
| OR6C75 | Olfactory transduction | 0.138 |
| LSM5 | RNA degradation, Spliceosome | 0.138 |
| UGT2B15 | Ascorbate and aldarate metabolism, Drug metabolism - cytochrome P450, Drug metabolism - other enzymes, Metabolic pathways, Metabolism of xenobiotics by cytochrome P450, Other types of O-glycan biosynthesis, Pentose and glucuronate interconversions, Porphyrin and chlorophyll metabolism, Retinol metabolism, Starch and sucrose metabolism, Steroid hormone biosynthesis | 0.138 |
| RAN | Cycling of Ran in nucleocytoplasmic transport, Mechanism of Protein Import into the Nucleus, Role of Ran in mitotic spindle regulation, Sumoylation by RanBP2 Regulates Transcriptional Repression, Ribosome biogenesis in eukaryotes, RNA transport | 0.138 |
| CSF3R | Cytokine-cytokine receptor interaction, Hematopoietic cell lineage, Jak-STAT signaling pathway, Pathways in cancer | 0.138 |
| PLCD3 | Calcium signaling pathway, Inositol phosphate metabolism, Metabolic pathways, Phosphatidylinositol signaling system | 0.138 |
| GALNT7 | Metabolic pathways, Mucin type O-Glycan biosynthesis | 0.138 |
| RRM2 | Glutathione metabolism, Metabolic pathways, p53 signaling pathway, Purine metabolism, Pyrimidine metabolism | 0.138 |
| XPC | Nucleotide excision repair | 0.138 |
| SEMA3C | Axon guidance | 0.138 |
| CHI3L1 | Amino sugar and nucleotide sugar metabolism | 0.138 |
| ERBB2 | Role of ERBB2 in Signal Transduction and Oncology, Trefoil Factors Initiate Mucosal Healing, Adherens junction, Bladder cancer, Calcium signaling pathway, Endometrial cancer, ErbB | 0.138 |

| | | |
|---------|---|-------|
| | signaling pathway, Focal adhesion, Non-small cell lung cancer, Pancreatic cancer, Pathways in cancer, Prostate cancer | |
| CHST13 | Glycosaminoglycan biosynthesis - chondroitin sulfate / dermatan sulfate, Sulfur metabolism | 0.138 |
| CCL21 | Chemokine signaling pathway, Cytokine-cytokine receptor interaction | 0.138 |
| PPP1R1A | Long-term potentiation | 0.138 |
| RAP2B | Phospholipase C-epsilon pathway | 0.138 |
| RPTOR | Insulin signaling pathway, mTOR signaling pathway | 0.131 |
| NOP56 | Ribosome biogenesis in eukaryotes | 0.131 |
| U2AF1 | Spliceosomal Assembly, Shigellosis, Spliceosome | 0.112 |
| MAPK9 | MAPKinase Signaling Pathway, Adipocytokine signaling pathway, Chagas disease (American trypanosomiasis), Colorectal cancer, Epithelial cell signaling in Helicobacter pylori infection, ErbB signaling pathway, Fc epsilon RI signaling pathway, Focal adhesion, GnRH signaling pathway, Hepatitis C, Insulin signaling pathway, MAPK signaling pathway, Neurotrophin signaling pathway, NOD-like receptor signaling pathway, Osteoclast differentiation, Pancreatic cancer, Pathways in cancer, Progesterone-mediated oocyte maturation, Protein processing in endoplasmic reticulum, RIG-I-like receptor signaling pathway, Shigellosis, T cell receptor signaling pathway, Toll-like receptor signaling pathway, Toxoplasmosis, Type II diabetes mellitus, Wnt signaling pathway | 0.111 |
| OR4C46 | Olfactory transduction | 0.111 |
| ATP2B2 | Calcium signaling pathway, Pancreatic secretion, Salivary secretion | 0.091 |
| CNTN1 | Cell adhesion molecules (CAMs) | 0.070 |
| TIAM2 | Chemokine signaling pathway, Regulation of actin cytoskeleton | 0.070 |
| CNOT7 | RNA degradation | 0.070 |
| CHRNA3 | Neuroactive ligand-receptor interaction | 0.070 |
| PARN | RNA degradation | 0.070 |
| PELP1 | CARM1 and Regulation of the Estrogen Receptor, Pelp1 Modulation of Estrogen Receptor Activity | 0.070 |
| POLG | Metabolic pathways | 0.070 |
| IL4R | IL 4 signaling pathway, Selective expression of chemokine receptors during T-cell polarization, Th1/Th2 Differentiation, Cytokine-cytokine receptor interaction, Hematopoietic cell lineage, Jak-STAT signaling pathway | 0.070 |
| OR4C15 | Olfactory transduction | 0.070 |
| BMS1 | Ribosome biogenesis in eukaryotes | 0.070 |
| NLRX1 | RIG-I-like receptor signaling pathway | 0.070 |

| | | |
|--------|--|-------|
| ODC1 | Arginine and proline metabolism, Glutathione metabolism, Metabolic pathways | 0.070 |
| ATXN3 | Protein processing in endoplasmic reticulum | 0.070 |
| ACSL6 | Adipocytokine signaling pathway, Fatty acid degradation, Metabolic pathways, Peroxisome, PPAR signaling pathway | 0.070 |
| TRAF5 | Pathways in cancer, Small cell lung cancer | 0.070 |
| GRIK3 | Neuroactive ligand-receptor interaction | 0.070 |
| ACTC1 | Cardiac muscle contraction, Dilated cardiomyopathy, Hypertrophic cardiomyopathy (HCM) | 0.070 |
| RPL41 | Ribosome | 0.070 |
| F13A1 | Fibrinolysis Pathway, Complement and coagulation cascades | 0.070 |
| CPSF4 | Polyadenylation of mRNA, mRNA surveillance pathway | 0.070 |
| CDH2 | Arrhythmogenic right ventricular cardiomyopathy (ARVC), Cell adhesion molecules (CAMs) | 0.070 |
| CXCL6 | Chemokine signaling pathway, Cytokine-cytokine receptor interaction, Rheumatoid arthritis | 0.070 |
| MRVI1 | Vascular smooth muscle contraction | 0.069 |
| THBS4 | ECM-receptor interaction, Focal adhesion, Malaria, Phagosome, TGF-beta signaling pathway | 0.067 |
| CD8B | Antigen processing and presentation, Cell adhesion molecules (CAMs), Hematopoietic cell lineage, Primary immunodeficiency, T cell receptor signaling pathway | 0.067 |
| CXCR6 | Chemokine signaling pathway, Cytokine-cytokine receptor interaction | 0.067 |
| CCNB2 | Estrogen-responsive protein Efp controls cell cycle and breast tumors growth, Cell cycle, Oocyte meiosis, p53 signaling pathway, Progesterone-mediated oocyte maturation | 0.064 |
| MBTPS2 | SREBP control of lipid synthesis, Protein processing in endoplasmic reticulum | 0.057 |
| LEF1 | Inactivation of Gsk3 by AKT causes accumulation of b-catenin in Alveolar Macrophages, Multi-step Regulation of Transcription by Pitx2, Acute myeloid leukemia, Adherens junction, Arrhythmogenic right ventricular cardiomyopathy (ARVC), Basal cell carcinoma, Colorectal cancer, Endometrial cancer, Melanogenesis, Pathways in cancer, Prostate cancer, Thyroid cancer, Wnt signaling pathway | 0.052 |
| DUSP3 | MAPK signaling pathway | 0.052 |

| B: Downregulated genes | | |
|-------------------------------|---|--------------------|
| 8 Hours | | |
| Symbol | Defined Gene Lists | Fold Change |
| MBTPS2 | SREBP control of lipid synthesis, Protein processing in endoplasmic reticulum | 0.788 |
| GSK3A | Phosphoinositides and their downstream targets., Chemokine signaling pathway | 0.786 |
| POLG | Metabolic pathways | 0.781 |
| THTPA | Metabolic pathways, Thiamine metabolism | 0.778 |
| GMPPA | Amino sugar and nucleotide sugar metabolism, Fructose and mannose metabolism, Metabolic pathways | 0.778 |
| IFIT1B | Hepatitis C | 0.766 |
| GABRG1 | Neuroactive ligand-receptor interaction | 0.766 |
| OR10C1 | Olfactory transduction | 0.766 |
| HTR5A | Calcium signaling pathway, Neuroactive ligand-receptor interaction | 0.766 |
| TRPC5 | Ion Channels and Their Functional Role in Vascular Endothelium | 0.766 |
| FZR1 | Cell cycle, Progesterone-mediated oocyte maturation, Ubiquitin mediated proteolysis | 0.764 |
| KCNJ13 | Protein digestion and absorption | 0.762 |
| ITPR1 | Alzheimer's disease, Calcium signaling pathway, Gap junction, Gastric acid secretion, GnRH signaling pathway, Huntington's disease, Long-term depression, Long-term potentiation, Oocyte meiosis, Pancreatic secretion, Phosphatidylinositol signaling system, Salivary secretion, Vascular smooth muscle contraction | 0.750 |
| ENPP1 | Regulators of Bone Mineralization, Metabolic pathways, Nicotinate and nicotinamide metabolism, Pantothenate and CoA biosynthesis, Purine metabolism, Riboflavin metabolism, Starch and sucrose metabolism | 0.747 |
| MPZL1 | Cell adhesion molecules (CAMs) | 0.741 |
| GRIK2 | Neuroactive ligand-receptor interaction | 0.737 |
| RAF1 | Angiotensin II mediated activation of JNK Pathway via Pyk2 dependent signaling, Aspirin Blocks Signaling Pathway Involved in Platelet Activation, BCR Signaling Pathway, Bioactive Peptide Induced Signaling Pathway, Cadmium induces DNA synthesis and proliferation in macrophages, CCR3 signaling in Eosinophils, Ceramide Signaling Pathway, CXCR4 Signaling Pathway, EGF Signaling Pathway, EPO Signaling Pathway, Erk and PI-3 Kinase Are Necessary for Collagen Binding in Corneal Epithelia, Erk1/Erk2 Mapk | 0.724 |

| | | |
|---------|--|-------|
| | Signaling pathway, Fc Epsilon Receptor I Signaling in Mast Cells, fMLP induced chemokine gene expression in HMC-1 cells, Growth Hormone Signaling Pathway, IGF-1 Signaling Pathway, IL 2 signaling pathway, IL 3 signaling pathway, IL 6 signaling pathway, IL-2 Receptor Beta Chain in T cell Activation, Influence of Ras and Rho proteins on G1 to S Transition, Inhibition of Cellular Proliferation by Gleevec, Insulin Signaling Pathway, Integrin Signaling Pathway, Keratinocyte Differentiation, | |
| RET | Endocytosis, Pathways in cancer, Thyroid cancer | 0.722 |
| CORO1A | Phagosome | 0.720 |
| SLC19A3 | Vitamin digestion and absorption | 0.714 |
| ADAM17 | g-Secretase mediated ErbB4 Signaling Pathway, Presenilin action in Notch and Wnt signaling, Proteolysis and Signaling Pathway of Notch, Alzheimer's disease, Epithelial cell signaling in Helicobacter pylori infection, Notch signaling pathway | 0.697 |
| MYL5 | Focal adhesion, Leukocyte transendothelial migration, Regulation of actin cytoskeleton, Tight junction | 0.695 |
| HIF1A | Erythropoietin mediated neuroprotection through NF-kB, Hypoxia and p53 in the Cardiovascular system, Hypoxia-Inducible Factor in the Cardiovascular System, VEGF, Hypoxia, and Angiogenesis, mTOR signaling pathway, Pathways in cancer, Renal cell carcinoma | 0.695 |
| GEMIN8 | RNA transport | 0.686 |
| RPL26 | Ribosome | 0.686 |
| DIAPH2 | Regulation of actin cytoskeleton | 0.684 |
| FMO5 | Drug metabolism - cytochrome P450 | 0.678 |
| OR51B2 | Olfactory transduction | 0.678 |
| ZCCHC7 | RNA degradation | 0.678 |
| SOS2 | Acute myeloid leukemia, B cell receptor signaling pathway, Chemokine signaling pathway, Chronic myeloid leukemia, Dorso-ventral axis formation, Endometrial cancer, ErbB signaling pathway, Fc epsilon RI signaling pathway, Focal adhesion, Gap junction, Glioma, GnRH signaling pathway, Hepatitis C, Insulin signaling pathway, Jak-STAT signaling pathway, MAPK signaling pathway, Natural killer cell mediated cytotoxicity, Neurotrophin signaling pathway, Non-small cell lung cancer, Pathways in cancer, Prostate cancer, Regulation of actin cytoskeleton, Renal cell carcinoma, T cell receptor signaling pathway | 0.678 |
| COX7C | Alzheimer's disease, Cardiac muscle contraction, Huntington's disease, Metabolic pathways, Oxidative phosphorylation, Parkinson's disease | 0.670 |
| GJD2 | Gap junction | 0.666 |

| | | |
|------------|--|-------|
| WHSC1L1 | Lysine degradation | 0.661 |
| LAMC2 | Amoebiasis, ECM-receptor interaction, Focal adhesion, Pathways in cancer, Small cell lung cancer, Toxoplasmosis | 0.634 |
| CPEB1 | Dorso-ventral axis formation, Oocyte meiosis, Progesterone-mediated oocyte maturation | 0.632 |
| EP300 | Acetylation and Deacetylation of RelA in The Nucleus, CARM1 and Regulation of the Estrogen Receptor, Cell Cycle: G2/M Checkpoint, Control of Gene Expression by Vitamin D Receptor, Hypoxia and p53 in the Cardiovascular system, Hypoxia-Inducible Factor in the Cardiovascular System, IL-7 Signal Transduction, Mechanism of Gene Regulation by Peroxisome Proliferators via PPARa(alpha), Melanocyte Development and Pigmentation Pathway, Multi-step Regulation of Transcription by Pitx2, NFkB activation by Nontypeable Hemophilus influenzae, Pelp1 Modulation of Estrogen Receptor Activity, Role of ERBB2 in Signal Transduction and Oncology, Role of MEF2D in T-cell Apoptosis, Role of PPAR-gamma Coactivators in Obesity and Thermogenesis, TGF beta signaling pathway, Transcription Regulation by Methyltransferase of CARM1, Adherens junction, Cell cycle, Huntington's disease, Jak-STAT signaling pathway, Long-term potentiation, Melanogenesis, Notch signaling pathway, Pathways in cancer, Prostate cancer, Rena ... | 0.632 |
| CNOT1 | RNA degradation | 0.628 |
| HIST1H2BI | Systemic lupus erythematosus | 0.624 |
| TRMU | Sulfur relay system | 0.623 |
| RBM8A | mRNA surveillance pathway, RNA transport, Spliceosome | 0.606 |
| ELAC2 | RNA transport | 0.585 |
| CSGALNACT2 | Glycosaminoglycan biosynthesis - chondroitin sulfate / dermatan sulfate, Metabolic pathways | 0.585 |
| SSR2 | Protein processing in endoplasmic reticulum | 0.585 |
| RFC2 | DNA replication, Mismatch repair, Nucleotide excision repair | 0.585 |
| SPCS3 | Protein export | 0.585 |
| COL4A4 | Acute Myocardial Infarction, Angiotensin-converting enzyme 2 regulates heart function, Intrinsic Prothrombin Activation Pathway, Platelet Amyloid Precursor Protein Pathway, Regulators of Bone Mineralization, Vitamin C in the Brain, Amoebiasis, ECM-receptor interaction, Focal adhesion, Pathways in cancer, Protein digestion and absorption, Small cell lung cancer | 0.585 |
| SPCS2 | Protein export | 0.585 |
| RASGRP3 | B cell receptor signaling pathway, MAPK signaling pathway | 0.570 |
| KCNJ11 | Type II diabetes mellitus | 0.564 |

| | | |
|---------|--|-------|
| STAT4 | IL12 and Stat4 Dependent Signaling Pathway in Th1 Development, NO2-dependent IL 12 Pathway in NK cells, Jak-STAT signaling pathway | 0.555 |
| CKS1B | Regulation of p27 Phosphorylation during Cell Cycle Progression, Pathways in cancer, Small cell lung cancer | 0.554 |
| MMP14 | Inhibition of Matrix Metalloproteinases, GnRH signaling pathway | 0.550 |
| NFYC | Overview of telomerase RNA component gene hTerc Transcriptional Regulation, Antigen processing and presentation | 0.547 |
| COX6B1 | Alzheimer's disease, Cardiac muscle contraction, Huntington's disease, Metabolic pathways, Oxidative phosphorylation, Parkinson's disease | 0.544 |
| RELA | Acetylation and Deacetylation of RelA in The Nucleus, Activation of PKC through G protein coupled receptor, AKT Signaling Pathway, ATM Signaling Pathway, Bone Remodelling, Cadmium induces DNA synthesis and proliferation in macrophages, CD40L Signaling Pathway, Ceramide Signaling Pathway, Chaperones modulate interferon Signaling Pathway, Corticosteroids and cardioprotection, CXCR4 Signaling Pathway, Double Stranded RNA Induced Gene Expression, Erythropoietin mediated neuroprotection through NF-kB, fMLP induced chemokine gene expression in HMC-1 cells, Free Radical Induced Apoptosis, HIV-I Nef: negative effector of Fas and TNF, Human Cytomegalovirus and Map Kinase Pathways, Inactivation of Gsk3 by AKT causes accumulation of b-catenin in Alveolar Macrophages, Induction of apoptosis through DR3 and DR4/5 Death Receptors , Influence of Ras and Rho proteins on G1 to S Transition, Keratinocyte Differentiation, MAPKinase Signaling Pathway, Mechanism of Gene Regulation by Peroxisome Proliferato ... | 0.541 |
| RPL39 | Ribosome | 0.536 |
| SEC11C | Protein export | 0.536 |
| HSPA1B | Antigen processing and presentation, Endocytosis, MAPK signaling pathway, Protein processing in endoplasmic reticulum, Spliceosome, Toxoplasmosis | 0.536 |
| GRIN1 | Erythropoietin mediated neuroprotection through NF-kB, Nitric Oxide Signaling Pathway, Synaptic Proteins at the Synaptic Junction, Alzheimer's disease, Amyotrophic lateral sclerosis (ALS), Calcium signaling pathway, Huntington's disease, Long-term potentiation, Neuroactive ligand-receptor interaction | 0.531 |
| NUDT9 | Purine metabolism | 0.526 |
| VAMP1 | SNARE interactions in vesicular transport | 0.524 |
| CHAD | ECM-receptor interaction, Focal adhesion | 0.524 |
| HLA-DRA | Activation of Csk by cAMP-dependent Protein Kinase Inhibits Signaling through the T Cell Receptor, Antigen Dependent B | 0.518 |

| | | |
|--------|---|-------|
| | Cell Activation, Antigen Processing and Presentation, B Lymphocyte Cell Surface Molecules, Bystander B Cell Activation, Cytokines and Inflammatory Response, IL 5 Signaling Pathway, Lck and Fyn tyrosine kinases in initiation of TCR Activation, Th1/Th2 Differentiation, The Co-Stimulatory Signal During T-cell Activation, The Role of Eosinophils in the Chemokine Network of Allergy, Allograft rejection, Antigen processing and presentation, Asthma, Autoimmune thyroid disease, Cell adhesion molecules (CAMs), Graft-versus-host disease, Hematopoietic cell lineage, Intestinal immune network for IgA production, Leishmaniasis, Phagosome, Rheumatoid arthritis, Staphylococcus aureus infection, Systemic lupus erythematosus, Toxoplasmosis, Type I diabetes mellitus, Viral myocarditis | |
| WDR36 | Ribosome biogenesis in eukaryotes | 0.510 |
| PIAS3 | Hepatitis C, Jak-STAT signaling pathway, Pathways in cancer, Small cell lung cancer, Ubiquitin mediated proteolysis | 0.509 |
| TIAM2 | Chemokine signaling pathway, Regulation of actin cytoskeleton | 0.507 |
| RORA | Circadian rhythm | 0.507 |
| COL5A3 | Amoebiasis, ECM-receptor interaction, Focal adhesion, Protein digestion and absorption | 0.505 |
| HK2 | Amino sugar and nucleotide sugar metabolism, Butirosin and neomycin biosynthesis, Carbohydrate digestion and absorption, Fructose and mannose metabolism, Galactose metabolism, Glycolysis / Gluconeogenesis, Insulin signaling pathway, Metabolic pathways, Starch and sucrose metabolism, Type II diabetes mellitus | 0.500 |
| THOC6 | RNA transport | 0.491 |
| PSMD6 | Proteasome | 0.485 |
| CA7 | Nitrogen metabolism | 0.485 |
| MGAT4A | Metabolic pathways, N-Glycan biosynthesis | 0.485 |
| PHKA2 | Calcium signaling pathway, Insulin signaling pathway | 0.485 |
| CAMK2A | Calcium signaling pathway, ErbB signaling pathway, Gastric acid secretion, Glioma, GnRH signaling pathway, Long-term potentiation, Melanogenesis, Neurotrophin signaling pathway, Olfactory transduction, Oocyte meiosis, Wnt signaling pathway | 0.485 |
| SNF8 | Endocytosis | 0.485 |
| CASP5 | NOD-like receptor signaling pathway | 0.481 |
| VAMP2 | Blockade of Neurotransmitter Release by Botulinum Toxin, Salivary secretion, SNARE interactions in vesicular transport, Vasopressin-regulated water reabsorption | 0.478 |
| CCL16 | Chemokine signaling pathway, Cytokine-cytokine receptor interaction | 0.476 |

| | | |
|----------|---|-------|
| POM121L2 | RNA transport | 0.474 |
| SLIT1 | Axon guidance | 0.472 |
| KLK2 | Erk1/Erk2 Mapk Signaling pathway, Nerve growth factor pathway (NGF), Phosphorylation of MEK1 by cdk5/p35 down regulates the MAP kinase pathway, Trka Receptor Signaling Pathway | 0.472 |
| CD276 | Cell adhesion molecules (CAMs) | 0.472 |
| TMEM173 | Cytosolic DNA-sensing pathway, RIG-I-like receptor signaling pathway | 0.472 |
| PSMB8 | Antigen Processing and Presentation, Proteasome | 0.472 |
| OR4D10 | Olfactory transduction | 0.469 |
| TPM1 | Cardiac muscle contraction, Dilated cardiomyopathy, Hypertrophic cardiomyopathy (HCM) | 0.459 |
| AP2S1 | Endocytosis, Huntington's disease | 0.455 |
| NTN3 | Axon guidance | 0.444 |
| ADCY4 | Bile secretion, Calcium signaling pathway, Chemokine signaling pathway, Dilated cardiomyopathy, Gap junction, Gastric acid secretion, GnRH signaling pathway, Melanogenesis, Oocyte meiosis, Pancreatic secretion, Progesterone-mediated oocyte maturation, Purine metabolism, Salivary secretion, Taste transduction, Vascular smooth muscle contraction | 0.444 |
| CLN5 | Lysosome | 0.444 |
| PCNA | p53 Signaling Pathway, Base excision repair, Cell cycle, DNA replication, Mismatch repair, Nucleotide excision repair | 0.441 |
| IDH3G | Citrate cycle (TCA cycle), Metabolic pathways | 0.433 |
| UBE2NL | Ubiquitin mediated proteolysis | 0.433 |
| ITGAD | Regulation of actin cytoskeleton | 0.433 |
| TAF9 | Basal transcription factors, Ribosome biogenesis in eukaryotes | 0.426 |
| PNLIP | Fat digestion and absorption, Glycerolipid metabolism, Metabolic pathways, Pancreatic secretion, Vitamin digestion and absorption | 0.426 |
| GSTK1 | Drug metabolism - cytochrome P450, Glutathione metabolism, Metabolism of xenobiotics by cytochrome P450, Peroxisome | 0.415 |
| PSMC6 | Proteasome | 0.415 |
| ABCG8 | ABC transporters, Bile secretion, Fat digestion and absorption | 0.415 |
| MOCS1 | Sulfur relay system | 0.406 |
| PRKCSH | Protein processing in endoplasmic reticulum | 0.404 |
| B3GAT1 | Glycosaminoglycan biosynthesis - chondroitin sulfate / dermatan sulfate, Glycosaminoglycan biosynthesis - heparan sulfate / heparin, Metabolic pathways | 0.401 |

| | | |
|-----------|--|-------|
| LRP1 | Alzheimer's disease, Malaria | 0.396 |
| DNAH8 | Lissencephaly gene (LIS1) in neuronal migration and development | 0.389 |
| ALDH18A1 | Arginine and proline metabolism, Metabolic pathways | 0.383 |
| CASC3 | mRNA surveillance pathway, RNA transport | 0.383 |
| RPS6KA1 | Cell Cycle: G2/M Checkpoint, Erk1/Erk2 Mapk Signaling pathway, Growth Hormone Signaling Pathway, How Progesterone Initiates the Oocyte Maturation, MAPKinase Signaling Pathway, Melanocyte Development and Pigmentation Pathway, Multiple antiapoptotic pathways from IGF-1R signaling lead to BAD phosphorylation, Regulation of BAD phosphorylation, Role of Erk5 in Neuronal Survival, Transcription factor CREB and its extracellular signals, Long-term potentiation, MAPK signaling pathway, mTOR signaling pathway, Neurotrophin signaling pathway, Oocyte meiosis, Progesterone-mediated oocyte maturation | 0.379 |
| EPO | EPO Signaling Pathway, Erythrocyte Differentiation Pathway, Erythropoietin mediated neuroprotection through NF-kB, Hypoxia-Inducible Factor in the Cardiovascular System, Regulation of hematopoiesis by cytokines, Cytokine-cytokine receptor interaction, Hematopoietic cell lineage, Jak-STAT signaling pathway | 0.379 |
| EXOC3 | Tight junction | 0.373 |
| ABCD4 | ABC transporters, Peroxisome | 0.363 |
| SEMA6A | Axon guidance | 0.351 |
| JAK3 | IL 2 signaling pathway, IL 4 signaling pathway, IL 6 signaling pathway, IL-2 Receptor Beta Chain in T cell Activation, IL22 Soluble Receptor Signaling Pathway , IL-7 Signal Transduction, Stat3 Signaling Pathway, Chemokine signaling pathway, Jak-STAT signaling pathway, Primary immunodeficiency | 0.351 |
| KCNMB1 | Vascular smooth muscle contraction | 0.350 |
| SHISA5 | p53 signaling pathway | 0.344 |
| IL9R | Cytokine-cytokine receptor interaction, Hematopoietic cell lineage, Jak-STAT signaling pathway | 0.334 |
| AGTR2 | Angiotensin-converting enzyme 2 regulates heart function, Bioactive Peptide Induced Signaling Pathway, Role of EGF Receptor Transactivation by GPCRs in Cardiac Hypertrophy, Neuroactive ligand-receptor interaction, Renin-angiotensin system | 0.331 |
| CYP27A1 | Metabolic pathways, PPAR signaling pathway, Primary bile acid biosynthesis | 0.330 |
| HIST2H2BE | Systemic lupus erythematosus | 0.330 |
| MAPK1 | Agrin in Postsynaptic Differentiation, Angiotensin II mediated activation of JNK Pathway via Pyk2 dependent signaling, Aspirin Blocks Signaling Pathway Involved in Platelet | 0.327 |

| | | |
|---------|--|-------|
| | Activation, Bioactive Peptide Induced Signaling Pathway, Cadmium induces DNA synthesis and proliferation in macrophages, CCR3 signaling in Eosinophils, Ceramide Signaling Pathway, CXCR4 Signaling Pathway, Erk and PI-3 Kinase Are Necessary for Collagen Binding in Corneal Epithelia, Erk1/Erk2 Mapk Signaling pathway, Fc Epsilon Receptor I Signaling in Mast Cells, fMLP induced chemokine gene expression in HMC-1 cells, Growth Hormone Signaling Pathway, How Progesterone Initiates the Oocyte Maturation, Human Cytomegalovirus and Map Kinase Pathways, IL-2 Receptor Beta Chain in T cell Activation, Influence of Ras and Rho proteins on G1 to S Transition, Integrin Signaling Pathway, Keratinocyte Differentiation, Links between Pyk2 and Map Kinases, MAPKinase Signaling Pathway, Mechanism of Gene Regulation by Peroxisome Prolifer. | |
| SDHC | Electron Transport Reaction in Mitochondria, Alzheimer's disease, Citrate cycle (TCA cycle), Huntington's disease, Metabolic pathways, Oxidative phosphorylation, Parkinson's disease | 0.322 |
| MRVI1 | Vascular smooth muscle contraction | 0.322 |
| ADA | Metabolic pathways, Primary immunodeficiency, Purine metabolism | 0.322 |
| ORC4 | CDK Regulation of DNA Replication, Cell cycle | 0.322 |
| ETV5 | IL12 and Stat4 Dependent Signaling Pathway in Th1 Development | 0.314 |
| COL9A3 | Protein digestion and absorption | 0.312 |
| GNRH2 | GnRH signaling pathway | 0.310 |
| NF1 | Chromatin Remodeling by hSWI/SNF ATP-dependent Complexes, MAPK signaling pathway | 0.300 |
| B4GALT2 | Galactose metabolism, Glycosaminoglycan biosynthesis - keratan sulfate, Glycosphingolipid biosynthesis - lacto and neolacto series, Metabolic pathways, N-Glycan biosynthesis, Other types of O-glycan biosynthesis | 0.297 |
| PHKA1 | Calcium signaling pathway, Insulin signaling pathway | 0.294 |
| AGK | Glycerolipid metabolism, Metabolic pathways | 0.293 |
| RENBP | Amino sugar and nucleotide sugar metabolism | 0.290 |
| HRH1 | Calcium signaling pathway, Neuroactive ligand-receptor interaction | 0.290 |
| ACOX1 | Mechanism of Gene Regulation by Peroxisome Proliferators via PPARa(alpha), alpha-Linolenic acid metabolism, Biosynthesis of unsaturated fatty acids, Fatty acid degradation, Metabolic pathways, Peroxisome, PPAR signaling pathway | 0.285 |
| CTSC | Lysosome | 0.278 |
| CD9 | Hematopoietic cell lineage | 0.276 |

| | | |
|--------|---|-------|
| TPM2 | Cardiac muscle contraction, Dilated cardiomyopathy, Hypertrophic cardiomyopathy (HCM) | 0.272 |
| CDKN1A | ATM Signaling Pathway, Cell Cycle: G1/S Check Point , Cell Cycle: G2/M Checkpoint, Cyclins and Cell Cycle Regulation, Effects of calcineurin in Keratinocyte Differentiation, Erythropoietin mediated neuroprotection through NF-kB, Hypoxia and p53 in the Cardiovascular system, Influence of Ras and Rho proteins on G1 to S Transition, p53 Signaling Pathway, Bladder cancer, Cell cycle, Chronic myeloid leukemia, ErbB signaling pathway, Glioma, Hepatitis C, Melanoma, p53 signaling pathway, Pathways in cancer, Prostate cancer | 0.268 |
| IL1A | Adhesion and Diapedesis of Granulocytes, Adhesion and Diapedesis of Lymphocytes, Cells and Molecules involved in local acute inflammatory response, Cytokine Network, Cytokines and Inflammatory Response, Erythrocyte Differentiation Pathway, IL-10 Anti-inflammatory Signaling Pathway, NF-kB Signaling Pathway, Signal transduction through IL1R, Stress Induction of HSP Regulation, Apoptosis, Cytokine-cytokine receptor interaction, Graft-versus-host disease, Hematopoietic cell lineage, Leishmaniasis, MAPK signaling pathway, Osteoclast differentiation, Prion diseases, Rheumatoid arthritis, Type I diabetes mellitus | 0.263 |
| TAAR9 | Neuroactive ligand-receptor interaction | 0.263 |
| PHF5A | Spliceosome | 0.263 |
| FAAH | Metabolism of Anandamide, an Endogenous Cannabinoid | 0.263 |
| OR1D5 | Olfactory transduction | 0.252 |
| A2M | Complement and coagulation cascades | 0.248 |
| SRSF2 | Spliceosomal Assembly, Spliceosome | 0.245 |
| POMT1 | Other types of O-glycan biosynthesis | 0.241 |
| SEMA3C | Axon guidance | 0.241 |
| NOB1 | Ribosome biogenesis in eukaryotes | 0.237 |
| CHST13 | Glycosaminoglycan biosynthesis - chondroitin sulfate / dermatan sulfate, Sulfur metabolism | 0.234 |
| OR52K2 | Olfactory transduction | 0.222 |
| MUSK | Agrin in Postsynaptic Differentiation, Role of nicotinic acetylcholine receptors in the regulation of apoptosis | 0.222 |
| RORC | Circadian rhythm | 0.218 |
| DUSP3 | MAPK signaling pathway | 0.216 |
| ALG13 | Metabolic pathways, N-Glycan biosynthesis | 0.214 |
| FRAT1 | WNT Signaling Pathway, Wnt signaling pathway | 0.206 |
| TSHR | Autoimmune thyroid disease, Neuroactive ligand-receptor interaction | 0.206 |

| | | |
|---------|--|-------|
| CD79A | B Cell Receptor Complex, BCR Signaling Pathway, CTCF: First Multivalent Nuclear Factor, B cell receptor signaling pathway, Primary immunodeficiency | 0.202 |
| IL23R | Cytokine-cytokine receptor interaction, Jak-STAT signaling pathway | 0.202 |
| PARN | RNA degradation | 0.202 |
| COMP | ECM-receptor interaction, Focal adhesion, Malaria, Phagosome, TGF-beta signaling pathway | 0.202 |
| TUBA1C | Gap junction, Pathogenic Escherichia coli infection, Phagosome | 0.202 |
| OR52E2 | Olfactory transduction | 0.202 |
| CUL4B | Nucleotide excision repair, Ubiquitin mediated proteolysis | 0.202 |
| CTSE | Lysosome | 0.200 |
| DDX3Y | RIG-I-like receptor signaling pathway | 0.193 |
| CHRNA3 | Neuroactive ligand-receptor interaction | 0.193 |
| ATP2B3 | Calcium signaling pathway, Pancreatic secretion, Salivary secretion | 0.188 |
| CLDN10 | Cell adhesion molecules (CAMs), Hepatitis C, Leukocyte transendothelial migration, Tight junction | 0.186 |
| CREB5 | Huntington's disease, Prostate cancer, Vasopressin-regulated water reabsorption | 0.177 |
| SESN3 | p53 signaling pathway | 0.175 |
| ATP5A1 | Electron Transport Reaction in Mitochondria, Alzheimer's disease, Huntington's disease, Metabolic pathways, Oxidative phosphorylation, Parkinson's disease | 0.175 |
| CNOT7 | RNA degradation | 0.173 |
| FOLR2 | Endocytosis | 0.170 |
| DSC2 | Arrhythmogenic right ventricular cardiomyopathy (ARVC) | 0.170 |
| GNG4 | Chemokine signaling pathway | 0.160 |
| CLDN4 | Cell adhesion molecules (CAMs), Hepatitis C, Leukocyte transendothelial migration, Tight junction | 0.158 |
| PLA2G2A | alpha-Linolenic acid metabolism, Arachidonic acid metabolism, Ether lipid metabolism, Fat digestion and absorption, Fc epsilon RI signaling pathway, Glycerophospholipid metabolism, GnRH signaling pathway, Linoleic acid metabolism, Long-term depression, MAPK signaling pathway, Metabolic pathways, Pancreatic secretion, Toxoplasmosis, Vascular smooth muscle contraction, VEGF signaling pathway | 0.156 |
| ATG3 | Regulation of autophagy | 0.140 |
| RRM2 | Glutathione metabolism, Metabolic pathways, p53 signaling pathway, Purine metabolism, Pyrimidine metabolism | 0.127 |
| PAQR7 | How Progesterone Initiates the Oocyte Maturation | 0.126 |

| | | |
|--------|---|-------|
| WASF3 | Y branching of actin filaments, Adherens junction, Fc gamma R-mediated phagocytosis | 0.126 |
| PICALM | Endocytotic role of NDK, Phosphins and Dynamin | 0.122 |
| OR4A16 | Olfactory transduction | 0.115 |
| NDUFS3 | Alzheimer's disease, Huntington's disease, Metabolic pathways, Oxidative phosphorylation, Parkinson's disease | 0.104 |
| IL3 | Cytokine Network, Cytokines and Inflammatory Response, Dendritic cells in regulating TH1 and TH2 Development, Erythrocyte Differentiation Pathway, IL 17 Signaling Pathway, IL 3 signaling pathway, Regulation of BAD phosphorylation, Regulation of hematopoiesis by cytokines, The Role of Eosinophils in the Chemokine Network of Allergy, Apoptosis, Asthma, Cytokine-cytokine receptor interaction, Fc epsilon RI signaling pathway, Hematopoietic cell lineage, Jak-STAT signaling pathway | 0.103 |
| TALDO1 | Metabolic pathways, Pentose phosphate pathway | 0.100 |
| SUMO4 | RNA transport | 0.096 |
| MYC | Cadmium induces DNA synthesis and proliferation in macrophages, CTCF: First Multivalent Nuclear Factor, Erk1/Erk2 Mapk Signaling pathway, IL-2 Receptor Beta Chain in T cell Activation, Inhibition of Cellular Proliferation by Gleevec, MAPKinase Signaling Pathway, Mechanism of Gene Regulation by Peroxisome Proliferators via PPARa(alpha), Neuropeptides VIP and PACAP inhibit the apoptosis of activated T cells, Overview of telomerase protein component gene hTert Transcriptional Regulation , p38 MAPK Signaling Pathway , Role of EGF Receptor Transactivation by GPCRs in Cardiac Hypertrophy, Telomeres, Telomerase, Cellular Aging, and Immortality, Tumor Suppressor Arf Inhibits Ribosomal Biogenesis, WNT Signaling Pathway, Acute myeloid leukemia, Bladder cancer, Cell cycle, Chronic myeloid leukemia, Colorectal cancer, Endometrial cancer, ErbB signaling pathway, Jak-STAT signaling pathway, MAPK signaling pathway, Pathways in cancer, Small cell lung cancer, TGF-beta signaling pathway, | 0.093 |
| OCLN | Cell adhesion molecules (CAMs), Hepatitis C, Leukocyte transendothelial migration, Pathogenic Escherichia coli infection, Tight junction | 0.091 |
| LEPR | Reversal of Insulin Resistance by Leptin, Adipocytokine signaling pathway, Cytokine-cytokine receptor interaction, Jak-STAT signaling pathway, Neuroactive ligand-receptor interaction | 0.084 |
| FOLH1 | Vitamin digestion and absorption | 0.074 |
| NPY5R | Neuroactive ligand-receptor interaction | 0.072 |
| PEX13 | Peroxisome | 0.061 |
| ACP2 | Lysosome, Riboflavin metabolism | 0.059 |

| | | |
|--------|---|-------|
| RCC1 | Cycling of Ran in nucleocytoplasmic transport, Mechanism of Protein Import into the Nucleus, Role of Ran in mitotic spindle regulation | 0.051 |
| GRIN2B | Nitric Oxide Signaling Pathway, Alzheimer's disease, Amyotrophic lateral sclerosis (ALS), Huntington's disease, Long-term potentiation, Neuroactive ligand-receptor interaction, Systemic lupus erythematosus | 0.049 |
| CCNB2 | Estrogen-responsive protein Efp controls cell cycle and breast tumors growth, Cell cycle, Oocyte meiosis, p53 signaling pathway, Progesterone-mediated oocyte maturation | 0.042 |
| GIT1 | Endocytosis, Epithelial cell signaling in Helicobacter pylori infection, Regulation of actin cytoskeleton | 0.041 |
| MEFV | NOD-like receptor signaling pathway | 0.041 |
| GNA14 | Amoebiasis, Calcium signaling pathway, Chagas disease (American trypanosomiasis) | 0.035 |
| GRIA1 | Amyotrophic lateral sclerosis (ALS), Long-term depression, Long-term potentiation, Neuroactive ligand-receptor interaction | 0.031 |
| TNKS | Telomeres, Telomerase, Cellular Aging, and Immortality | 0.027 |
| XPC | Nucleotide excision repair | 0.019 |

| B: Downregulated genes | | |
|-------------------------------|---|--------------------|
| 12 Hours | | |
| Symbol | Defined Gene Lists | Fold Change |
| ATP2B2 | Calcium signaling pathway, Pancreatic secretion, Salivary secretion | 0.799 |
| PHKA1 | Calcium signaling pathway, Insulin signaling pathway | 0.798 |
| ATP2A1 | Alzheimer's disease, Calcium signaling pathway, Pancreatic secretion | 0.787 |
| JAG2 | Notch signaling pathway | 0.787 |
| CAMK2A | Calcium signaling pathway, ErbB signaling pathway, Gastric acid secretion, Glioma, GnRH signaling pathway, Long-term potentiation, Melanogenesis, Neurotrophin signaling pathway, Olfactory transduction, Oocyte meiosis, Wnt signaling pathway | 0.781 |
| E2F1 | Cell Cycle: G1/S Check Point , Cyclin E Destruction Pathway, Cyclins and Cell Cycle Regulation, E2F1 Destruction Pathway, IL-2 Receptor Beta Chain in T cell Activation, Influence of Ras and Rho proteins on G1 to S Transition, METS affect on Macrophage Differentiation, p53 Signaling Pathway, Regulation of p27 Phosphorylation during Cell Cycle Progression, Tumor Suppressor Arf Inhibits Ribosomal Biogenesis, Bladder cancer, Cell cycle, Chronic myeloid leukemia, Glioma, Melanoma, Non-small cell lung cancer, Pancreatic cancer, Pathways in cancer, Prostate cancer, Small cell lung cancer | 0.781 |
| CXCR6 | Chemokine signaling pathway, Cytokine-cytokine receptor interaction | 0.781 |
| VIPR2 | Neuropeptides VIP and PACAP inhibit the apoptosis of activated T cells, Neuroactive ligand-receptor interaction | 0.781 |
| OR13C3 | Olfactory transduction | 0.781 |
| CTNS | Lysosome | 0.772 |
| OR4C16 | Olfactory transduction | 0.751 |
| HK2 | Amino sugar and nucleotide sugar metabolism, Butirosin and neomycin biosynthesis, Carbohydrate digestion and absorption, Fructose and mannose metabolism, Galactose metabolism, Glycolysis / Gluconeogenesis, Insulin signaling pathway, Metabolic pathways, Starch and sucrose metabolism, Type II diabetes mellitus | 0.748 |
| MARS2 | Aminoacyl-tRNA biosynthesis, Selenocompound metabolism | 0.748 |
| SLC25A5 | Calcium signaling pathway, Huntington's disease, Parkinson's disease | 0.748 |
| ZBP1 | Cytosolic DNA-sensing pathway | 0.748 |

| | | |
|---------|--|-------|
| AGPAT4 | Glycerolipid metabolism, Glycerophospholipid metabolism, Metabolic pathways | 0.748 |
| FADD | Acetylation and Deacetylation of RelA in The Nucleus, Ceramide Signaling Pathway, FAS signaling pathway (CD95), HIV-I Nef: negative effector of Fas and TNF, Induction of apoptosis through DR3 and DR4/5 Death Receptors , NF-kB Signaling Pathway, SODD/TNFR1 Signaling Pathway, TNFR1 Signaling Pathway, Alzheimer's disease, Apoptosis, Chagas disease (American trypanosomiasis), Pathways in cancer, RIG-I-like receptor signaling pathway, Toll-like receptor signaling pathway | 0.735 |
| EPB41L3 | Tight junction | 0.727 |
| NPFFR1 | Neuroactive ligand-receptor interaction | 0.725 |
| HTR5A | Calcium signaling pathway, Neuroactive ligand-receptor interaction | 0.717 |
| CDK7 | Cyclins and Cell Cycle Regulation, Degradation of the RAR and RXR by the proteasome, Estrogen-responsive protein Efp controls cell cycle and breast tumors growth, Sonic Hedgehog (SHH) Receptor Ptc1 Regulates cell cycle, Cell cycle, Nucleotide excision repair | 0.714 |
| LEF1 | Inactivation of Gsk3 by AKT causes accumulation of b-catenin in Alveolar Macrophages, Multi-step Regulation of Transcription by Pitx2, Acute myeloid leukemia, Adherens junction, Arrhythmogenic right ventricular cardiomyopathy (ARVC), Basal cell carcinoma, Colorectal cancer, Endometrial cancer, Melanogenesis, Pathways in cancer, Prostate cancer, Thyroid cancer, Wnt signaling pathway | 0.714 |
| TSC1 | mTOR Signaling Pathway, Insulin signaling pathway, mTOR signaling pathway | 0.714 |
| LRP5 | Wnt signaling pathway | 0.708 |
| GALNT7 | Metabolic pathways, Mucin type O-Glycan biosynthesis | 0.693 |
| FCAR | Phagosome, Staphylococcus aureus infection | 0.693 |
| ACSL6 | Adipocytokine signaling pathway, Fatty acid degradation, Metabolic pathways, Peroxisome, PPAR signaling pathway | 0.679 |
| RELT | Cytokine-cytokine receptor interaction | 0.679 |
| PRKCD | HIV-I Nef: negative effector of Fas and TNF, Keratinocyte Differentiation, Chemokine signaling pathway, Fc epsilon RI signaling pathway, Fc gamma R-mediated phagocytosis, GnRH signaling pathway, Neurotrophin signaling pathway, Tight junction, Type II diabetes mellitus, Vascular smooth muscle contraction | 0.679 |
| MNX1 | Maturity onset diabetes of the young | 0.679 |
| PRDM4 | Neurotrophin signaling pathway | 0.679 |
| OR52H1 | Olfactory transduction | 0.679 |
| TRAF5 | Pathways in cancer, Small cell lung cancer | 0.679 |
| NUDT9 | Purine metabolism | 0.679 |

| | | |
|---------|---|-------|
| CRB3 | Tight junction | 0.679 |
| SEMA4D | Axon guidance | 0.678 |
| FOSL2 | Bone Remodelling, Osteoclast differentiation | 0.676 |
| OR52D1 | Olfactory transduction | 0.676 |
| AKT3 | Acute myeloid leukemia, Adipocytokine signaling pathway, Apoptosis, B cell receptor signaling pathway, Carbohydrate digestion and absorption, Chagas disease (American trypanosomiasis), Chemokine signaling pathway, Chronic myeloid leukemia, Colorectal cancer, Endometrial cancer, ErbB signaling pathway, Fc epsilon RI signaling pathway, Fc gamma R-mediated phagocytosis, Focal adhesion, Glioma, Hepatitis C, Insulin signaling pathway, Jak-STAT signaling pathway, MAPK signaling pathway, Melanoma, mTOR signaling pathway, Neurotrophin signaling pathway, Non-small cell lung cancer, Osteoclast differentiation, Pancreatic cancer, Pathways in cancer, Progesterone-mediated oocyte maturation, Prostate cancer, Renal cell carcinoma, Small cell lung cancer, T cell receptor signaling pathway, Tight junction, Toll-like receptor signaling pathway, Toxoplasmosis, VEGF signaling pathway | 0.674 |
| PGM2 | Amino sugar and nucleotide sugar metabolism, Galactose metabolism, Glycolysis / Gluconeogenesis, Metabolic pathways, Pentose phosphate pathway, Purine metabolism, Starch and sucrose metabolism | 0.669 |
| ATXN3 | Protein processing in endoplasmic reticulum | 0.669 |
| CNOT1 | RNA degradation | 0.660 |
| PAX3 | Regulation of transcriptional activity by PML | 0.656 |
| NEFH | Amyotrophic lateral sclerosis (ALS) | 0.644 |
| HMGB2 | Apoptotic DNA fragmentation and tissue homeostasis, Granzyme A mediated Apoptosis Pathway | 0.644 |
| ITGA10 | Arrhythmogenic right ventricular cardiomyopathy (ARVC), Dilated cardiomyopathy, ECM-receptor interaction, Focal adhesion, Hypertrophic cardiomyopathy (HCM), Regulation of actin cytoskeleton | 0.644 |
| FGF1 | BTG family proteins and cell cycle regulation, MAPK signaling pathway, Melanoma, Pathways in cancer, Regulation of actin cytoskeleton | 0.644 |
| CAMK2B | Calcium signaling pathway, ErbB signaling pathway, Gastric acid secretion, Glioma, GnRH signaling pathway, Long-term potentiation, Melanogenesis, Neurotrophin signaling pathway, Olfactory transduction, Oocyte meiosis, Wnt signaling pathway | 0.644 |
| PLCD3 | Calcium signaling pathway, Inositol phosphate metabolism, Metabolic pathways, Phosphatidylinositol signaling system | 0.644 |
| GADD45B | Cell cycle, MAPK signaling pathway, p53 signaling pathway | 0.644 |
| IMPDH2 | Drug metabolism - other enzymes, Metabolic pathways, Purine metabolism | 0.644 |

| | | |
|---------|--|-------|
| CCR5 | HIV Induced T Cell Apoptosis, IL12 and Stat4 Dependent Signaling Pathway in Th1 Development, NO2-dependent IL 12 Pathway in NK cells, Pertussis toxin-insensitive CCR5 Signaling in Macrophage, Selective expression of chemokine receptors during T-cell polarization, Chemokine signaling pathway, Cytokine-cytokine receptor interaction, Endocytosis, Toxoplasmosis | 0.644 |
| CNR2 | Metabolism of Anandamide, an Endogenous Cannabinoid, Neuroactive ligand-receptor interaction | 0.644 |
| LAT | Ras-Independent pathway in NK cell-mediated cytotoxicity, T Cell Receptor Signaling Pathway, Fc epsilon RI signaling pathway, Fc gamma R-mediated phagocytosis, Natural killer cell mediated cytotoxicity, T cell receptor signaling pathway | 0.644 |
| CHRNA1 | Role of nicotinic acetylcholine receptors in the regulation of apoptosis, Neuroactive ligand-receptor interaction | 0.644 |
| GRIA1 | Amyotrophic lateral sclerosis (ALS), Long-term depression, Long-term potentiation, Neuroactive ligand-receptor interaction | 0.632 |
| TNKS | Telomeres, Telomerase, Cellular Aging, and Immortality | 0.615 |
| ITGAD | Regulation of actin cytoskeleton | 0.611 |
| CARS | Aminoacyl-tRNA biosynthesis | 0.607 |
| HTR7 | Calcium signaling pathway, Neuroactive ligand-receptor interaction | 0.607 |
| NUP43 | RNA transport | 0.607 |
| TAS2R60 | Taste transduction | 0.607 |
| CXXC4 | Wnt signaling pathway | 0.607 |
| ACP2 | Lysosome, Riboflavin metabolism | 0.589 |
| SLC27A1 | PPAR signaling pathway | 0.573 |
| RPS29 | Ribosome | 0.573 |
| PDE6A | Visual Signal Transduction, Phototransduction, Purine metabolism | 0.573 |
| HSPA1B | Antigen processing and presentation, Endocytosis, MAPK signaling pathway, Protein processing in endoplasmic reticulum, Spliceosome, Toxoplasmosis | 0.570 |
| CDKN1A | ATM Signaling Pathway, Cell Cycle: G1/S Check Point , Cell Cycle: G2/M Checkpoint, Cyclins and Cell Cycle Regulation, Effects of calcineurin in Keratinocyte Differentiation, Erythropoietin mediated neuroprotection through NF-kB, Hypoxia and p53 in the Cardiovascular system, Influence of Ras and Rho proteins on G1 to S Transition, p53 Signaling Pathway, Bladder cancer, Cell cycle, Chronic myeloid leukemia, ErbB signaling pathway, Glioma, Hepatitis C, Melanoma, p53 signaling pathway, Pathways in cancer, Prostate cancer | 0.570 |
| ADCY2 | Bile secretion, Calcium signaling pathway, Chemokine signaling pathway, Dilated cardiomyopathy, Gap junction, Gastric acid secretion, GnRH signaling pathway, Melanogenesis, Oocyte meiosis, Pancreatic secretion, Progesterone-mediated oocyte | 0.570 |

| | | |
|--------|---|-------|
| | maturation, Purine metabolism, Salivary secretion, Vascular smooth muscle contraction | |
| EIF4A2 | Eukaryotic protein translation, Internal Ribosome entry pathway, mTOR Signaling Pathway, Regulation of eIF4e and p70 S6 Kinase, RNA transport | 0.570 |
| OR4A47 | Olfactory transduction | 0.570 |
| ITPKA | Calcium signaling pathway, Inositol phosphate metabolism, Metabolic pathways, Phosphatidylinositol signaling system | 0.551 |
| LMNB2 | Caspase Cascade in Apoptosis, FAS signaling pathway (CD95), HIV-1 Nef: negative effector of Fas and TNF, TNFR1 Signaling Pathway | 0.540 |
| FGA | Acute Myocardial Infarction, Extrinsic Prothrombin Activation Pathway, Fibrinolysis Pathway, Intrinsic Prothrombin Activation Pathway, Complement and coagulation cascades | 0.537 |
| COL4A4 | Acute Myocardial Infarction, Angiotensin-converting enzyme 2 regulates heart function, Intrinsic Prothrombin Activation Pathway, Platelet Amyloid Precursor Protein Pathway, Regulators of Bone Mineralization, Vitamin C in the Brain, Amoebiasis, ECM-receptor interaction, Focal adhesion, Pathways in cancer, Protein digestion and absorption, Small cell lung cancer | 0.531 |
| ATP2B3 | Calcium signaling pathway, Pancreatic secretion, Salivary secretion | 0.531 |
| IL2RB | IL 2 signaling pathway, IL-2 Receptor Beta Chain in T cell Activation, Cytokine-cytokine receptor interaction, Endocytosis, Jak-STAT signaling pathway | 0.531 |
| INPP4A | Inositol phosphate metabolism, Metabolic pathways, Phosphatidylinositol signaling system | 0.531 |
| CLN5 | Lysosome | 0.531 |
| OR6B1 | Olfactory transduction | 0.531 |
| NFYC | Overview of telomerase RNA component gene hTerc Transcriptional Regulation, Antigen processing and presentation | 0.531 |
| ZCCHC7 | RNA degradation | 0.531 |
| MAPK1 | Agrin in Postsynaptic Differentiation, Angiotensin II mediated activation of JNK Pathway via Pyk2 dependent signaling, Aspirin Blocks Signaling Pathway Involved in Platelet Activation, Bioactive Peptide Induced Signaling Pathway, Cadmium induces DNA synthesis and proliferation in macrophages, CCR3 signaling in Eosinophils, Ceramide Signaling Pathway, CXCR4 Signaling Pathway, Erk and PI-3 Kinase Are Necessary for Collagen Binding in Corneal Epithelia, Erk1/Erk2 Mapk Signaling pathway, Fc Epsilon Receptor I Signaling in Mast Cells, fMLP induced chemokine gene expression in HMC-1 cells, Growth Hormone Signaling Pathway, How Progesterone Initiates the Oocyte Maturation, Human Cytomegalovirus and Map Kinase Pathways, IL-2 Receptor Beta Chain in T cell Activation, Influence of Ras and Rho proteins on G1 to S Transition, Integrin Signaling Pathway, Keratinocyte Differentiation, Links | 0.530 |

| | | |
|---------|--|-------|
| | between Pyk2 and Map Kinases, MAPKinase Signaling Pathway, Mechanism of Gene Regulation by Peroxisome Prolifer. | |
| PHKA2 | Calcium signaling pathway, Insulin signaling pathway | 0.528 |
| ORC5 | CDK Regulation of DNA Replication, Cell cycle | 0.528 |
| COL5A3 | Amoebiasis, ECM-receptor interaction, Focal adhesion, Protein digestion and absorption | 0.524 |
| DNAH8 | Lissencephaly gene (LIS1) in neuronal migration and development | 0.524 |
| DUSP16 | MAPK signaling pathway | 0.524 |
| WHSC1L1 | Lysine degradation | 0.521 |
| RORA | Circadian rhythm | 0.518 |
| CYP19A1 | Metabolic pathways, Steroid hormone biosynthesis | 0.513 |
| H2AFJ | Systemic lupus erythematosus | 0.504 |
| VHL | Hypoxia-Inducible Factor in the Cardiovascular System, VEGF, Hypoxia, and Angiogenesis, Pathways in cancer, Renal cell carcinoma, Ubiquitin mediated proteolysis | 0.499 |
| FSHR | Regulation of Spermatogenesis by CREM, Neuroactive ligand-receptor interaction | 0.498 |
| CBLB | Bacterial invasion of epithelial cells, Chronic myeloid leukemia, Endocytosis, ErbB signaling pathway, Insulin signaling pathway, Jak-STAT signaling pathway, Pathways in cancer, T cell receptor signaling pathway, Ubiquitin mediated proteolysis | 0.492 |
| OGDH | Citrate cycle (TCA cycle), Lysine degradation, Metabolic pathways, Tryptophan metabolism | 0.492 |
| ITCH | Endocytosis, Ubiquitin mediated proteolysis | 0.492 |
| MMP14 | Inhibition of Matrix Metalloproteinases, GnRH signaling pathway | 0.492 |
| PFN3 | Regulation of actin cytoskeleton, Shigellosis | 0.492 |
| RPS11 | Ribosome | 0.492 |
| DSC2 | Arrhythmogenic right ventricular cardiomyopathy (ARVC) | 0.488 |
| OR4C46 | Olfactory transduction | 0.485 |
| EXOSC2 | RNA degradation | 0.474 |
| NEUROG3 | Maturity onset diabetes of the young | 0.461 |
| HLA-DRA | Activation of Csk by cAMP-dependent Protein Kinase Inhibits Signaling through the T Cell Receptor, Antigen Dependent B Cell Activation, Antigen Processing and Presentation, B Lymphocyte Cell Surface Molecules, Bystander B Cell Activation, Cytokines and Inflammatory Response, IL 5 Signaling Pathway, Lck and Fyn tyrosine kinases in initiation of TCR Activation, Th1/Th2 Differentiation, The Co-Stimulatory Signal During T-cell Activation, The Role of Eosinophils in the Chemokine Network of Allergy, Allograft rejection, Antigen processing and presentation, Asthma, Autoimmune thyroid | 0.451 |

| | | |
|-----------|---|-------|
| | disease, Cell adhesion molecules (CAMs), Graft-versus-host disease, Hematopoietic cell lineage, Intestinal immune network for IgA production, Leishmaniasis, Phagosome, Rheumatoid arthritis, Staphylococcus aureus infection, Systemic lupus erythematosus, Toxoplasmosis, Type I diabetes mellitus, Viral myocarditis | |
| RELN | Lissencephaly gene (LIS1) in neuronal migration and development, Reelin Signaling Pathway, ECM-receptor interaction, Focal adhesion | 0.451 |
| HIST1H2BI | Systemic lupus erythematosus | 0.451 |
| ADA | Metabolic pathways, Primary immunodeficiency, Purine metabolism | 0.446 |
| MTHFR | Metabolic pathways, One carbon pool by folate | 0.437 |
| RPL36 | Ribosome | 0.432 |
| POGLUT1 | Other types of O-glycan biosynthesis | 0.426 |
| AP3M1 | Lysosome | 0.421 |
| TAOK1 | MAPK signaling pathway | 0.416 |
| FRAT2 | Wnt signaling pathway | 0.416 |
| SMS | Arginine and proline metabolism, beta-Alanine metabolism, Cysteine and methionine metabolism, Glutathione metabolism, Metabolic pathways | 0.409 |
| CCL16 | Chemokine signaling pathway, Cytokine-cytokine receptor interaction | 0.409 |
| GPX4 | Glutathione metabolism | 0.409 |
| ARSA | Lysosome, Sphingolipid metabolism | 0.409 |
| ACOX1 | Mechanism of Gene Regulation by Peroxisome Proliferators via PPARa(alpha), alpha-Linolenic acid metabolism, Biosynthesis of unsaturated fatty acids, Fatty acid degradation, Metabolic pathways, Peroxisome, PPAR signaling pathway | 0.393 |
| CUL3 | Ubiquitin mediated proteolysis | 0.392 |
| ODC1 | Arginine and proline metabolism, Glutathione metabolism, Metabolic pathways | 0.391 |
| CLEC7A | Phagosome | 0.388 |
| LDHAL6B | Cysteine and methionine metabolism, Glycolysis / Gluconeogenesis, Metabolic pathways, Propanoate metabolism, Pyruvate metabolism | 0.368 |
| EFNA2 | Axon guidance | 0.366 |
| NUMBL | Notch signaling pathway | 0.366 |
| MAFK | Oxidative Stress Induced Gene Expression Via Nrf2 | 0.366 |
| CKS1B | Regulation of p27 Phosphorylation during Cell Cycle Progression, Pathways in cancer, Small cell lung cancer | 0.366 |
| HEY2 | Segmentation Clock | 0.366 |
| DBF4 | Cell cycle | 0.354 |

| | | |
|-----------|---|-------|
| MCM3 | CDK Regulation of DNA Replication, Cell cycle, DNA replication | 0.348 |
| TNFRSF11B | Cytokine-cytokine receptor interaction, Osteoclast differentiation | 0.348 |
| TPH1 | Metabolic pathways, Tryptophan metabolism | 0.344 |
| NLRX1 | RIG-I-like receptor signaling pathway | 0.326 |
| SERPINB9 | Amoebiasis | 0.322 |
| VAMP2 | Blockade of Neurotransmitter Release by Botulinum Toxin, Salivary secretion, SNARE interactions in vesicular transport, Vasopressin-regulated water reabsorption | 0.322 |
| TIMP1 | Inhibition of Matrix Metalloproteinases | 0.322 |
| PON1 | Metabolic pathways | 0.322 |
| AKR1C1 | Metabolism of xenobiotics by cytochrome P450, Steroid hormone biosynthesis | 0.322 |
| S1PR1 | Phospholipids as signalling intermediaries, Neuroactive ligand-receptor interaction | 0.322 |
| SIKE1 | RIG-I-like receptor signaling pathway | 0.322 |
| SNAP29 | SNARE interactions in vesicular transport | 0.322 |
| ALDH18A1 | Arginine and proline metabolism, Metabolic pathways | 0.304 |
| C8A | Alternative Complement Pathway, Classical Complement Pathway, Complement Pathway, Lectin Induced Complement Pathway, Amoebiasis, Complement and coagulation cascades, Prion diseases, Systemic lupus erythematosus | 0.276 |
| CSF3R | Cytokine-cytokine receptor interaction, Hematopoietic cell lineage, Jak-STAT signaling pathway, Pathways in cancer | 0.276 |
| CTSD | Downregulated of MTA-3 in ER-negative Breast Tumors, Lysosome | 0.276 |
| GCAT | Glycine, serine and threonine metabolism | 0.276 |
| NMRK1 | Nicotinate and nicotinamide metabolism | 0.276 |
| RAN | Cycling of Ran in nucleocytoplasmic transport, Mechanism of Protein Import into the Nucleus, Role of Ran in mitotic spindle regulation, Sumoylation by RanBP2 Regulates Transcriptional Repression, Ribosome biogenesis in eukaryotes, RNA transport | 0.272 |
| CARD8 | NOD-like receptor signaling pathway | 0.268 |
| CDC40 | Spliceosome | 0.255 |
| CD44 | Adhesion Molecules on Lymphocyte, Monocyte and its Surface Molecules, Neutrophil and Its Surface Molecules, ECM-receptor interaction, Hematopoietic cell lineage, Shigellosis | 0.229 |
| EIF2S1 | Apoptotic Signaling in Response to DNA Damage, Double Stranded RNA Induced Gene Expression, Eukaryotic protein translation, Regulation of eIF2, Skeletal muscle hypertrophy is regulated via AKT/mTOR pathway, VEGF, Hypoxia, and Angiogenesis, Hepatitis C, Protein processing in endoplasmic reticulum, RNA transport | 0.229 |

| | | |
|---------|--|-------|
| ACTN3 | Cell to Cell Adhesion Signaling, Integrin Signaling Pathway, uCalpain and friends in Cell spread, Adherens junction, Amoebiasis, Arrhythmogenic right ventricular cardiomyopathy (ARVC), Focal adhesion, Leukocyte transendothelial migration, Regulation of actin cytoskeleton, Systemic lupus erythematosus, Tight junction | 0.229 |
| POLR2F | Huntington's disease, Metabolic pathways, Purine metabolism, Pyrimidine metabolism, RNA polymerase | 0.229 |
| SETD7 | Lysine degradation | 0.229 |
| RXFP1 | Neuroactive ligand-receptor interaction | 0.229 |
| CPA3 | Pancreatic secretion, Protein digestion and absorption, Renin-angiotensin system | 0.229 |
| RBKS | Pentose phosphate pathway | 0.213 |
| ALDH3A2 | Arginine and proline metabolism, Ascorbate and aldarate metabolism, beta-Alanine metabolism, Fatty acid degradation, Glycerolipid metabolism, Glycolysis / Gluconeogenesis, Histidine metabolism, Lysine degradation, Metabolic pathways, Pentose and glucuronate interconversions, Propanoate metabolism, Pyruvate metabolism, Tryptophan metabolism, Valine, leucine and isoleucine degradation | 0.203 |
| TOP3B | Homologous recombination | 0.194 |
| EIF4E1B | Insulin signaling pathway, mTOR signaling pathway, RNA transport | 0.184 |
| UGT2B15 | Ascorbate and aldarate metabolism, Drug metabolism - cytochrome P450, Drug metabolism - other enzymes, Metabolic pathways, Metabolism of xenobiotics by cytochrome P450, Other types of O-glycan biosynthesis, Pentose and glucuronate interconversions, Porphyrin and chlorophyll metabolism, Retinol metabolism, Starch and sucrose metabolism, Steroid hormone biosynthesis | 0.180 |
| SEMA5B | Axon guidance | 0.180 |
| TBPL1 | Basal transcription factors, Huntington's disease | 0.180 |
| LIPT2 | Lipoic acid metabolism, Metabolic pathways | 0.180 |
| ULK1 | mTOR signaling pathway, Regulation of autophagy | 0.180 |
| MBTPS2 | SREBP control of lipid synthesis, Protein processing in endoplasmic reticulum | 0.180 |
| FZD9 | Basal cell carcinoma, Melanogenesis, Pathways in cancer, Wnt signaling pathway | 0.174 |
| ADCY3 | Bile secretion, Calcium signaling pathway, Chemokine signaling pathway, Dilated cardiomyopathy, Gap junction, Gastric acid secretion, GnRH signaling pathway, Melanogenesis, Olfactory transduction, Oocyte meiosis, Pancreatic secretion, Progesterone-mediated oocyte maturation, Purine metabolism, Salivary secretion, Vascular smooth muscle contraction, Vasopressin-regulated water reabsorption, Vibrio cholerae infection | 0.174 |

| | | |
|---------|---|-------|
| BMS1 | Ribosome biogenesis in eukaryotes | 0.162 |
| IL6R | IL 6 signaling pathway, Role of ERBB2 in Signal Transduction and Oncology, Cytokine-cytokine receptor interaction, Hematopoietic cell lineage, Jak-STAT signaling pathway | 0.158 |
| RASGRP3 | B cell receptor signaling pathway, MAPK signaling pathway | 0.153 |
| FOLH1 | Vitamin digestion and absorption | 0.139 |
| TNNI3 | Cardiac muscle contraction, Dilated cardiomyopathy, Hypertrophic cardiomyopathy (HCM) | 0.129 |
| COMP | ECM-receptor interaction, Focal adhesion, Malaria, Phagosome, TGF-beta signaling pathway | 0.129 |
| B4GALT2 | Galactose metabolism, Glycosaminoglycan biosynthesis - keratan sulfate, Glycosphingolipid biosynthesis - lacto and neolacto series, Metabolic pathways, N-Glycan biosynthesis, Other types of O-glycan biosynthesis | 0.129 |
| NAMPT | Nicotinate and nicotinamide metabolism | 0.129 |
| FGD1 | Regulation of actin cytoskeleton | 0.129 |
| RPL12 | Ribosome | 0.129 |
| NDUFS5 | Alzheimer's disease, Huntington's disease, Metabolic pathways, Oxidative phosphorylation, Parkinson's disease | 0.110 |
| CR1 | B Lymphocyte Cell Surface Molecules, Complement and coagulation cascades, Hematopoietic cell lineage, Leishmaniasis, Malaria | 0.110 |
| CTSO | Lysosome | 0.110 |
| CD8B | Antigen processing and presentation, Cell adhesion molecules (CAMs), Hematopoietic cell lineage, Primary immunodeficiency, T cell receptor signaling pathway | 0.103 |
| POLR2K | Huntington's disease, Metabolic pathways, Purine metabolism, Pyrimidine metabolism, RNA polymerase | 0.086 |
| MAPK9 | MAPKinase Signaling Pathway, Adipocytokine signaling pathway, Chagas disease (American trypanosomiasis), Colorectal cancer, Epithelial cell signaling in Helicobacter pylori infection, ErbB signaling pathway, Fc epsilon RI signaling pathway, Focal adhesion, GnRH signaling pathway, Hepatitis C, Insulin signaling pathway, MAPK signaling pathway, Neurotrophin signaling pathway, NOD-like receptor signaling pathway, Osteoclast differentiation, Pancreatic cancer, Pathways in cancer, Progesterone-mediated oocyte maturation, Protein processing in endoplasmic reticulum, RIG-I-like receptor signaling pathway, Shigellosis, T cell receptor signaling pathway, Toll-like receptor signaling pathway, Toxoplasmosis, Type II diabetes mellitus, Wnt signaling pathway | 0.078 |
| ATP5B | Alzheimer's disease, Huntington's disease, Metabolic pathways, Oxidative phosphorylation, Parkinson's disease | 0.077 |
| RAF1 | Angiotensin II mediated activation of JNK Pathway via Pyk2 dependent signaling, Aspirin Blocks Signaling Pathway Involved in Platelet Activation, BCR Signaling Pathway, Bioactive Peptide Induced Signaling Pathway, Cadmium induces DNA synthesis | 0.077 |

| | | |
|---------|---|-------|
| | and proliferation in macrophages, CCR3 signaling in Eosinophils, Ceramide Signaling Pathway, CXCR4 Signaling Pathway, EGF Signaling Pathway, EPO Signaling Pathway, Erk and PI-3 Kinase Are Necessary for Collagen Binding in Corneal Epithelia, Erk1/Erk2 Mapk Signaling pathway, Fc Epsilon Receptor I Signaling in Mast Cells, fMLP induced chemokine gene expression in HMC-1 cells, Growth Hormone Signaling Pathway, IGF-1 Signaling Pathway, IL 2 signaling pathway, IL 3 signaling pathway, IL 6 signaling pathway, IL-2 Receptor Beta Chain in T cell Activation, Influence of Ras and Rho proteins on G1 to S Transition, Inhibition of Cellular Proliferation by Gleevec, Insulin Signaling Pathway, Integrin Signaling Pathway, Keratinocyte Differentiation. | |
| PSMB8 | Antigen Processing and Presentation, Proteasome | 0.077 |
| NPC1L1 | Fat digestion and absorption | 0.077 |
| TACR2 | Calcium signaling pathway, Neuroactive ligand-receptor interaction | 0.074 |
| GJD2 | Gap junction | 0.073 |
| CHDH | Glycine, serine and threonine metabolism | 0.059 |
| GNAT1 | Phototransduction | 0.038 |
| ZAP70 | Activation of Csk by cAMP-dependent Protein Kinase Inhibits Signaling through the T Cell Receptor, Lck and Fyn tyrosine kinases in initiation of TCR Activation, T Cell Receptor Signaling Pathway, Natural killer cell mediated cytotoxicity, Primary immunodeficiency, T cell receptor signaling pathway | 0.022 |
| AGTR2 | Angiotensin-converting enzyme 2 regulates heart function, Bioactive Peptide Induced Signaling Pathway, Role of EGF Receptor Transactivation by GPCRs in Cardiac Hypertrophy, Neuroactive ligand-receptor interaction, Renin-angiotensin system | 0.022 |
| IL33 | Cytosolic DNA-sensing pathway | 0.022 |
| DEGS2 | Metabolic pathways, Sphingolipid metabolism | 0.022 |
| WASF3 | Y branching of actin filaments, Adherens junction, Fc gamma R-mediated phagocytosis | 0.022 |
| NDUFA11 | Alzheimer's disease, Huntington's disease, Metabolic pathways, Oxidative phosphorylation, Parkinson's disease | 0.011 |

DISCUSSION

Yuan et al. (2003) reported that Tetrahydrofuran (THF) from Annonaceae plants arrested *Bax* and *CASP3* related pathways in G1 phase of human urinary bladder cancer (T24 cells). *Bax* and *CASP3* which both shows up regulation in this study are two key proteins for signaling the onset of cell death. Sun et al. (2014) showed that HPLC fractions of *Annonaceous acetogenins* fruit extract contained mono-tetrahydrofuran rings which resulted in anti-proliferation among human prostate cancer cells (PC-3 cell line). These results were corroborated by Matsumoto et al. (2017) using THF in 39 human cancer cell lines.

L19 showed induction of apoptosis and inflammation. From the microarray, qRT-PCR, and RT² Profiler™ PCR Array techniques the following pathways are proposed:

Pathway 1: Apoptosis

CASP6 and *3*, executioner caspases, which represent apoptosis, showed high level of expression (Foveaux et al., 2014) in protein level by Apo assay. They

also showed high level gene expression by qRT-PCR and RT² Profiler™ PCR Array techniques.

Apoptotic pathways that seem to be involved in the DLD1 cells in response to the L19, seem to be FAS mediated with induction of ER Stress. ER Stress pathway is demonstrated by high level of gene expression of *CASP12* and 3. *CASP12* which is known as the important genes of inflammation showed maximum expression which means the gene is turned on within 6 hours then declined gradually (25.13 ± 4.81 -fold change). Zhang et al. (2016) showed *CASP12* could also induce apoptosis by cleaving pro-caspase 3 to activate CASP3 (Figure 24).

TNF (Tumor necrosis factor) activating *TNF-R1* (Tumor necrosis factor receptor superfamily, member 10a) is not changed at all time points; however, *TNF-R1* is downregulated. *TNF-R1* can activate *TRAF2* (TNFRSF1A-associated via death domain) which can further activate *TRADD*. *TRADD* is co-factor of *FADD* (Fas (TNFRSF6)-associated via death domain *FADD*) which function is to cleave pro-caspase 8 or 10. These CASPs are the initiator caspases of apoptosis. Based on down-regulation on *TNF*, all other genes were down regulated consisting of *TNF-R1*, *TRAF2*, *TRADD* and *FADD* (Komarov et al., 2016). Thus, TNF pathway is not up-regulated in the DLD-1 cells. *CASP8* and 10 are up regulated based in RT² Profiler™ PCR Array and qRT-PCR results. These CASPs are activated by *FAS-L* (Fas ligand (*TNF* superfamily, member 6) pathway (Malike et al., 2016). *FAS-L*, a protein on the surface of the cell membrane, is a death receptor which binds to *FAS* (Fas (TNF receptor superfamily, member 6)). *FAS-FAS* Ligand can

activate *CASP8* and *10* by *FADD* (Figure 24). Although *FADD* showed no significant changes in RT² Profiler™ PCR data. Therefore, *FADD* cleaved pro-caspase 8 and 10 and activate *CASP8* and *10*. *CASP8* or *10* releases DISC to cytosol and activates other executioner caspases such as *CASP3*, 6 or 7. *CASP3* and 6 are upregulated and induced apoptosis (Malik et al., 2016); however, *CASP7* represents down regulation at all time points. The genes up-regulation may represent FAS pathway and activate executioner CASPs which turn on apoptosis.

BAD (BCL2-associated agonist of cell death) shows no changes but *BAX* (BCL2-associated X protein) is up regulated in 6-hours. According to Adams and Cory (2017) these two genes are inducing apoptosis individually by inhibiting *BCL-2* which is down regulated in RT² Profiler™ PCR data. Kawamoto et al. (2016) showed inhibition of *BCL-2* also activated *BID* (BH3 interacting domain death agonist) and *BID* could either release *CYTC* (Cytochrome c) from mitochondria membranes or activate *AIF*. *BID* and *CYTC* are both down-regulated in 8-hours, while *AIF* is upregulated at 12-hours (Figure 24). *CYTC* activated *APAF-1* which can cleave pro-caspase 9 and activated *CASP9* (Kawamoto et al., 2016). *CASP9* expressed in 6-hours showed upregulation which can activate *CYTC* (Cytochrome c) and cleave Pro-*CASP9* and activate *CASP9* (Figure 24). *CASP9* can activate *CASP3* by cleaving pro-caspase 3 protein. *CASP9* showed up regulation at 6 hours and then fell off in 8 hours. Thus, *CASP3* showed a gradual increase from 6 hours to 12 hours (Fox & Macfarlane, 2016) which is also shown on graph 14 in results section from this study. Therefore, all these up- and down- regulated genes, indicate ER stress and show *AIF* pathway activation (apoptosis pathways),

because *CASP3*, *Apaf-1*, *Bax*, *AIF*, *CASP9* and *p53* genes, which are key factors for apoptosis, are up regulated and *BCL2* is down regulated. In addition, according to Kadam et al. (2017) *AIF* shows apoptosis activity which is upregulated in this study.

Pathway 2: Inflammatory

Within the 6-hour exposure period to L19, *CASP12* had a huge increase in expression, as much as a 25-fold increase. This change indicated the immediate onset of inflammation. Consistent with this was *CASP1*, which is a key factor of inflammation and not apoptosis key factor showed increase in gene up regulation from 6 to 24 hours. RT² Profiler™ is not consistent with 12 hour results showing no significant changes in *CASP1* gene. The discrepancy could have been caused by the primers being different in the SA Bioscience plate as compared to the ones designed for the qRT PCR using the NCI primer database. *CASP1* is activated by HIN (domain containing (PYHIN) family) and NLR (nucleoid-binding domain, leucine-rich repeat containing) which are inflammasome factors. *CASP1* also has a role in autoinflammatory disease, tumor suppression and tissue repair (Man & Kanneganti, 2016). Based on Foveaux et al. (2014), *CASP1* can activate inflammatory pathways as well as *CASP6*. Maximum level of *CASP5* which is an inflammatory CASP is expressed within 8 hours (McIlwain et al., 2013). Recent research showed *CASP3* activation was dependent on *CASP5* in stretch-induced

apoptosis (Zhao et al., 2017). *Casp5* expression was elevated followed by an increase in *CASP1* consistent with inflammation as described by McIlwain et al. (2013). The L19 has an immediate inflammatory response that would be undesirable as a chemotherapy agent.

Non-Apoptotic Genes Affected by L19

As with most chemotherapy agents, off target responses cause unexpected and/or harmful side effects. It is important in drug discovery to identify as many off target pathways as possible prior to moving the drug further in development. On the positive side, identifying other pathways that are affected by the drug, in this case L19, can provide new uses for the drug. Microarray technology allows screening changes that may occur in the entire transcriptome of cells in response to compounds. As evidenced by Table 11 A and B, there are numerous pathways and cellular functions that L19 impacts either causing up-regulation or down-regulation. The next step in this project will be to examine these pathways more closely to determine if L19 may be a good candidate for treatments other than anti-cancer.

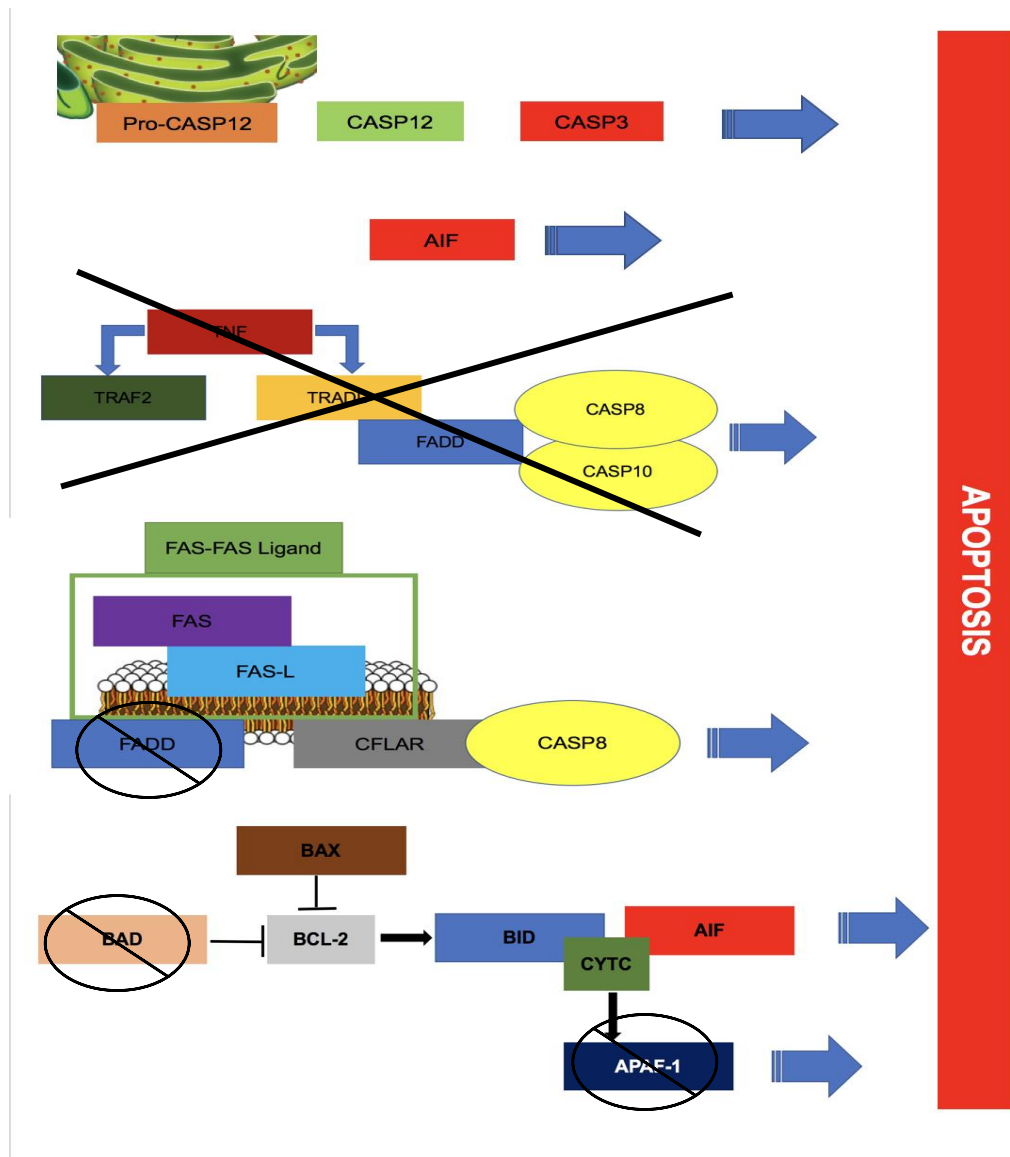


Figure 24. Hypothetical apoptosis pathway in treated colorectal cancer cells (DLD-1) by L19 through the qRT-PCR, and RT2 Profiler™ PCR Array results for 6, 8, and 12 hours.

REFERENCES

- Adams, J. M., & Cory, S. (2018). The BCL-2 arbiters of apoptosis and their growing role as cancer targets. *Cell Death and Differentiation*, 25(1), 27–36. <https://doi.org/10.1038/cdd.2017.161>
- Ahmed, D., Eide, P. W., Eilertsen, I. A., Danielsen, S. A., Eknaes, M., Hektoen, M., & Lothe, R. A. (2013). Epigenetic and genetic features of 24 colon cancer cell lines. *Oncogenesis*, 2(9), e71
- American Cancer Society (2017) Cancer facts & figures. Bulletin 861714. *The American Cancer Society*. American Type Culture (2016) Dld-1 (ATCC® ccl-221™). Bulletin 8409. *American Type Culture Collection*, 1–3.
- Bhandari, M. (2015) Extraction and identification of water soluble compounds from Rumex Crispus leaf and root; an in-vivo analysis as a suppressive agent for colon carcinoma. MS Thesis, Stephen F. Austin State University: UMI Publishing.
- Bhardwaj, M., Kim, N.-H., Paul, S., Jakhar, R., Han, J., & Kang, S. C. (2016). 5-Hydroxy-7-Methoxyflavone Triggers Mitochondrial-Associated Cell Death via Reactive Oxygen Species Signaling in Human Colon Carcinoma Cells. *PLOS ONE*, 11(4), e0154525. <https://doi.org/10.1371/journal.pone.0154525>
- Czabotar, P. E., Lessene, G., Strasser, A., & Adams, J. M. (2014). Control of apoptosis by the BCL-2 protein family: implications for physiology and therapy. *Nature Reviews Molecular Cell Biology*, 15(1), 49–63. <https://doi.org/10.1038/nrm3722>
- Dexter, D. L., Barbosa, J. A., & Calabresi, P. (1979). N,N-dimethylformamide-induced alteration of cell culture characteristics and loss of tumorigenicity in cultured human colon carcinoma cells. *Cancer Research*, 39(3), 1020–1025.
- Eom, Y-W., Kim, M. A., Park, S. S., Goo, M. J., Kwon, H. J., Sohn, S., Choi, K. S. (2005). Two distinct modes of cell death induced by doxorubicin: apoptosis and cell death through mitotic catastrophe accompanied by senescence-like phenotype. *Oncogene*, 24(30), 4765–4777. <https://doi.org/10.1038/sj.onc.1208627>

- Favaloro, B., Allocati, N., Graziano, V., Di Ilio, C., & De Laurenzi, V. (2012). Role of Apoptosis in disease. *Aging*, 4(5), 330–349.
<https://doi.org/10.18632/aging.100459>
- Foveaux, B., Van Der Kraak, L., Beauchemin, N., Albrecht, S., & LeBlanc, A. C. (2014). Inflammation-Induced Tumorigenesis in Mouse Colon Is Caspase-6 Independent. *PLoS ONE*, 9(12), e114270.
<https://doi.org/10.1371/journal.pone.0114270>
- Fox, J. L., & MacFarlane, M. (2016). Targeting cell death signalling in cancer: minimising 'Collateral damage.' *British Journal of Cancer*, 115(1), 5–11.
<https://doi.org/10.1038/bjc.2016.111>
- Gerl, R., & Vaux, D. L. (2004). Apoptosis in the development and treatment of cancer. *Carcinogenesis*, 26(2), 263–270.
<https://doi.org/10.1093/carcin/bgh283>
- Huang, Y.-C., Kuo, C.-L., Lu, K.-W., Lin, J.-J., Yang, J.-L., Wu, R., ... Chung, J.-G. (2016). 18 α -Glycyrrhetic Acid Induces Apoptosis of HL-60 Human Leukemia Cells through Caspases- and Mitochondria-Dependent Signaling Pathways. *Molecules*, 21(7), 872.
<https://doi.org/10.3390/molecules21070872>
- Inkollu, S. K. (2007). Identification of anticancer compounds from *Rumex crispus* root. MS Thesis, Department of Biology, Stephen F. Austin State University: Nacogdoches, TX. UMI Publishing.
- Jang, J., Jeong, S.-J., Kwon, H.Y., Jung, J. H., Sohn, E. J., Lee, H.-J., ... Kim, S.-H. (2013). Decursin and Doxorubicin Are in Synergy for the Induction of Apoptosis via STAT3 and/or mTOR Pathways in Human Multiple Myeloma Cells. *Evidence-Based Complementary and Alternative Medicine : ECAM*, 2013, 506324. <https://doi.org/10.1155/2013/506324>
- Jing, Z., Sui, X., Yao, J., Xie, J., Jiang, L., Zhou, Y., Han, W. (2016). SKF-96365 activates cytoprotective autophagy to delay apoptosis in colorectal cancer cells through inhibition of the calcium/CaMKII γ /AKT-mediated pathway. *Cancer Letters*, 372(2), 226–238.
<https://doi.org/10.1016/j.canlet.2016.01.006>
- Kadam, A. A., Jubin, T., Mir, H. A., & Begum, R. (2017). Potential role of Apoptosis Inducing Factor in evolutionarily significant eukaryote,

- Dictyostelium discoideum survival. *Biochimica et Biophysica Acta (BBA) - General Subjects*, 1861(1), 2942–2955.
<https://doi.org/10.1016/j.bbagen.2016.09.021>
- Kawamoto, Y., Ayaki, T., Urushitani, M., Ito, H., & Takahashi, R. (2016). Activated caspase-9 immunoreactivity in glial and neuronal cytoplasmic inclusions in multiple system atrophy. *Neuroscience Letters*, 628, 207–212.
<https://doi.org/10.1016/j.neulet.2016.06.036>
- Komarov, A. P., Komarova, E. A., Green, K., Novototskaya, L. R., Baker, P. S., Eroshkin, A., Gudkov, A. V. (2016). Functional genetics-directed identification of novel pharmacological inhibitors of FAS- and TNF-dependent apoptosis that protect mice from acute liver failure. *Cell Death & Disease*, 7(3), e2145–e2145. <https://doi.org/10.1038/cddis.2016.45>
- Kondaveeti, S. (2015) Induction of apoptosis in DLD-1 colon cancer cells to elucidate apoptosis mechanism over time. MS Thesis, Department of Biology, Stephen F. Austin State University, Nacogdoches TX: UMI Publishing.
- Kralik, P., & Ricchi, M. (2017). A Basic Guide to Real Time PCR in Microbial Diagnostics: Definitions, Parameters, and Everything. *Frontiers in Microbiology*, 8, 108. <https://doi.org/10.3389/fmicb.2017.00108>
- Lee, D. A. (2015). *Apoptosis induction in dld-1 colorectal cancer cells with extracts of Rumex crispus*. MS Thesis, Department of Biology, Stephen F. Austin State University, Nacogdoches, TX: UMI Publishing
- Lowe, S. W., & Lin, A. W. (2000). Apoptosis in cancer. *Carcinogenesis*, 21(3), 485–495. <https://doi.org/10.1093/carcin/21.3.485>
- Lucena-Aguilar, G., Sánchez-López, A. M., Barberán-Aceituno, C., Carrillo-Ávila, J. A., López-Guerrero, J. A., & Aguilar-Quesada, R. (2016). DNA Source Selection for Downstream Applications Based on DNA Quality Indicators Analysis. *Biopreservation and Biobanking*, 14(4), 264–270.
<https://doi.org/10.1089/bio.2015.0064>
- Malike, K., Asif, K., & Ambreen, A. (2016). Role of FAS in Apoptosis. *BEPLS Bulletin of Environment Pharmacology and Life Sciences Bull. Env. Pharmacol. Life Sci*, 5(5).

- Man, S. M., & Kanneganti, T.-D. (2016). Converging roles of caspases in inflammasome activation, cell death and innate immunity. *Nature Reviews Immunology*, 16(1), 7–21. <https://doi.org/10.1038/nri.2015.7>
- Matsumoto, T., Kojima, N., Akatsuka, A., Yamori, T., Dan, S., Iwasaki, H., & Yamashita, M. (2017). Convergent synthesis of stereoisomers of THF ring moiety of acetogenin thiophene analogue and their antiproliferative activities against human cancer cell lines. *Tetrahedron*, 73(17), 2359–2366. <https://doi.org/10.1016/j.tet.2017.03.011>
- McIlwain, D. R., Berger, T., & Mak, T. W. (2013). Caspase Functions in Cell Death and Disease. *Cold Spring Harbor Perspectives in Biology*, 5(4), a008656–a008656. <https://doi.org/10.1101/cshperspect.a008656>
- McIlwaine, M., Bradley, J., Elborn, J. S., & Moran, F. (2017). Personalising airway clearance in chronic lung disease. *European Respiratory Review*, 26(143), 1-12. <https://doi.org/10.1183/16000617.0086-2016>
- Nakagawa, T., Zhu, H., Morishima, N., Li, E., Xu, J., Yankner, B. A., & Yuan, J. (2000). Caspase-12 mediates endoplasmic-reticulum-specific apoptosis and cytotoxicity by amyloid- β . *Nature*, 403(6765), 98–103. <https://doi.org/10.1038/47513>
- Patra, K., Jana, S., Sarkar, A., Karmakar, S., Jana, J., Gupta, M., Bhattacharjee, S. (2016). *Parkia javanica* Extract Induces Apoptosis in S-180 Cells via the Intrinsic Pathway of Apoptosis. *Nutrition and Cancer*, 68(4), 689–707. <https://doi.org/10.1080/01635581.2016.1158298>
- Potaman, V. N., & Sinden, R. R. (2000). Madame Curie Bioscience Database [Internet]. Landes Bioscience, Austin (TX).
- Quackenbush, J. (2002). Microarray data normalization and transformation. *Nature Genetics*, 32(Supp), 496–501. <https://doi.org/10.1038/ng1032>
- Redondo-Blanco, S., Fernández, J., Gutiérrez-Del-Río, I., Villar, C. J., & Lombó, F. (2017). New Insights toward colorectal cancer chemotherapy using natural bioactive compounds. *Frontiers in Pharmacology*, 8, 109. <https://doi.org/10.3389/fphar.2017.00109>

- Riganti, C., Miraglia, E., Viarisio, D., Costamagna, C., Pescarmona, G., Ghigo, D., & Bosia, A. (2005). Nitric oxide reverts the resistance to doxorubicin in human colon cancer cells by inhibiting the drug efflux. *Cancer Research*, 65(2), 516–525.
- Rodrigues, N. R., Rowan, A., Smith, M. E., Kerr, I. B., Bodmer, W. F., Gannon, J. V., & Lane, D. P. (1990). p53 mutations in colorectal cancer. *Proceedings of the National Academy of Sciences*, 87(19), 7555–7559.
<https://doi.org/10.1073/PNAS.87.19.7555>
- Rosati, E., Sabatini, R., Rampino, G., De Falco, F., Di Ianni, M., Falzetti, F., & Marconi, P. (2010). Novel targets for endoplasmic reticulum stress-induced apoptosis in B-CLL. *Blood*, 116(15), 2713–2723.
<https://doi.org/10.1182/blood-2010-03-275628>
- Saeed, A. I., Bhagabati, N. K., Braisted, J. C., Liang, W., Sharov, V., Howe, E. A., & Quackenbush, J. (2006). TM4 microarray software suite. *Methods in Enzymology*, 411, 134–193.
[https://doi.org/10.1016/S0076-6879\(06\)11009-5](https://doi.org/10.1016/S0076-6879(06)11009-5)
- SA Biosciences Corp. (2017) The RT² Profiler™ PCR Array Human Apoptosis. Technical Bulletin #G7790, QIAGEN Inc., Germantown, MD.
- Schmittgen, T. D., & Livak, K. J. (2008). Analyzing real-time PCR data by the comparative C(T) method. *Nature Protocols*, 3(6), 1101–1108.
[doi:10.1038/nprot.2008.73](https://doi.org/10.1038/nprot.2008.73)
- Shiwani, S., Singh, N. K., & Wang, M. H. (2012). Carbohydrase inhibition and anti-cancerous and free radical scavenging properties along with DNA and protein protection ability of methanolic root extracts of *Rumex crispus*. *Nutrition Research and Practice*, 6(5), 389–395.
<https://doi.org/10.4162/nrp.2012.6.5.389>
- Stekel, D. (2003). Microarray Bioinformatics. *Cambridge University Press*.
- Sørensen, B. H., Nielsen, D., Thorsteinsdottir, U. A., Hoffmann, E. K., & Lambert, I. H. (2016). Downregulation of LRRC8A protects human ovarian and alveolar carcinoma cells against Cisplatin-induced expression of p53, MDM2, p21^{Waf1/Cip1}, and Caspase-9/-3 activation. *American Journal of Physiology-Cell Physiology*, 310(11), C857–C873.
<https://doi.org/10.1152/ajpcell.00256.2015>

- Sonavane, R. M. (2012) Profiling gene expression of caspas 3 and 7 in human colon cancer DLD-1 cells in response to Doxorubicin. MS Thesis, Department of Biology, Stephen F. Austin State University, Nacogdoches, TX: UMI Publishing.
- Stewart, B. W., Wild, C., International Agency for Research on Cancer, & World Health Organization. (2017). *World Cancer Report 2014*.
- Sun, S., Liu, J., Kadouh, H., Sun, X., & Zhou, K. (2014). Three new anti-proliferative Annonaceous acetogenins with mono-tetrahydrofuran ring from graviola fruit (*Annona muricata*). *Bioorganic & Medicinal Chemistry Letters*, 24(12), 2773–2776. <https://doi.org/10.1016/j.bmcl.2014.03.099>
- Tibbetts, L. M., Chu, M. Y., Hager, J. C., Dexter, D. L., & Calabresi, P. (1977). Chemotherapy of cell-line-derived human colon carcinomas in mice immunosuppressed with antithymocyte serum. *Cancer*, 40(S5), 2651-2659.
- Tokarnia, C. H., Döbereiner, J., & Peixoto, P. V. (2002). Poisonous plants affecting livestock in Brazil. *Toxicon*, 40(12), 1635–1660. doi: 10.1016/s0041-0101(02)00239-8
- Wynn, S. (2007) Veterinary herbal medicine. *Popular “Anticancer” Herbal Remedies*, St. Louis, Mo. Mosby Elsevier.
- Ye, J., Coulouris, G., Zaretskaya, I., Cutcutache, I., Rozen, S., & Madden, T. L. (2012). Primer-BLAST: A tool to design target-specific primers for polymerase chain reaction. *BMC Bioinformatics*, 13(1), 134. <https://doi.org/10.1186/1471-2105-13-134>
- Yuan, S.-S. F., Chang, H.-L., Chen, H.-W., Yeh, Y.-T., Kao, Y.-H., Lin, K.-H., ... Su, J.-H. (2003). Annonacin, a mono-tetrahydrofuran acetogenin, arrests cancer cells at the G1 phase and causes cytotoxicity in a Bax- and caspase-3-related pathway. *Life Sciences*, 72(25), 2853–2861. doi: 10.1016/S0024-3205(03)00190-5
- Zhang, Q., Liu, J., Chen, S., Liu, J., Liu, L., Liu, G., ... Yuan, X. (2016). Caspase-12 is involved in stretch-induced apoptosis mediated endoplasmic reticulum stress. *Apoptosis*, 21(4), 432–442. <https://doi.org/10.1007/s10495-016-1217-6>

- Zhang, R., Xu, J., Zhao, J., & Bai, J. (2017). Knockdown of miR-27a sensitizes colorectal cancer stem cells to TRAIL by promoting the formation of Apaf-1-caspase-9 complex. *Oncotarget*, 8(28), 45213–45223. <https://doi.org/10.18632/oncotarget.16779>
- Zhao, D., Wu, Y., Xu, C., & Zhang, F. (2017). Cyclic-stretch induces apoptosis in human periodontal ligament cells by activation of caspase-5. *Archives of Oral Biology*, 73, 129–135. <https://doi.org/10.1016/j.archoralbio.2016.10.009>
- Zhao, Y., & Simon, R. (2008). BRB-ArrayTools Data Archive for human cancer gene expression: a unique and efficient data sharing resource. *Cancer Informatics*, 6, 9–15.

APPENDIX I

Gene descriptions for RT² Profiler™ PCR Human Apoptosis Array (SABiosciences, Cat no: PAHS-012Z) results, contained of the transcriptome (UniGene) from NCBI website, The Reference Sequence (RefSeq), Gene Symbol, Gene Description and Gene name from left to right.

| UniGene | Refseq | Symbol | Description | Gname |
|-----------|-----------|--------|--|--|
| Hs.431048 | NM_005157 | ABL1 | C-abl oncogene 1, non-receptor tyrosine kinase | ABL/JTK7/bcr/abl/c-ABL/c-ABL1/p150/v-abl |
| Hs.424932 | NM_004208 | AIFM1 | Apoptosis-inducing factor, mitochondrion-associated, 1 | AIF/CMT2D/CMTX4/COWCK/COXPD6/NADMR/NAMSD/PDCD8 |
| Hs.525622 | NM_005163 | AKT1 | V-akt murine thymoma viral oncogene homolog 1 | AKT/CWS6/PKB/PKB-ALPHA/PRKBA/RAC/RAC-ALPHA |
| Hs.552567 | NM_001160 | APAF1 | Apoptotic peptidase activating factor 1 | APAF-1/CED4 |
| Hs.370254 | NM_004322 | BAD | BCL2-associated agonist of cell death | BBC2/BCL2L8 |
| Hs.377484 | NM_004323 | BAG1 | BCL2-associated athanogene | BAG-1/HAP/RAP46 |
| Hs.523309 | NM_004281 | BAG3 | BCL2-associated athanogene 3 | BAG-3/BIS/CAIR-1/MFM6 |
| Hs.485139 | NM_001188 | BAK1 | BCL2-antagonist/killer 1 | BAK/BAK-LIKE/BCL2L7/CDN1 |
| Hs.624291 | NM_004324 | BAX | BCL2-associated X protein | BCL2L4 |
| Hs.193516 | NM_003921 | BCL10 | B-cell CLL/lymphoma 10 | CARMEN/CIPER/CLAP/IMD37/c-E10/mE10 |
| Hs.150749 | NM_000633 | BCL2 | B-cell CLL/lymphoma 2 | Bcl-2/PPP1R50 |
| Hs.227817 | NM_004049 | BCL2A1 | BCL2-related protein A1 | ACC-1/ACC-2/ACC1/ACC2/BCL2L5/BFL1/GRS/HBPA1 |

| | | | | |
|-----------|-----------|---------|---|--|
| Hs.516966 | NM_138578 | BCL2L1 | BCL2-like 1 | BCL-XL/S/BCL2L/BCLX/BCXL/BCLXS/Bcl-X/PPP1R52/bcl-xL/bcl-xS |
| Hs.283672 | NM_020396 | BCL2L10 | BCL2-like 10 (apoptosis facilitator) | BCL-B/Boo/Diva/bcl2-L-10 |
| Hs.469658 | NM_006538 | BCL2L11 | BCL2-like 11 (apoptosis facilitator) | BAM/BIM/BOD |
| Hs.410026 | NM_004050 | BCL2L2 | BCL2-like 2 | BCL-W/BCL2-L-2/BCLW/PPP1R51 |
| Hs.435556 | NM_016561 | BFAR | Bifunctional apoptosis regulator | BAR/RNF47 |
| Hs.517145 | NM_001196 | BID | BH3 interacting domain death agonist | FP497 |
| Hs.475055 | NM_001197 | BIK | BCL2-interacting killer (apoptosis-inducing) | BIP1/BP4/NBK |
| Hs.696238 | NM_001166 | BIRC2 | Baculoviral IAP repeat containing 2 | API1/HIAP2/Hiap-2/MIHB/RNF48/c-IAP1/cIAP1 |
| Hs.127799 | NM_001165 | BIRC3 | Baculoviral IAP repeat containing 3 | AIP1/API2/CIAP2/HAIP1/HIAP1/MALT2/MIHC/RNF49/c-IAP2 |
| Hs.744872 | NM_001168 | BIRC5 | Baculoviral IAP repeat containing 5 | API4/EPR-1 |
| Hs.150107 | NM_016252 | BIRC6 | Baculoviral IAP repeat containing 6 | APOLLON/BRUCE |
| Hs.646490 | NM_004330 | BNIP2 | BCL2/adenovirus E1B 19kDa interacting protein 2 | BNIP-2/NIP2 |
| Hs.144873 | NM_004052 | BNIP3 | BCL2/adenovirus E1B 19kDa interacting protein 3 | NIP3 |
| Hs.131226 | NM_004331 | BNIP3L | BCL2/adenovirus E1B 19kDa interacting protein 3-like | BNIP3a/NIX |
| Hs.550061 | NM_004333 | BRAF | V-raf murine sarcoma viral oncogene homolog B1 | B-RAF1/BRAF1/NS7/RAFB1 |
| Hs.2490 | NM_033292 | CASP1 | Caspase 1, apoptosis-related cysteine peptidase (interleukin 1, beta, convertase) | ICE/IL1BC/P45 |

| | | | | |
|-----------|-----------|--------|--|--|
| Hs.5353 | NM_001230 | CASP10 | Caspase 10, apoptosis-related cysteine peptidase | ALPS2/FLICE2/MCH4 |
| Hs.466057 | NM_012114 | CASP14 | Caspase 14, apoptosis-related cysteine peptidase | - |
| Hs.368982 | NM_032982 | CASP2 | Caspase 2, apoptosis-related cysteine peptidase | CASP-2/ICH1/NEDD-2/NEDD2/PPP1R57 |
| Hs.141125 | NM_004346 | CASP3 | Caspase 3, apoptosis-related cysteine peptidase | CPP32/ CPP32B/SCA-1 |
| Hs.138378 | NM_001225 | CASP4 | Caspase 4, apoptosis-related cysteine peptidase | ICE(rel)II/ICEREL-II/ICH-2/Mih1/TX/TX |
| Hs.213327 | NM_004347 | CASP5 | Caspase 5, apoptosis-related cysteine peptidase | ICE(rel)III/ICEREL-III/ICH-3 |
| Hs.654616 | NM_032992 | CASP6 | Caspase 6, apoptosis-related cysteine peptidase | MCH2 |
| Hs.9216 | NM_001227 | CASP7 | Caspase 7, apoptosis-related cysteine peptidase | CASP-7/CMH-1/ICE-LAP3/LICE2/MCH3 |
| Hs.599762 | NM_001228 | CASP8 | Caspase 8, apoptosis-related cysteine peptidase | ALPS2B/CAP4/Casp-8/FLICE/MACH/MCH5 |
| Hs.329502 | NM_001229 | CASP9 | Caspase 9, apoptosis-related cysteine peptidase | APAF-3/APAF3/ICE-LAP6/MCH6/PPP1R56 |
| Hs.355307 | NM_001242 | CD27 | CD27 molecule | S152/S152. LPFS2/T14/TNFRSF7/Tp55 |
| Hs.472860 | NM_001250 | CD40 | CD40 molecule, TNF receptor superfamily member 5 | Bp50/CDW40/TNFRSF5/p50 |
| Hs.592244 | NM_000074 | CD40LG | CD40 ligand | CD154/CD40L/HIGM1/IGM/IMD3/T-BAM/TNFSF5/TRAP/gp39/hCD40L |
| Hs.501497 | NM_001252 | CD70 | CD70 molecule | CD27L/CD27LG/TNFSF7 |
| Hs.390736 | NM_003879 | CFLAR | CASP8 and FADD-like apoptosis regulator | CASH/CASP8AP1/CLARP/Casper/FLAME/FL |

| | | | | |
|-----------|-----------|---------|---|---|
| | | | | AME-1/FLAME1/FLIP/I-FLICE/MRIT/c-FLIP/c-FLIPL/c-FLIPR/c-FLIPS |
| Hs.249129 | NM_001279 | CIDEA | Cell death-inducing DFFA-like effector a | CIDE-A |
| Hs.642693 | NM_014430 | CIDEB | Cell death-inducing DFFA-like effector b | - |
| Hs.38533 | NM_003805 | CRADD | CASP2 and RIPK1 domain containing adaptor with death domain | MRT34/RAIDD |
| Hs.437060 | NM_018947 | CYCS | Cytochrome c, somatic | CYC/HCS/THC4 |
| Hs.380277 | NM_004938 | DAPK1 | Death-associated protein kinase 1 | DAPK |
| Hs.484782 | NM_004401 | DFFA | DNA fragmentation factor, 45kDa, alpha polypeptide | DFF-45/DFF1/ICAD |
| Hs.169611 | NM_019887 | DIABLO | Diablo, IAP-binding mitochondrial protein | DFNA64/SMAC |
| Hs.86131 | NM_003824 | FADD | Fas (TNFRSF6)-associated via death domain | GIG3/MORT1 |
| Hs.667309 | NM_000043 | FAS | Fas (TNF receptor superfamily, member 6) | ALPS1A/APO-1/APT1/CD95/FAS1/FSTM/TNFRSF6 |
| Hs.2007 | NM_000639 | FASLG | Fas ligand (TNF superfamily, member 6) | ALPS1B/APT1LG1/APTL/CD178/CD95-L/CD95L/FASL/TNFSF6 |
| Hs.80409 | NM_001924 | GADD45A | Growth arrest and DNA-damage-inducible, alpha | DDIT1/GADD45 |
| Hs.87247 | NM_003806 | HRK | Harakiri, BCL2 interacting protein (contains only BH3 domain) | DP5/HARAKIRI |
| Hs.643120 | NM_000875 | IGF1R | Insulin-like growth factor 1 receptor | CD221/IGFIR/IGFR/JTK13 |
| Hs.193717 | NM_000572 | IL10 | Interleukin 10 | CSIF/GVHDS/IL-10/IL10A/TGIF |

| | | | | |
|-----------|-----------|-----------|--|--|
| Hs.36 | NM_000595 | LTA | Lymphotoxin alpha (TNF superfamily, member 1) | LT/TNFB/TNFSF1 |
| Hs.1116 | NM_002342 | LTBR | Lymphotoxin beta receptor (TNFR superfamily, member 3) | CD18/D12S370/LT-BETA-R/TNF-R-III/TNFCR/TNFR-RP/TNFR2-RP/TNFR3/TNFRSF3 |
| Hs.632486 | NM_021960 | MCL1 | Myeloid cell leukemia sequence 1 (BCL2-related) | BCL2L3/EAT/MCL1-ES/MCL1L/MCL1S/Mcl-1/TM/bcl2-L-3/mcl1/EAT |
| Hs.646951 | NM_004536 | NAIP | NLR family, apoptosis inhibitory protein | BIRC1/NLRB1/psiNAIP |
| Hs.618430 | NM_003998 | NFKB1 | Nuclear factor of kappa light polypeptide gene enhancer in B-cells 1 | EBP-1/KBF1/NF-kB1/NF-kappa-B/NF-kappaB/NFKB-p105/NFKB-p50/NFkappaB/p105/p50 |
| Hs.738731 | NM_006092 | NOD1 | Nucleotide-binding oligomerization domain containing 1 | CARD4/CLR7.1/NLRC1 |
| Hs.513667 | NM_003946 | NOL3 | Nucleolar protein 3 (apoptosis repressor with CARD domain) | ARC/FCM/MYP/NOP/NOP30 |
| Hs.499094 | NM_013258 | PYCARD | PYD and CARD domain containing | ASC/CARD5/TMS/TMS-1/TMS1 |
| Hs.103755 | NM_003821 | RIPK2 | Receptor-interacting serine-threonine kinase 2 | CARD3/CARDIAK/CCK/GIG30/RICK/RIP2 |
| Hs.241570 | NM_000594 | TNF | Tumor necrosis factor | DIF/TNF-alpha/TNFA/TNFSF2 |
| Hs.591834 | NM_003844 | TNFRSF10A | Tumor necrosis factor receptor superfamily, member 10a | APO2/CD261/DR4/TRAILR-1/TRAILR1 |
| Hs.661668 | NM_003842 | TNFRSF10B | Tumor necrosis factor receptor superfamily, member 10b | CD262/DR5/KILLER/KILLER/DR5/TRAILR2/TRAILR2/TRICK2/TRICK2A/TRICK2B/TRICKB/ZTNFR9 |
| Hs.81791 | NM_002546 | TNFRSF11B | Tumor necrosis factor receptor superfamily, member 11b | OCIF/OPG/PDB5/TR1 |

| | | | | |
|-----------|-----------|----------|---|---|
| Hs.713833 | NM_001065 | TNFRSF1A | Tumor necrosis factor receptor superfamily, member 1A | CD120a/FPF/MS5/TBP1/TNF-R/TNF-R-I/TNF-R55/TNFR/TNFR1/TNFR1-d2/TNFR55/TNFR60/p55/p55-R/p60 |
| Hs.256278 | NM_001066 | TNFRSF1B | Tumor necrosis factor receptor superfamily, member 1B | CD120b/TBPII/TNF-R-II/TNF-R75/TNFR/TNFR1B/TNFR2/TNFR80/p75/p75TNFR |
| Hs.443577 | NM_014452 | TNFRSF21 | Tumor necrosis factor receptor superfamily, member 21 | BM-018/CD358/DR6 |
| Hs.462529 | NM_003790 | TNFRSF25 | Tumor necrosis factor receptor superfamily, member 25 | APO-3/DDR3/DR3/LARD/TNFRSF12/TR3/TRAMP/WSL-1/WSL-LR |
| Hs.738942 | NM_001561 | TNFRSF9 | Tumor necrosis factor receptor superfamily, member 9 | 4-1BB/CD137/CDw137/IL137 |
| Hs.478275 | NM_003810 | TNFSF10 | Tumor necrosis factor (ligand) superfamily, member 10 | APO2L/Apo-2L/CD253/TL2/TRAIL |
| Hs.654445 | NM_001244 | TNFSF8 | Tumor necrosis factor (ligand) superfamily, member 8 | CD153/CD30L/CD30LG |
| Hs.437460 | NM_000546 | TP53 | Tumor protein p53 | BCC7/LFS1/P53/TRP53 |
| Hs.523968 | NM_005426 | TP53BP2 | Tumor protein p53 binding protein, 2 | 53BP2/ASPP2/BBP/P53BP2/PPP1R13A |
| Hs.192132 | NM_005427 | TP73 | Tumor protein p73 | P73 |
| Hs.460996 | NM_003789 | TRADD | TNFRSF1A-associated via death domain | Hs.89862 |
| Hs.522506 | NM_021138 | TRAF2 | TNF receptor-associated factor 2 | MGC:45012/TRAF2/TRAF3 |
| Hs.510528 | NM_003300 | TRAF3 | TNF receptor-associated factor 3 | CAP-1/CAP1/CD40bp/CRAF1/IIAE5/LAP1 |
| Hs.356076 | NM_001167 | XIAP | X-linked inhibitor of apoptosis | API3/BIRC4/IAP-3/ILP1/MIHA/XLP2/hIAP-3/hIAP3 |

| | | | | |
|-----------|-----------|-------|--|------------------------|
| Hs.520640 | NM_001101 | ACTB | Actin, beta | BRWS1/PS1TP5BP1 |
| Hs.534255 | NM_004048 | B2M | Beta-2-microglobulin | - |
| Hs.592355 | NM_002046 | GAPDH | Glyceraldehyde-3-phosphate dehydrogenase | G3PD/GAPD/HEL-S-162eP |
| Hs.412707 | NM_000194 | HPRT1 | Hypoxanthine phosphoribosyltransferase 1 | HGPRT/HPRT |
| Hs.546285 | NM_001002 | RPLP0 | Ribosomal protein, large, P0 | L10E/LP0/P0/PRLP0/RPP0 |
| N/A | SA_00105 | HGDC | Human Genomic DNA Contamination | HIGX1A |
| N/A | SA_00104 | RTC | Reverse Transcription Control | RTC |
| N/A | SA_00104 | RTC | Reverse Transcription Control | RTC |
| N/A | SA_00104 | RTC | Reverse Transcription Control | RTC |
| N/A | SA_00103 | PPC | Positive PCR Control | PPC |
| N/A | SA_00103 | PPC | Positive PCR Control | PPC |
| N/A | SA_00103 | PPC | Positive PCR Control | PPC |

APPENDIX II

The whole human genes, with UniqueID, that were used in the microarray experiments.

| Name | Symbol |
|--|---------|
| zinc finger, CCHC domain containing 9 | ZCCHC9 |
| WD repeat domain 49 | WDR49 |
| signal transducer and activator of transcription 5B | STAT5B |
| olfactory receptor, family 2, subfamily C, member 1 | OR2C1 |
| ribosomal L1 domain containing 1 | RSL1D1 |
| phospholipid scramblase 2 | PLSCR2 |
| odd-skipped related transcription factor 1 | OSR1 |
| leucine-rich repeats and calponin homology (CH) domain containing 4 | LRCH4 |
| DnaJ (Hsp40) homolog, subfamily C, member 9 | DNAJC9 |
| RAP2B, member of RAS oncogene family | RAP2B |
| galactosidase, beta 1-like 2 | GLB1L2 |
| transmembrane and coiled-coil domain family 2 | TMCC2 |
| forkhead box E3 | FOXE3 |
| nudix (nucleoside diphosphate linked moiety X)-type motif 12 | NUDT12 |
| coiled-coil domain containing 105 | CCDC105 |
| collagen, type XXIII, alpha 1 | COL23A1 |
| zinc finger, matrin-type 3 | ZMAT3 |
| family with sequence similarity 69, member A | FAM69A |
| adenylate cyclase 2 (brain) | ADCY2 |
| IQ motif containing J | IQCJ |
| muscle, skeletal, receptor tyrosine kinase | MUSK |
| SUMO1/sentrin specific peptidase 1 | SEN1 |
| selectin P ligand | SELPLG |
| protein phosphatase 2, regulatory subunit B, gamma | PPP2R2C |
| polycystic kidney and hepatic disease 1 (autosomal recessive)-like 1 | PKHD1L1 |
| DENN/MADD domain containing 1A | DENND1A |

| | |
|--|------------|
| TBC1 domain family, member 24 | TBC1D24 |
| solute carrier family 2 (facilitated glucose transporter), member 6 | SLC2A6 |
| myc target 1 | MYCT1 |
| PHD finger protein 20-like 1 | PHF20L1 |
| potassium channel, voltage gated eag related subfamily H, member 7 | KCNH7 |
| NLR family, pyrin domain containing 10 | NLRP10 |
| klotho beta | KLB |
| chemokine (C-X-C motif) ligand 6 | CXCL6 |
| interferon gamma receptor 2 (interferon gamma transducer 1) | IFNGR2 |
| ubiquitin specific peptidase 20 | USP20 |
| HGF activator | HGFAC |
| solute carrier family 15 (oligopeptide transporter), member 2 | SLC15A2 |
| prolactin releasing hormone receptor | PRLHR |
| IQ motif containing GTPase activating protein 1 | IQGAP1 |
| SET and MYND domain containing 4 | SMYD4 |
| dihydrolipoamide S-succinyltransferase (E2 component of 2-oxo-glutarate complex) | DLST |
| hydroxycarboxylic acid receptor 1 | HCAR1 |
| phosphatidylinositol glycan anchor biosynthesis, class H | PIGH |
| leucine-rich repeat LGI family, member 4 | LGI4 |
| POM121 and ZP3 fusion | POMZP3 |
| COMM domain containing 7 | COMMD7 |
| docking protein 1, 62kDa (downstream of tyrosine kinase 1) | DOK1 |
| RAN binding protein 2 | RANBP2 |
| solute carrier family 6 (neutral amino acid transporter), member 15 | SLC6A15 |
| DnaJ (Hsp40) homolog, subfamily C, member 18 | DNAJC18 |
| chondroitin sulfate N-acetylgalactosaminyltransferase 2 | CSGALNACT2 |
| ubiquitin specific peptidase 45 | USP45 |
| calcium channel, voltage-dependent, gamma subunit 1 | CACNG1 |
| STEAP family member 1B | STEAP1B |
| zinc finger protein 345 | ZNF345 |
| Nipped-B homolog (Drosophila) | NIPBL |
| IQ motif containing H | IQCH |
| lysine (K)-specific demethylase 3A | KDM3A |
| ribosomal protein L39 | RPL39 |
| SH3 and SYLF domain containing 1 | SH3YL1 |

| | |
|--|-----------|
| solute carrier family 22, member 20 | SLC22A20 |
| minichromosome maintenance 9 homologous recombination repair factor | MCM9 |
| peroxisomal biogenesis factor 13 | PEX13 |
| YY1 associated factor 2 | YAF2 |
| zinc finger protein 225 | ZNF225 |
| carbonic anhydrase VII | CA7 |
| ribonuclease P/MRP 25kDa subunit | RPP25 |
| chromosome 9 open reading frame 142 | C9orf142 |
| transmembrane protein 184A | TMEM184A |
| ribosomal protein S6 kinase, 90kDa, polypeptide 1 | RPS6KA1 |
| RAB37, member RAS oncogene family | RAB37 |
| serpin peptidase inhibitor, clade F (alpha-2 antiplasmin, pigment epithelium derived factor), member 1 | SERPINF1 |
| carcinoembryonic antigen-related cell adhesion molecule 22, pseudogene | CEACAM22P |
| SWI5 homologous recombination repair protein | SWI5 |
| kallikrein-related peptidase 8 | KLK8 |
| flavin containing monooxygenase 5 | FMO5 |
| integrator complex subunit 12 | INTS12 |
| eukaryotic translation initiation factor 3, subunit J | EIF3J |
| progesterin and adipoQ receptor family member VII | PAQR7 |
| apoptosis-associated tyrosine kinase | AATK |
| autophagy related 9B | ATG9B |
| MON1 secretory trafficking family member A | MON1A |
| replication factor C (activator 1) 2, 40kDa | RFC2 |
| tudor domain containing 6 | TDRD6 |
| solute carrier family 16 (aromatic amino acid transporter), member 10 | SLC16A10 |
| elaC ribonuclease Z 2 | ELAC2 |
| single stranded DNA binding protein 3 | SSBP3 |
| transmembrane protein 169 | TMEM169 |
| leucine rich repeat neuronal 2 | LRRN2 |
| growth arrest and DNA-damage-inducible, beta | GADD45B |
| Rap guanine nucleotide exchange factor (GEF) 1 | RAPGEF1 |
| ribonucleoprotein, PTB-binding 2 | RAVER2 |
| long intergenic non-protein coding RNA 442 | LINC00442 |
| ets variant 5 | ETV5 |
| golgi phosphoprotein 3 (coat-protein) | GOLPH3 |
| glypican 6 | GPC6 |

| | |
|---|---------|
| zinc finger protein 446 | ZNF446 |
| zinc finger protein 655 | ZNF655 |
| tetratricopeptide repeat domain 21B | TTC21B |
| zinc finger protein 702, pseudogene | ZNF702P |
| chromosome 6 open reading frame 48 | C6orf48 |
| translational activator of mitochondrially encoded cytochrome c oxidase I | TACO1 |
| proline dehydrogenase (oxidase) 1 | PRODH |
| Ras association (RalGDS/AF-6) domain family (N-terminal) member 8 | RASSF8 |
| Kv channel interacting protein 2 | KCNIP2 |
| thiamine triphosphatase | THTPA |
| chromosome 3 open reading frame 67 | C3orf67 |
| unkempt family zinc finger-like | UNKL |
| chromosome 1 open reading frame 95 | C1orf95 |
| gap junction protein, beta 1, 32kDa | GJB1 |
| olfactory receptor, family 51, subfamily B, member 2 (gene/pseudogene) | OR51B2 |
| hydroletharus syndrome 1 | HYLS1 |
| fibroblast growth factor binding protein 3 | FGFBP3 |
| family with sequence similarity 117, member A | FAM117A |
| keratin 80, type II | KRT80 |
| family with sequence similarity 20, member A | FAM20A |
| NK2 homeobox 2 | NKX2-2 |
| phosphate cytidyltransferase 2, ethanolamine | PCYT2 |
| myosin VA | MYO5A |
| prolylcarboxypeptidase (angiotensinase C) | PRCP |
| proteasome 26S subunit, non-ATPase 3 | PSMD3 |
| ceramide synthase 3 | CERS3 |
| zinc finger protein 780A | ZNF780A |
| acyl-CoA synthetase bubblegum family member 1 | ACSBG1 |
| transmembrane protease, serine 2 | TMPRSS2 |
| solute carrier family 25 (mitochondrial carrier; phosphate carrier), member 3 | SLC25A3 |
| NANOG neighbor homeobox | NANOGNB |
| interferon-induced protein with tetratricopeptide repeats 1B | IFIT1B |
| prohibitin | PHB |
| breast carcinoma amplified sequence 4 | BCAS4 |
| doublecortin domain containing 2C | DCDC2C |

| | |
|--|----------|
| UTP15, U3 small nucleolar ribonucleoprotein, homolog (S. cerevisiae) | UTP15 |
| Myb-like, SWIRM and MPN domains 1 | MYSM1 |
| ATH1, acid trehalase-like 1 (yeast) | ATHL1 |
| zinc finger protein 22 | ZNF22 |
| solute carrier organic anion transporter family, member 3A1 | SLCO3A1 |
| proteasome 26S subunit, non-ATPase 6 | PSMD6 |
| protease, serine, 54 | PRSS54 |
| BBSome interacting protein 1 | BBIP1 |
| actin binding LIM protein 1 | ABLIM1 |
| ADAM metalloproteinase with thrombospondin type 1 motif, 6 | ADAMTS6 |
| abhydrolase domain containing 8 | ABHD8 |
| placenta-specific 1 | PLAC1 |
| myelin protein zero-like 1 | MPZL1 |
| RIC8 guanine nucleotide exchange factor B | RIC8B |
| cysteine-rich protein 3 | CRIP3 |
| chloride channel accessory 4 | CLCA4 |
| glutathione S-transferase kappa 1 | GSTK1 |
| gamma-aminobutyric acid (GABA) A receptor, gamma 1 | GABRG1 |
| polypeptide N-acetylgalactosaminyltransferase 6 | GALNT6 |
| son of sevenless homolog 2 (Drosophila) | SOS2 |
| protein phosphatase 1, regulatory (inhibitor) subunit 1A | PPP1R1A |
| chromosome 9 open reading frame 84 | C9orf84 |
| protein phosphatase 2A activator, regulatory subunit 4 | PPP2R4 |
| serine/arginine-rich splicing factor 2 | SRSF2 |
| late endosomal/lysosomal adaptor, MAPK and MTOR activator 1 | LAMTOR1 |
| ring finger protein 19A, RBR E3 ubiquitin protein ligase | RNF19A |
| 4-aminobutyrate aminotransferase | ABAT |
| sterile alpha motif domain containing 3 | SAMD3 |
| KIAA1468 | KIAA1468 |
| fem-1 homolog c (C. elegans) | FEM1C |
| protein phosphatase 6, regulatory subunit 2 | PPP6R2 |
| serine/arginine repetitive matrix 4 | SRRM4 |
| scavenger receptor class A, member 3 | SCARA3 |
| RNA binding motif protein 8A | RBM8A |
| T-cell leukemia/lymphoma 1A | TCL1A |
| dipeptidyl-peptidase 7 | DPP7 |
| T-box 5 | TBX5 |
| frequently rearranged in advanced T-cell lymphomas 1 | FRAT1 |

| | |
|---|-----------|
| NK3 homeobox 2 | NKX3-2 |
| parathyroid hormone 1 receptor | PTH1R |
| G protein-coupled receptor 45 | GPR45 |
| EF-hand calcium binding domain 9 | EFCAB9 |
| signal sequence receptor, beta (translocon-associated protein beta) | SSR2 |
| isocitrate dehydrogenase 3 (NAD+) gamma | IDH3G |
| proteasome subunit alpha 8 | PSMA8 |
| chromosome 11 open reading frame 53 | C11orf53 |
| RANBP2-like and GRIP domain containing 1 | RGPD1 |
| peptidyl-prolyl cis-trans isomerase A pseudogene | LOC390956 |
| carcinoembryonic antigen-related cell adhesion molecule 18 | CEACAM18 |
| leucine-rich repeats and IQ motif containing 3 | LRRIQ3 |
| GDP-mannose pyrophosphorylase A | GMPPA |
| ELOVL fatty acid elongase 1 | ELOVL1 |
| thioredoxin-related transmembrane protein 1 | TMX1 |
| RFT1 homolog | RFT1 |
| ribosomal protein L4 | RPL4 |
| paralemmin 3 | PALM3 |
| deafness, autosomal dominant 5 | DFNA5 |
| regulating synaptic membrane exocytosis 4 | RIMS4 |
| plexin A4 | PLXNA4 |
| doublecortin domain containing 1 | DCDC1 |
| ribosomal protein L31 pseudogene 11 | RPL31P11 |
| erythropoietin receptor | EPOR |
| angiomin like 2 | AMOTL2 |
| chromosome 3 open reading frame 38 | C3orf38 |
| Usher syndrome 1G (autosomal recessive) | USH1G |
| WD repeat domain 91 | WDR91 |
| ral guanine nucleotide dissociation stimulator-like 3 | RGL3 |
| snail family zinc finger 2 | SNAI2 |
| kinesin family member 1A | KIF1A |
| H6 family homeobox 3 | HMX3 |
| breast carcinoma amplified sequence 1 | BCAS1 |
| olfactory receptor, family 1, subfamily D, member 5 | OR1D5 |
| atonal bHLH transcription factor 8 | ATOH8 |
| endoplasmic reticulum aminopeptidase 2 | ERAP2 |
| carboxypeptidase D | CPD |
| miR-17-92 cluster host gene | MIR17HG |
| missing oocyte, meiosis regulator, homolog (Drosophila) | MIOS |

| | |
|---|---------|
| somatostatin receptor 1 | SSTR1 |
| alanyl (membrane) aminopeptidase | ANPEP |
| olfactory receptor, family 4, subfamily C, member 6 | OR4C6 |
| DiGeorge syndrome critical region gene 5 (non-protein coding) | DGCR5 |
| G protein-coupled receptor 22 | GPR22 |
| canopy FGF signaling regulator 1 | CNPY1 |
| centromere protein I | CENPI |
| mitochondrial translational initiation factor 3 | MTIF3 |
| chromosome 5 open reading frame 63 | C5orf63 |
| CD74 molecule, major histocompatibility complex, class II invariant chain | CD74 |
| STEAP family member 3, metalloredutase | STEAP3 |
| 3'(2'), 5'-bisphosphate nucleotidase 1 | BPNT1 |
| G protein-coupled receptor 39 | GPR39 |
| heat shock factor binding protein 1 | HSBP1 |
| v-myc avian myelocytomatosis viral oncogene homolog | MYC |
| olfactory receptor, family 52, subfamily K, member 2 | OR52K2 |
| zinc finger protein 44 | ZNF44 |
| gap junction protein, delta 3, 31.9kDa | GJD3 |
| gem (nuclear organelle) associated protein 6 | GEMIN6 |
| paired-like homeodomain 1 | PITX1 |
| olfactory receptor, family 56, subfamily A, member 1 | OR56A1 |
| transmembrane channel-like 8 | TMC8 |
| contactin 1 | CNTN1 |
| thyroid stimulating hormone receptor | TSHR |
| neuron navigator 1 | NAV1 |
| receptor (G protein-coupled) activity modifying protein 1 | RAMP1 |
| barrier to autointegration factor 2 | BANF2 |
| interleukin 3 | IL3 |
| secretagogin, EF-hand calcium binding protein | SCGN |
| kinase suppressor of ras 2 | KSR2 |
| echinoderm microtubule associated protein like 3 | EML3 |
| WD repeat domain 13 | WDR13 |
| phosphoinositide-3-kinase, regulatory subunit 2 (beta) | PIK3R2 |
| podocan-like 1 | PODNL1 |
| PR domain containing 4 | PRDM4 |
| MAP/microtubule affinity-regulating kinase 2 | MARK2 |
| late cornified envelope 2A | LCE2A |
| transducin (beta)-like 2 | TBL2 |

| | |
|---|--------------|
| spermatogenesis associated 18 | SPATA18 |
| metallophosphoesterase domain containing 2 | MPPED2 |
| G protein-coupled receptor 37 (endothelin receptor type B-like) | GPR37 |
| WNK lysine deficient protein kinase 1 | WNK1 |
| tetra-peptide repeat homeobox 1 | TPRX1 |
| chromosome 15 open reading frame 26 | C15orf26 |
| SRY (sex determining region Y)-box 4 | SOX4 |
| periostin, osteoblast specific factor | POSTN |
| leucine rich repeat containing 59 | LRRC59 |
| myosin, light chain 5, regulatory | MYL5 |
| family with sequence similarity 134, member C | FAM134C |
| family with sequence similarity 160, member B2 | FAM160B2 |
| calcium/calmodulin-dependent protein kinase II beta | CAMK2B |
| solute carrier family 25 (mitochondrial carrier; adenine nucleotide translocator), member 5 | SLC25A5 |
| otopetrin 2 | OTOP2 |
| translocase of inner mitochondrial membrane 8 homolog A (yeast) | TIMM8A |
| fasciculation and elongation protein zeta 1 (zygin I) | FEZ1 |
| ADP-ribosylation factor-like 6 interacting protein 6 | ARL6IP6 |
| solute carrier family 27 (fatty acid transporter), member 2 | SLC27A2 |
| sodium channel, voltage gated, type III beta subunit | SCN3B |
| HERV-H LTR-associating 3 | HHLA3 |
| synovial sarcoma translocation gene on chromosome 18-like 2 | SS18L2 |
| small nuclear ribonucleoprotein 27kDa (U4/U6.U5) | SNRNP27 |
| long intergenic non-protein coding RNA 111 | LINC00111 |
| acid phosphatase 2, lysosomal | ACP2 |
| cytoglobin | CYGB |
| uncharacterized LOC100130872 | LOC100130872 |
| zinc finger protein 654 | ZNF654 |
| far upstream element (FUSE) binding protein 1 | FUBP1 |
| glycerate kinase | GLYCK |
| polymerase (RNA) III (DNA directed) polypeptide H (22.9kD) | POLR3H |
| ephrin-A2 | EFNA2 |
| coiled-coil domain containing 68 | CCDC68 |
| sterile alpha motif domain containing 10 | SAMD10 |
| BPI fold containing family A, member 1 | BPIFA1 |
| ZFP62 zinc finger protein | ZFP62 |
| adhesion molecule with Ig-like domain 2 | AMIGO2 |

| | |
|---|--------------|
| chemokine (C-C motif) ligand 14 | CCL14 |
| transmembrane protein 160 | TMEM160 |
| chromosome 1 open reading frame 54 | C1orf54 |
| zinc finger protein 214 | ZNF214 |
| hypoxia inducible factor 1, alpha subunit (basic helix-loop-helix transcription factor) | HIF1A |
| DEAD (Asp-Glu-Ala-Asp) box helicase 3, Y-linked | DDX3Y |
| myeloid/lymphoid or mixed-lineage leukemia; translocated to, 10 | MLLT10 |
| coiled-coil domain containing 53 | CCDC53 |
| uncharacterized LOC100506813 | LOC100506813 |
| SPANX family, member N4 | SPANXN4 |
| FK506 binding protein 1A, 12kDa | FKBP1A |
| potassium channel, voltage gated eag related subfamily H, member 4 | KCNH4 |
| NIN1/RPN12 binding protein 1 homolog | NOB1 |
| deoxyribonuclease II beta | DNASE2B |
| olfactory receptor, family 6, subfamily Y, member 1 | OR6Y1 |
| keratin associated protein 12-4 | KRTAP12-4 |
| polyglutamine binding protein 1 | PQBP1 |
| gonadotropin-releasing hormone (type 2) receptor 2, pseudogene | GNRHR2 |
| cyclin Y | CCNY |
| coiled-coil domain containing 63 | CCDC63 |
| BTB (POZ) domain containing 3 | BTBD3 |
| sterol carrier protein 2 | SCP2 |
| EPH receptor A5 | EPHA5 |
| SH3-domain binding protein 2 | SH3BP2 |
| bone morphogenetic protein 8a | BMP8A |
| Kruppel-like factor 6 | KLF6 |
| transducer of ERBB2, 1 | TOB1 |
| ectonucleotide pyrophosphatase/phosphodiesterase 6 | ENPP6 |
| RAD51 associated protein 2 | RAD51AP2 |
| cAMP responsive element binding protein 3-like 1 | CREB3L1 |
| dihydropyrimidine dehydrogenase | DPYD |
| mannosyl (alpha-1,3-)-glycoprotein beta-1,4-N-acetylglucosaminyltransferase, isozyme A | MGAT4A |
| churchill domain containing 1 | CHURC1 |
| F-box protein 38 | FBXO38 |
| polypeptide N-acetylgalactosaminyltransferase-like 6 | GALNTL6 |
| SEC24 homolog C, COPII coat complex component | SEC24C |

| | |
|---|----------|
| sperm flagellar 1 | SPEF1 |
| WW and C2 domain containing 1 | WWC1 |
| G patch domain and KOW motifs | GPKOW |
| uridine-cytidine kinase 1 | UCK1 |
| fibroblast growth factor receptor-like 1 | FGFRL1 |
| glyceronephosphate O-acyltransferase | GNPAT |
| Ras and Rab interactor-like | RINL |
| transmembrane protein 145 | TMEM145 |
| failed axon connections homolog | FAXC |
| small G protein signaling modulator 2 | SGSM2 |
| ALG13, UDP-N-acetylglucosaminyltransferase subunit | ALG13 |
| non-SMC condensin I complex, subunit D2 | NCAPD2 |
| shisa family member 3 | SHISA3 |
| arylacetamide deacetylase-like 3 | AADACL3 |
| solute carrier family 25 (mitochondrial carrier; citrate transporter), member 1 | SLC25A1 |
| thyroid hormone receptor interactor 13 | TRIP13 |
| potassium channel tetramerization domain containing 2 | KCTD2 |
| dynactin 1 | DCTN1 |
| immature colon carcinoma transcript 1 | ICT1 |
| forkhead box K2 | FOXK2 |
| HNF1 homeobox B | HNF1B |
| phosphofructokinase, muscle | PFKM |
| S100 calcium binding protein A8 | S100A8 |
| mitochondrial ribosomal protein L39 | MRPL39 |
| SNF8, ESCRT-II complex subunit | SNF8 |
| cytochrome P450, family 2, subfamily F, polypeptide 1 | CYP2F1 |
| beta-carotene oxygenase 2 | BCO2 |
| solute carrier family 17 (organic anion transporter), member 1 | SLC17A1 |
| transmembrane protein 134 | TMEM134 |
| adenomatosis polyposis coli down-regulated 1 | APCDD1 |
| ring finger protein 183 | RNF183 |
| heat shock transcription factor 2 | HSF2 |
| chromosome 15 open reading frame 53 | C15orf53 |
| integrin-binding sialoprotein | IBSP |
| olfactory receptor, family 4, subfamily C, member 16 (gene/pseudogene) | OR4C16 |
| extracellular matrix protein 2, female organ and adipocyte specific | ECM2 |
| MIR205 host gene | MIR205HG |

| | |
|---|-----------|
| zinc finger, C3H1-type containing | ZFC3H1 |
| fibroblast growth factor binding protein 2 | FGFBP2 |
| parvin, alpha | PARVA |
| long intergenic non-protein coding RNA 336 | LINC00336 |
| proline dehydrogenase (oxidase) 2 | PRODH2 |
| major histocompatibility complex, class I-related | MR1 |
| dysbindin (dystrobrevin binding protein 1) domain containing 2 | DBNDD2 |
| PNN-interacting serine/arginine-rich protein | PNISR |
| glycine receptor, beta | GLRB |
| neurexophilin 3 | NXPH3 |
| ubiquinol-cytochrome c reductase, complex III subunit VII, 9.5kDa | UQCRQ |
| solute carrier family 24 (sodium/potassium/calcium exchanger), member 2 | SLC24A2 |
| sorting nexin 22 | SNX22 |
| chromosome 11 open reading frame 40 | C11orf40 |
| kin of IRRE like 2 (Drosophila) | KIRREL2 |
| zinc finger protein 524 | ZNF524 |
| elongation factor RNA polymerase II | ELL |
| Rho family GTPase 3 | RND3 |
| phosphotyrosine interaction domain containing 1 | PID1 |
| chromosome 20 open reading frame 78 | C20orf78 |
| keratin 28, type I | KRT28 |
| transcription elongation regulator 1-like | TCERG1L |
| t-complex 10-like 2 | TCP10L2 |
| NFAT activating protein with ITAM motif 1 | NFAM1 |
| filaggrin | FLG |
| chromosome 19 open reading frame 81 | C19orf81 |
| solute carrier family 39 (zinc transporter), member 14 | SLC39A14 |
| Rho GTPase activating protein 35 | ARHGAP35 |
| solute carrier family 38, member 9 | SLC38A9 |
| lipocalin-like 1 | LCNL1 |
| tyrosine kinase 2 | TYK2 |
| transforming growth factor beta regulator 1 | TBRG1 |
| aarF domain containing kinase 1 | ADCK1 |
| YLP motif containing 1 | YLPM1 |
| islet cell autoantigen 1,69kDa-like | ICA1L |
| zinc finger protein 551 | ZNF551 |
| olfactory receptor, family 4, subfamily A, member 15 | OR4A15 |
| actin binding LIM protein family, member 2 | ABLIM2 |

| | |
|--|-----------|
| secretoglobin, family 1D, member 1 | SCGB1D1 |
| class II, major histocompatibility complex, transactivator | CIITA |
| keratin associated protein 20-2 | KRTAP20-2 |
| sphingosine-1-phosphate receptor 3 | S1PR3 |
| chromosome 8 open reading frame 34 | C8orf34 |
| EF-hand calcium binding domain 12 | EFCAB12 |
| methyltransferase like 10 | METTLL10 |
| adipocyte plasma membrane associated protein | APMAP |
| interleukin 6 receptor | IL6R |
| carbohydrate (N-acetylglucosamine 6-O) sulfotransferase 5 | CHST5 |
| chromosome 9 open reading frame 72 | C9orf72 |
| paired box 3 | PAX3 |
| pleckstrin homology-like domain, family A, member 2 | PHLDA2 |
| synaptotagmin XVI | SYT16 |
| CD99 molecule pseudogene 1 | CD99P1 |
| apolipoprotein E | APOE |
| leukocyte immunoglobulin-like receptor, subfamily B (with TM and ITIM domains), member 2 | LILRB2 |
| sema domain, immunoglobulin domain (Ig), transmembrane domain (TM) and short cytoplasmic domain, (semaphorin) 4D | SEMA4D |
| ring finger protein 121 | RNF121 |
| trafficking protein particle complex 10 | TRAPPC10 |
| reelin | RELN |
| RNA guanylyltransferase and 5'-phosphatase | RNGTT |
| anaplastic lymphoma receptor tyrosine kinase | ALK |
| structural maintenance of chromosomes 1B | SMC1B |
| zinc finger protein 680 | ZNF680 |
| apolipoprotein L, 5 | APOL5 |
| N-acetylglutamate synthase | NAGS |
| FERM domain containing 1 | FRMD1 |
| aquaporin 3 (Gill blood group) | AQP3 |
| Sin3A-associated protein, 25kDa | SAP25 |
| keratin 85, type II | KRT85 |
| ubiquitously transcribed tetratricopeptide repeat containing, Y-linked | UTY |
| protein arginine methyltransferase 6 | PRMT6 |
| potassium channel subfamily M regulatory beta subunit 1 | KCNMB1 |
| uncharacterized LOC283440 | LOC283440 |
| androgen-induced 1 | AIG1 |
| synaptopodin 2-like | SYNPO2L |

| | |
|---|-----------|
| tRNA 5-methylaminomethyl-2-thiouridylate methyltransferase | TRMU |
| SET domain and mariner transposase fusion gene | SETMAR |
| transmembrane protein 192 | TMEM192 |
| F-box protein 41 | FBXO41 |
| TBC1 domain family, member 24 | TBC1D24 |
| cadherin 8, type 2 | CDH8 |
| SWI/SNF related, matrix associated, actin dependent regulator of chromatin, subfamily c, member 1 | SMARCC1 |
| potassium channel, voltage gated eag related subfamily H, member 7 | KCNH7 |
| AT hook containing transcription factor 1 | AHCTF1 |
| Fanconi anemia, complementation group A | FANCA |
| ATM serine/threonine kinase | ATM |
| cyclin-dependent kinase 5, regulatory subunit 2 (p39) | CDK5R2 |
| reticulocalbin 2, EF-hand calcium binding domain | RCN2 |
| low density lipoprotein receptor-related protein 1 | LRP1 |
| COMM domain containing 6 | COMMD6 |
| lin-28 homolog B (C. elegans) | LIN28B |
| SH3 and multiple ankyrin repeat domains 2 | SHANK2 |
| caspase 5, apoptosis-related cysteine peptidase | CASP5 |
| sorcin | SRI |
| chromosome 10 open reading frame 111 | C10orf111 |
| centrosomal protein 85kDa | CEP85 |
| filaggrin family member 2 | FLG2 |
| melanoregulin | MREG |
| coiled-coil domain containing 50 | CCDC50 |
| v-rel avian reticuloendotheliosis viral oncogene homolog A | RELA |
| abhydrolase domain containing 16A | ABHD16A |
| hes family bHLH transcription factor 2 | HES2 |
| MIS18 kinetochore protein A | MIS18A |

VITA

Sepideh Mohammadhosseinpour hold a Bachelor of Science degree in Agricultural Engineering in 2010 and a Master of Science Degree in Plant Breeding in 2013 from University of Tehran in Tehran, Iran. In Fall 2015, she entered graduate school at Stephen F. Austin State University, Nacogdoches, Texas. She received a Master of Science degree in Biotechnology in May 2018.

Permanent Address: 8 No, Haftpeikar Alley, Tavanir St,
Tehran, Iran.

Email address: mohammads@jacks.sfasu.edu

This thesis was typed by Sepideh Mohammadhosseinpour.

